GRB modelling

Željka Bošnjak
University of Zagreb, Croatia

Workshop on Numerical Multi-messenger Modeling - Paris, February 21-23, 2024

Synchrotron spectrum

Sari, Piran & Narayan 1998

Briggs et al. 1999

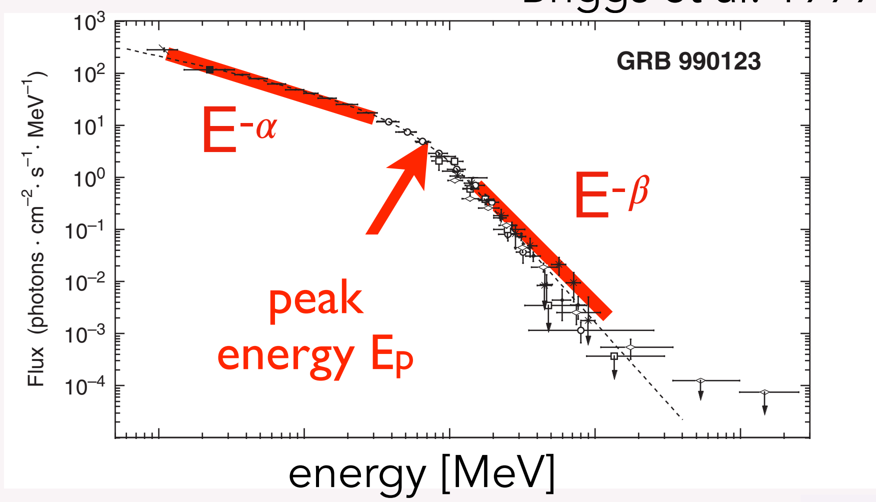

Relativistic electrons:

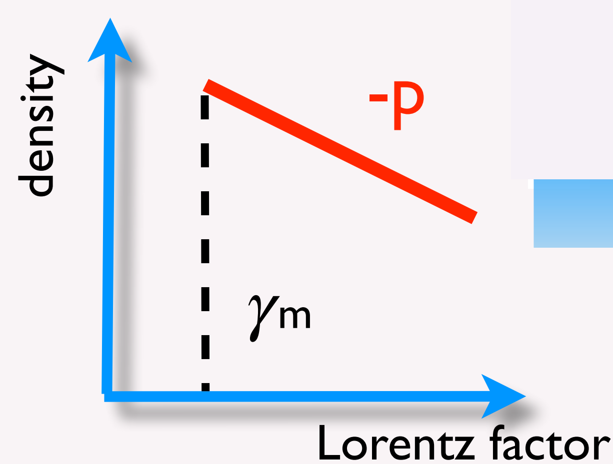

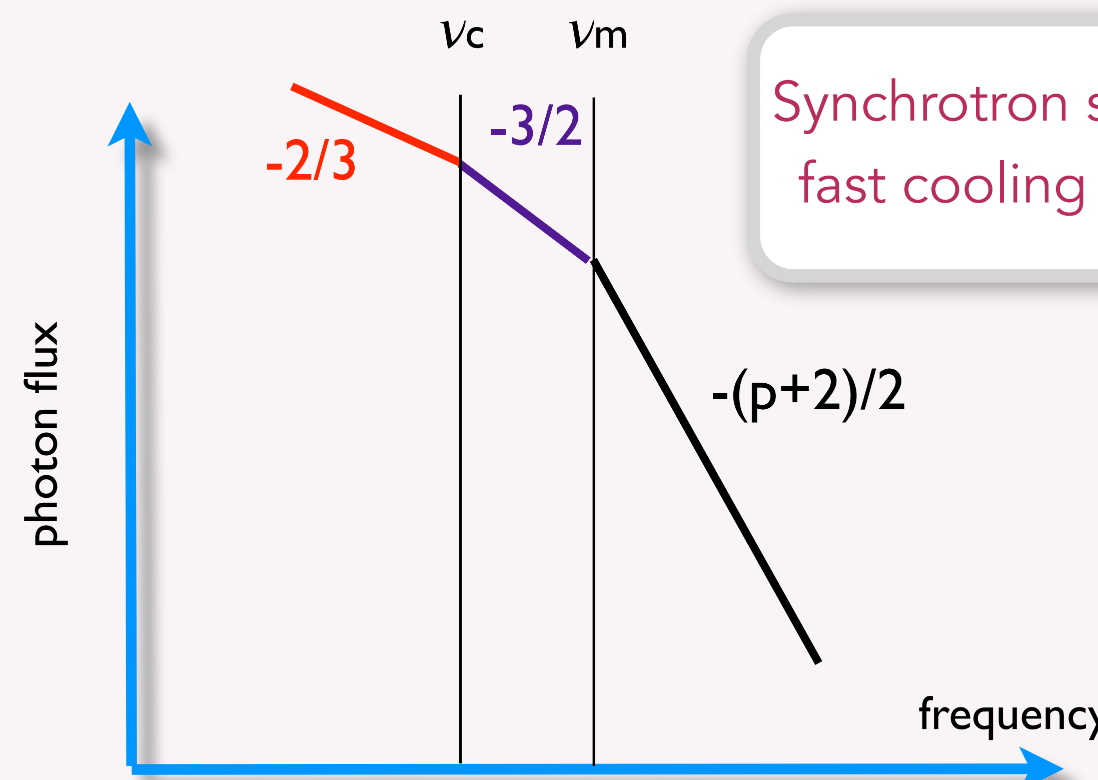

Synchrotron spectrum: fast cooling ($\gamma_c < \gamma_m$)

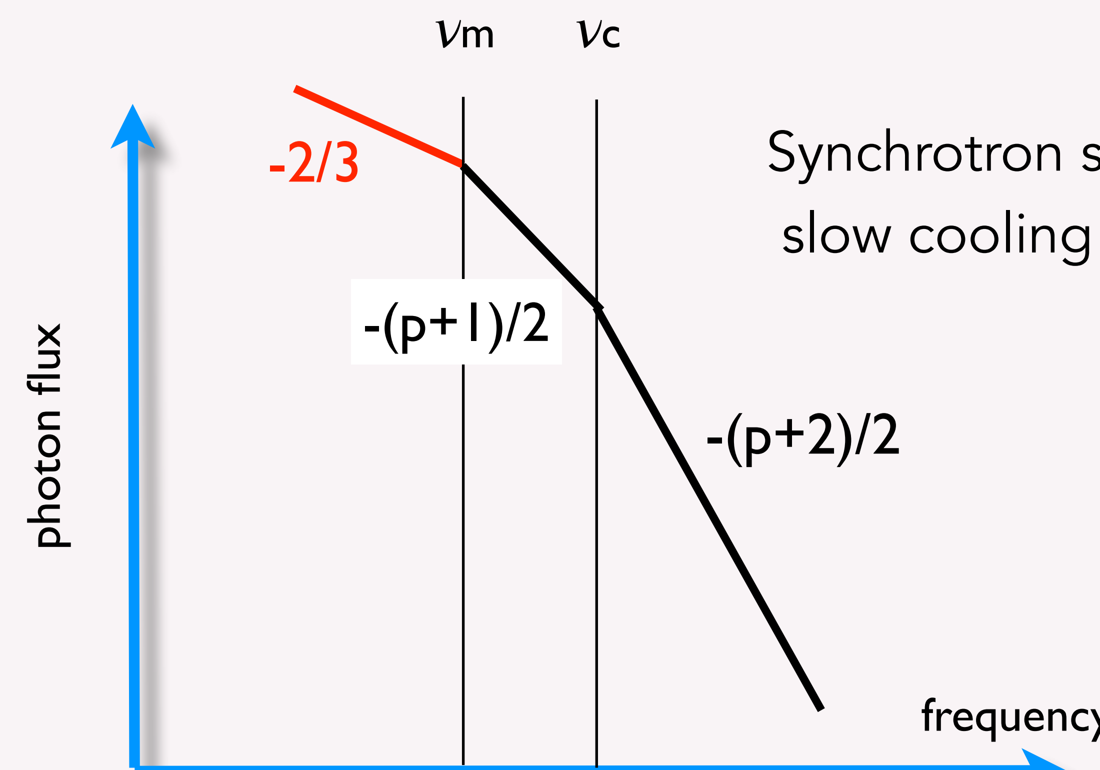

Synchrotron spectrum: slow cooling ($\gamma_c > \gamma_m$)

γ_m: minimum Lorentz factor at injection

γ_c: radiative timescale = dynamical timescale

Synchrotron spectrum

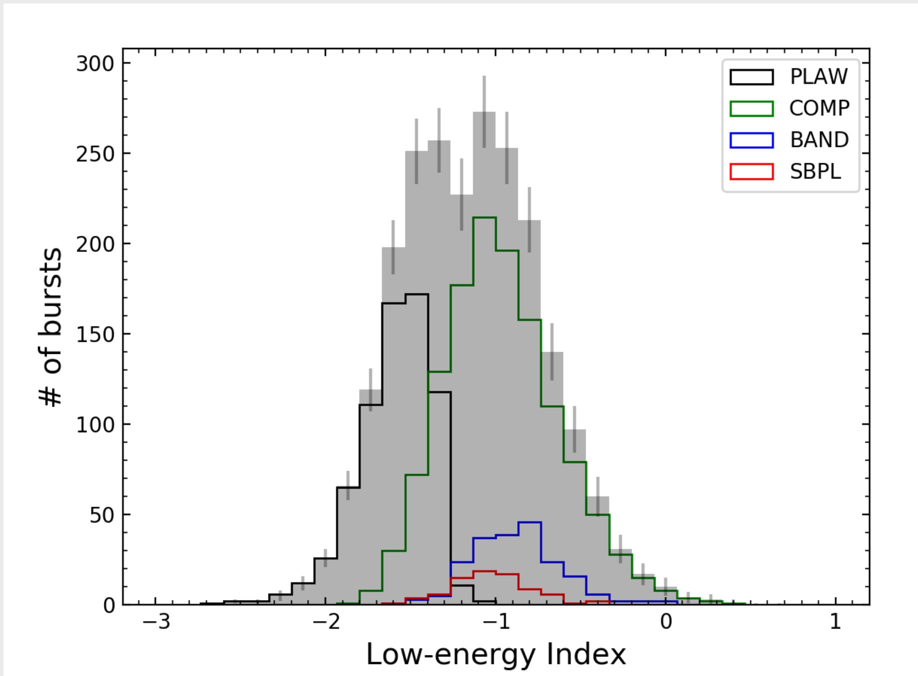

Time-integrated spectral fits: $\alpha = -1.08^{+0.45}_{-0.44}$

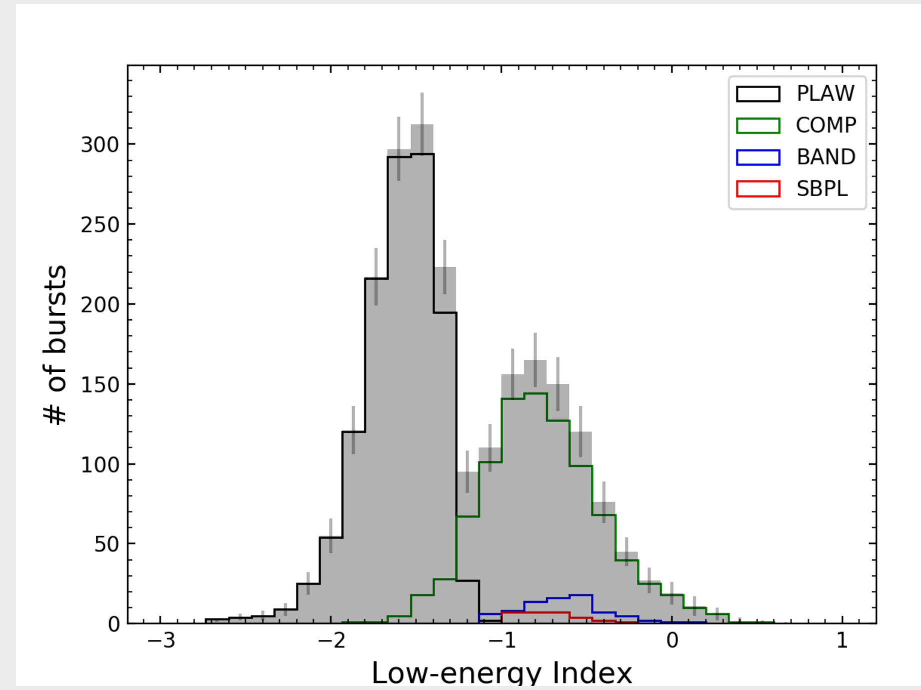

Peak-flux spectral fits: $\alpha = -1.30^{+0.77}_{-0.33}$

Poolakkil et al. 2021

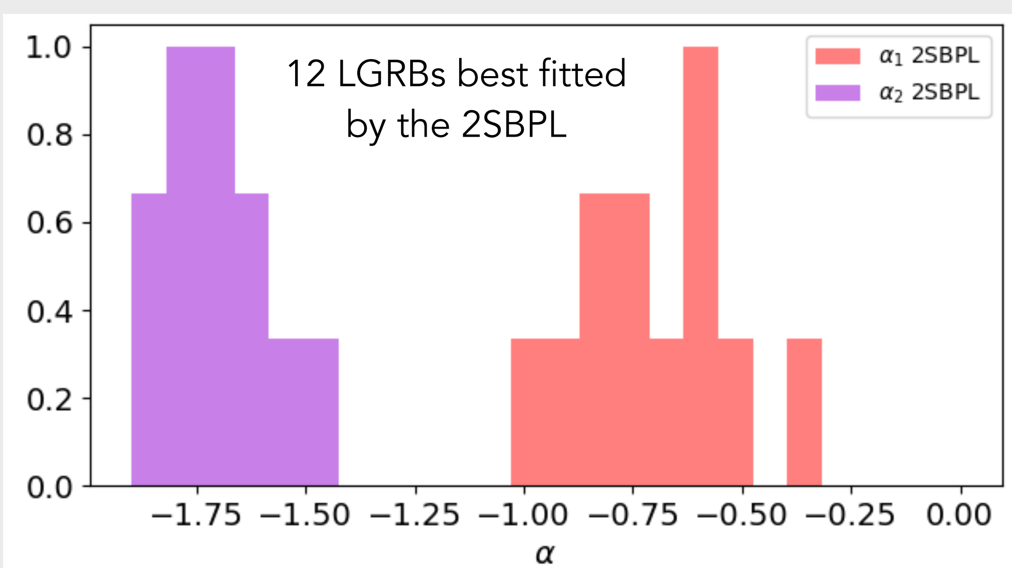

Toffano et al. 2021: 12 LGRBs observed by Fermi GBM, having large fluences and large E_{peak} values

→ the distributions of spectral slopes peak at -0.71 and -1.71, not far from the typical values -2/3 and -3/2 expected for synchrotron spectrum from marginally fast cooling electrons

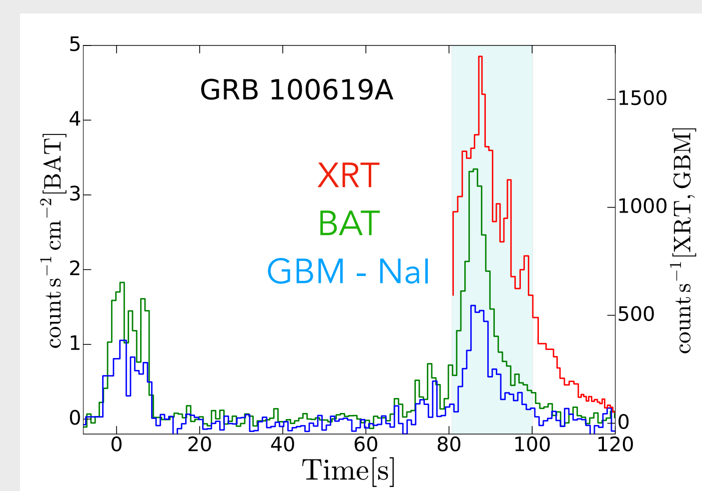

Oganesyan et al. 2018; 2017

joint XRT+BAT spectral analysis for 34 GRBs

Internal shock model

The jet is assumed to be weakly magnetized at large distance and the prompt emission is emitted above the photosphere by shock accelerated electrons.

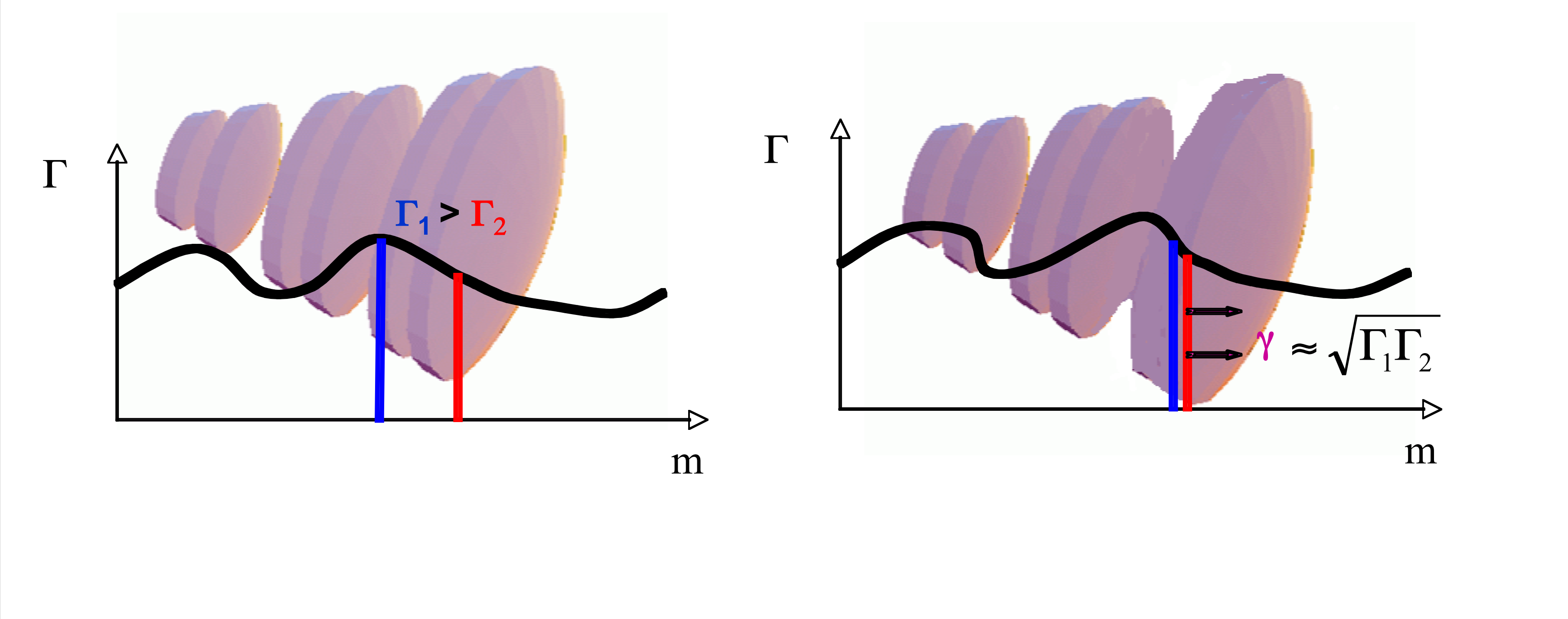

Modeling:

1. dynamics of internal shocks

2. radiative processes in the shocked medium

3. observed spectra and time profiles

Bosnjak, Daigne & Dubus 2009
Daigne, Bosnjak & Dubus 2011
Bosnjak & Daigne 2014
Daigne & Bosnjak 2024
Rudolph, Bosnjak, Palladino, Sadeh, Winter 2022
Rudolph, Petropoulou, Bosnjak, Winter 2023
Rudolph, Petropoulou, Winter, Bosnjak 2023

Internal shock model

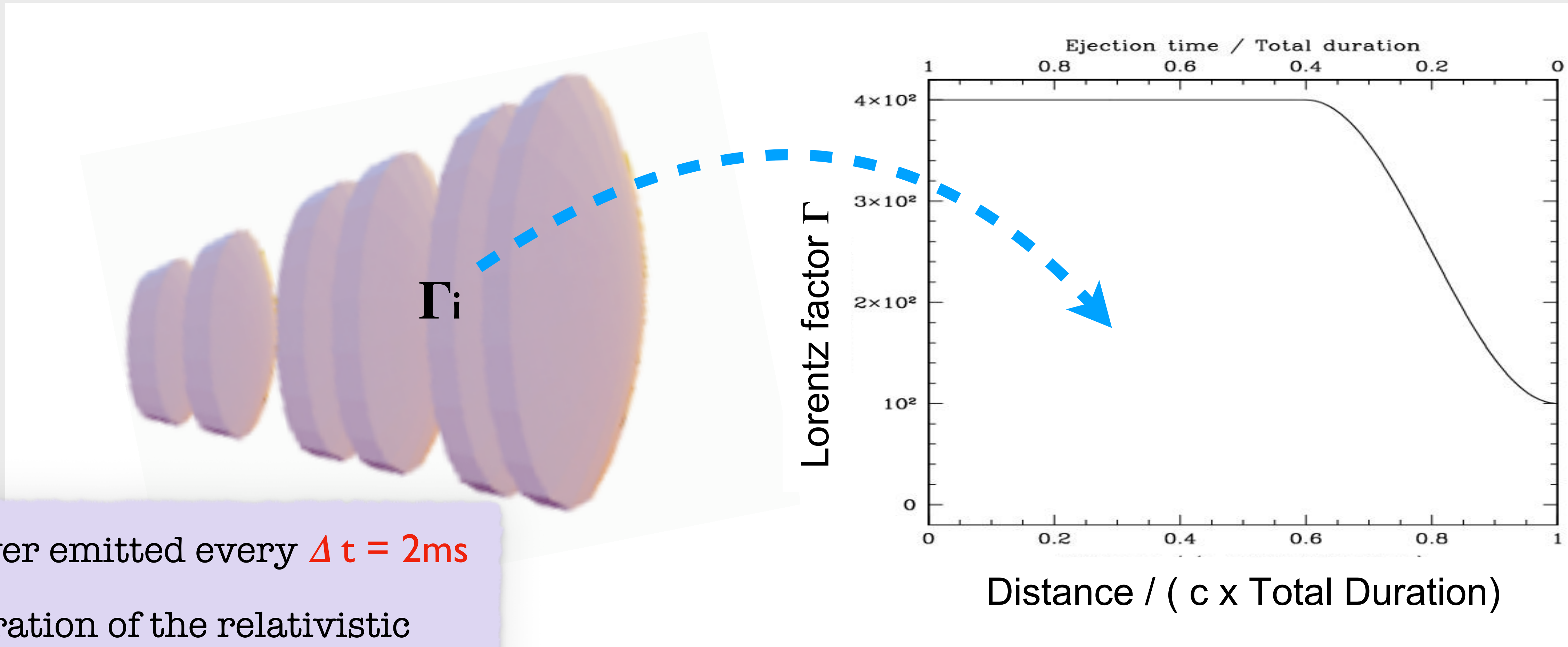

Layer emitted every $\Delta t = 2$ms

Duration of the relativistic ejection phase: $t_w \sim 2$ s

Number of shells: N = 1000

Layer mass: $M_i \sim 1 / \Gamma_i$

Shortest timescale of variability: t_{var}

$R_{IS,\,start} \sim \Gamma\ ct_{var} \sim 3 \times 10^{11}$ cm $(\Gamma/100)$ $(t_{var}/1\text{ ms})$

$R_{IS,\,end} \sim \Gamma\ ct_w \sim 3 \times 10^{15}$ cm $(\Gamma/100)$ $(t_w/10\text{ s})$

Dissipated energy: from 6% ($\Gamma_2 / \Gamma_1 = 2$) to 43 % ($\Gamma_2 / \Gamma_1 = 10$)

Internal shock model

Daigne & Mochkovitch 2000: the simplified approach for dynamics has been confirmed by comparison with a full hydrodynamical calculation

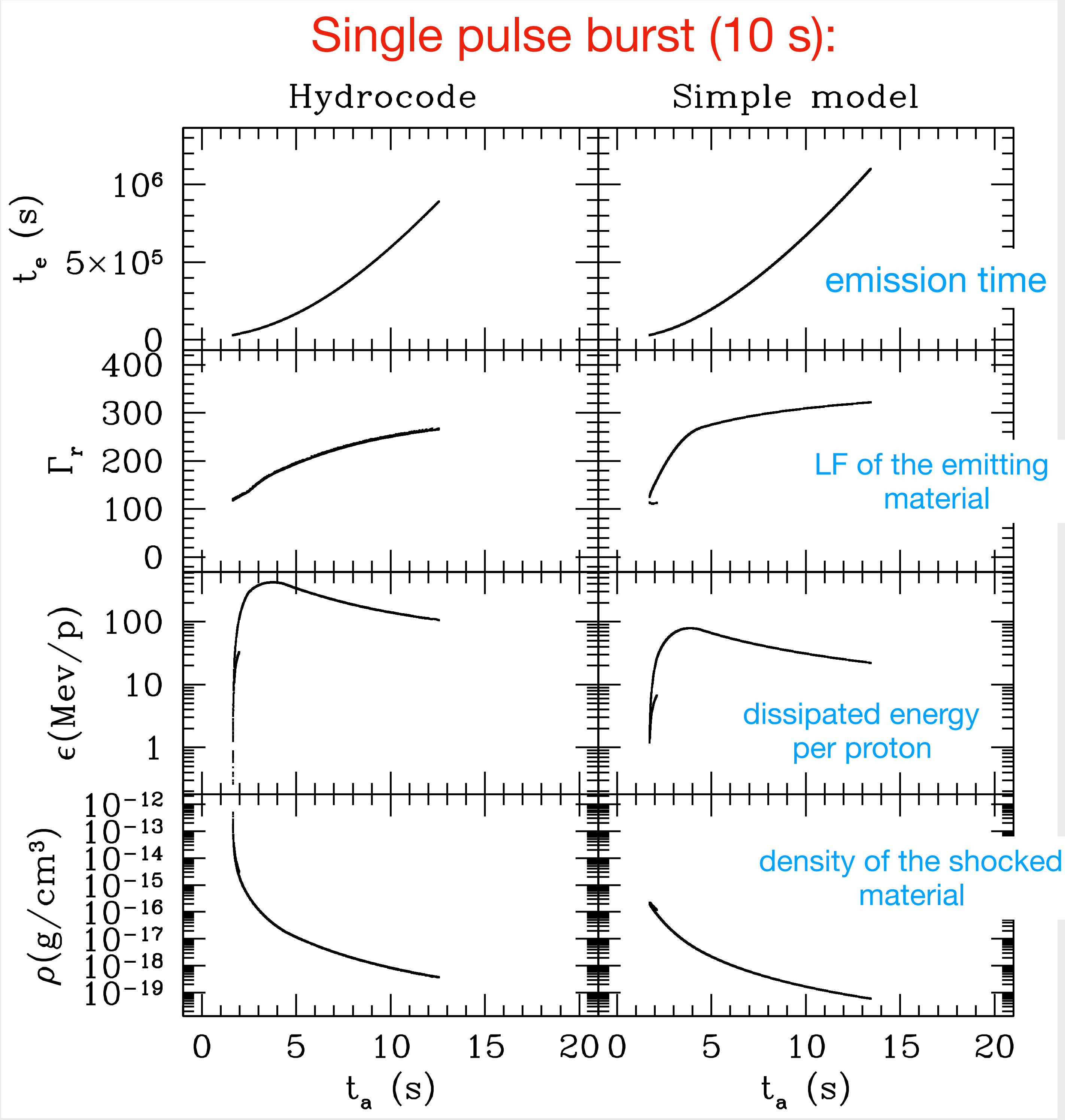

Internal shock model

Physical conditions in the shocked medium: Lorentz factor Γ^*, comoving density ρ^*, comoving specific energy density ε^*

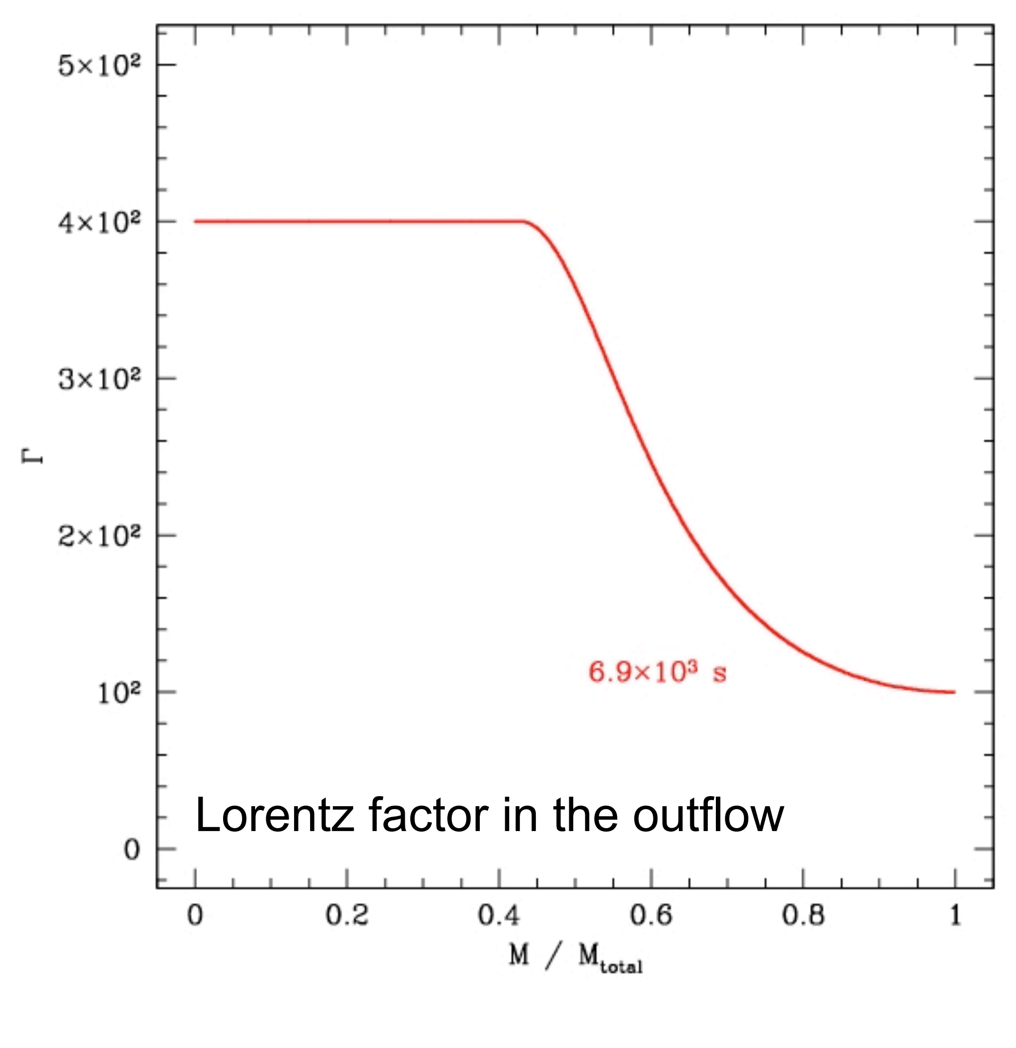

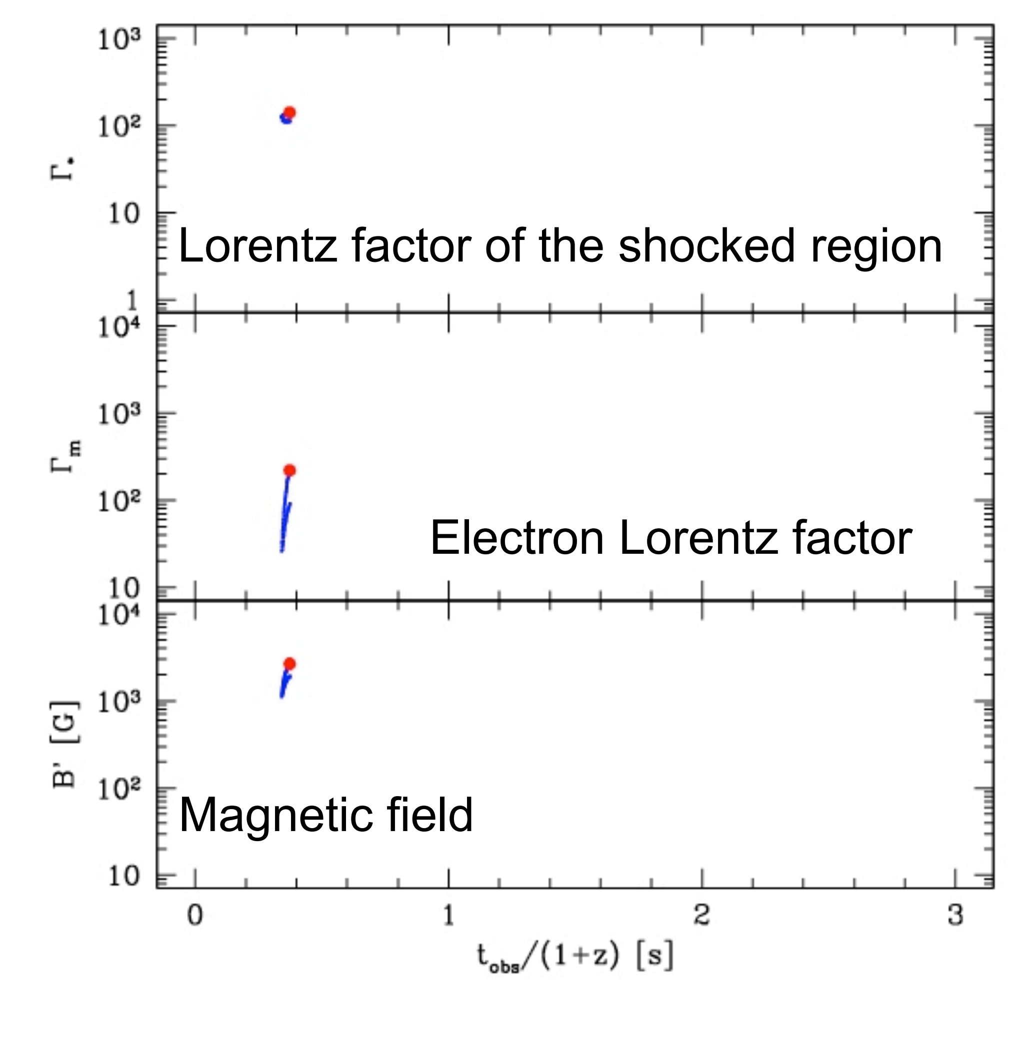

Dissipated energy is distributed between protons, electrons (fraction ε_e) and magnetic field (fraction ε_B)

Internal shock model

Physical conditions in the shocked medium: Lorentz factor Γ^*, comoving density ρ^*, comoving specific energy density ε^*

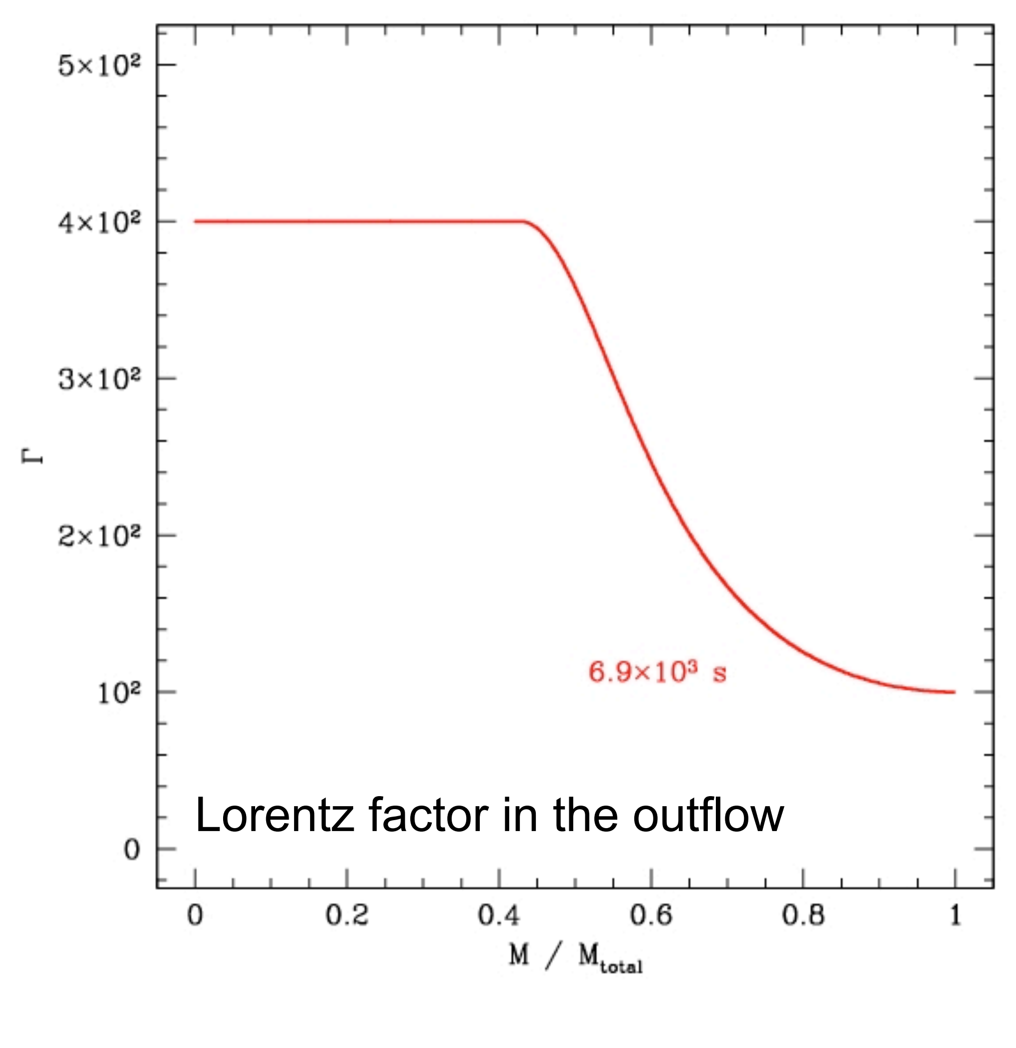

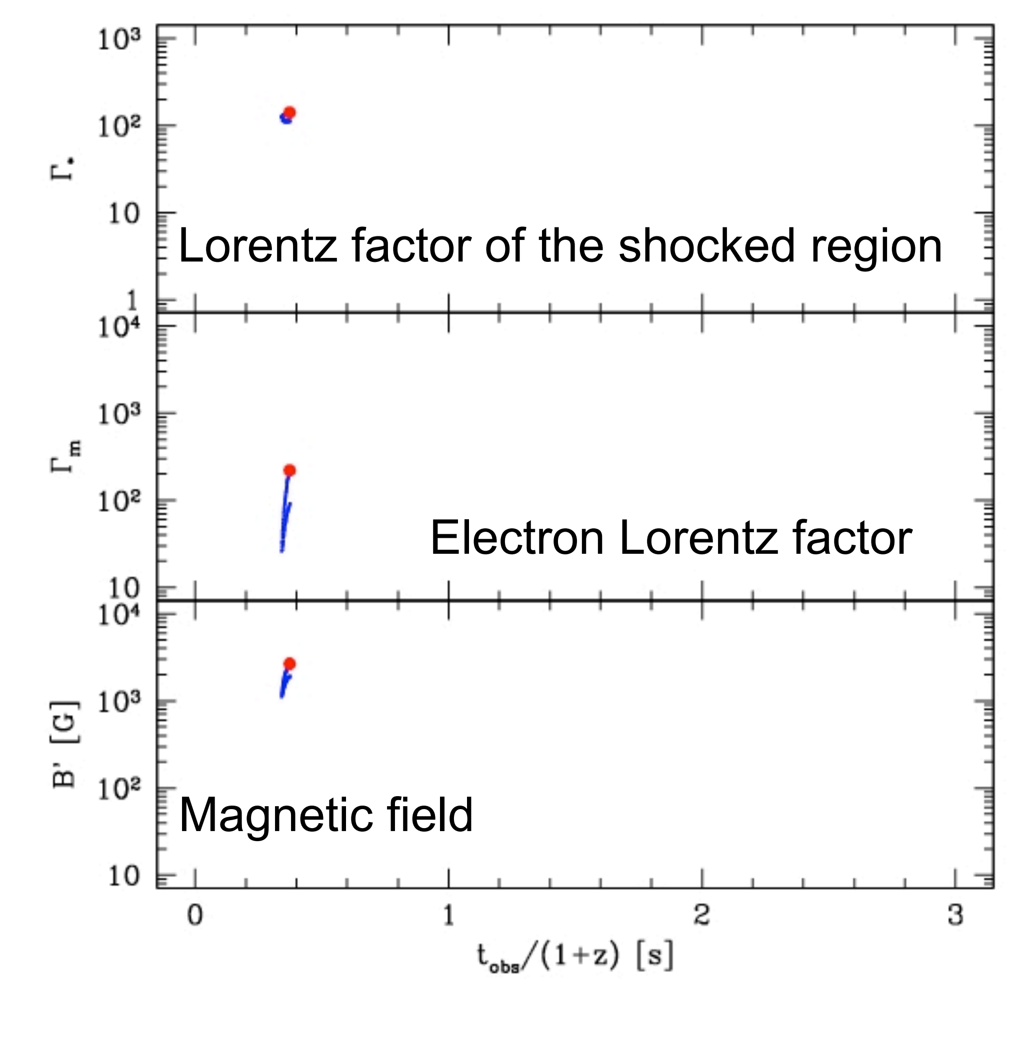

Dissipated energy is distributed between protons, electrons (fraction ε_e) and magnetic field (fraction ε_B)

Internal shock model

Physical conditions in the shocked medium: Lorentz factor Γ^*, comoving density ρ^*, comoving specific energy density ε^*

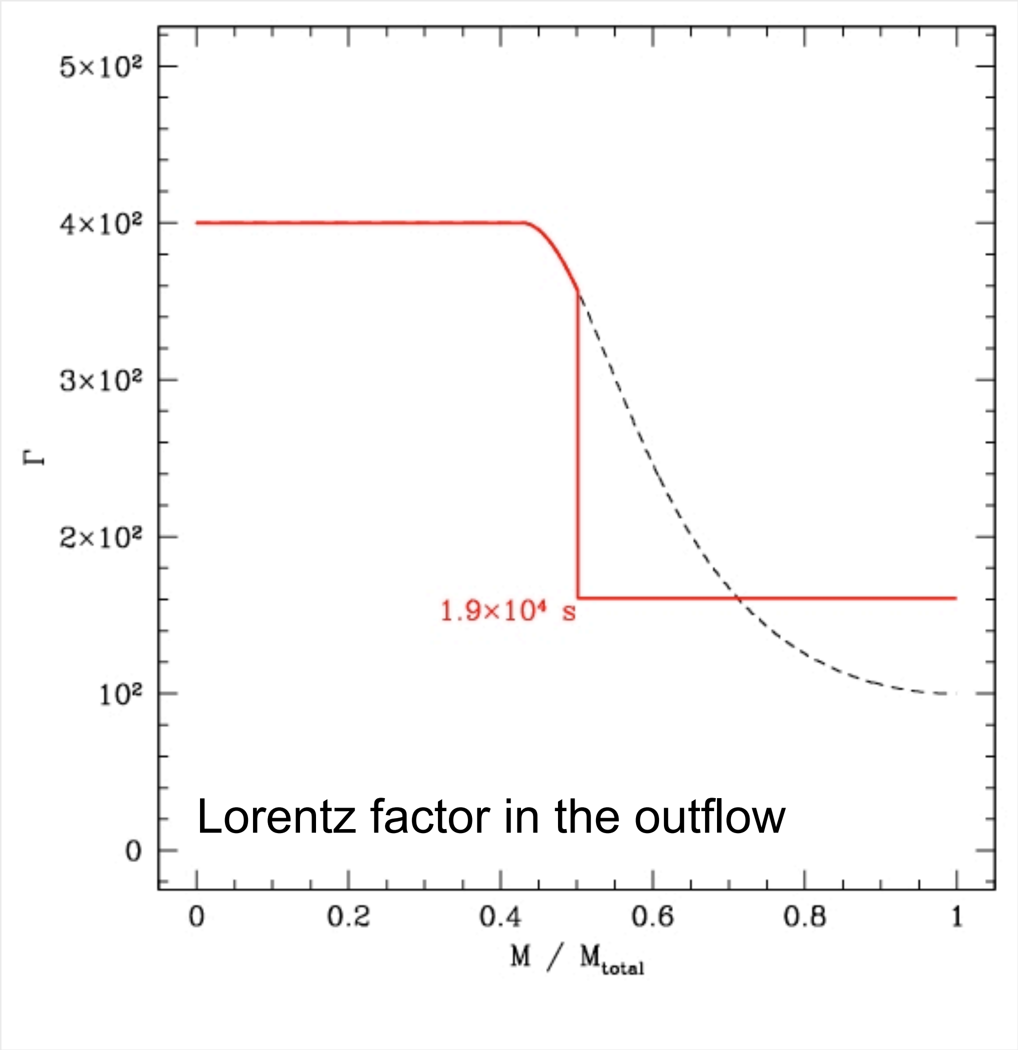

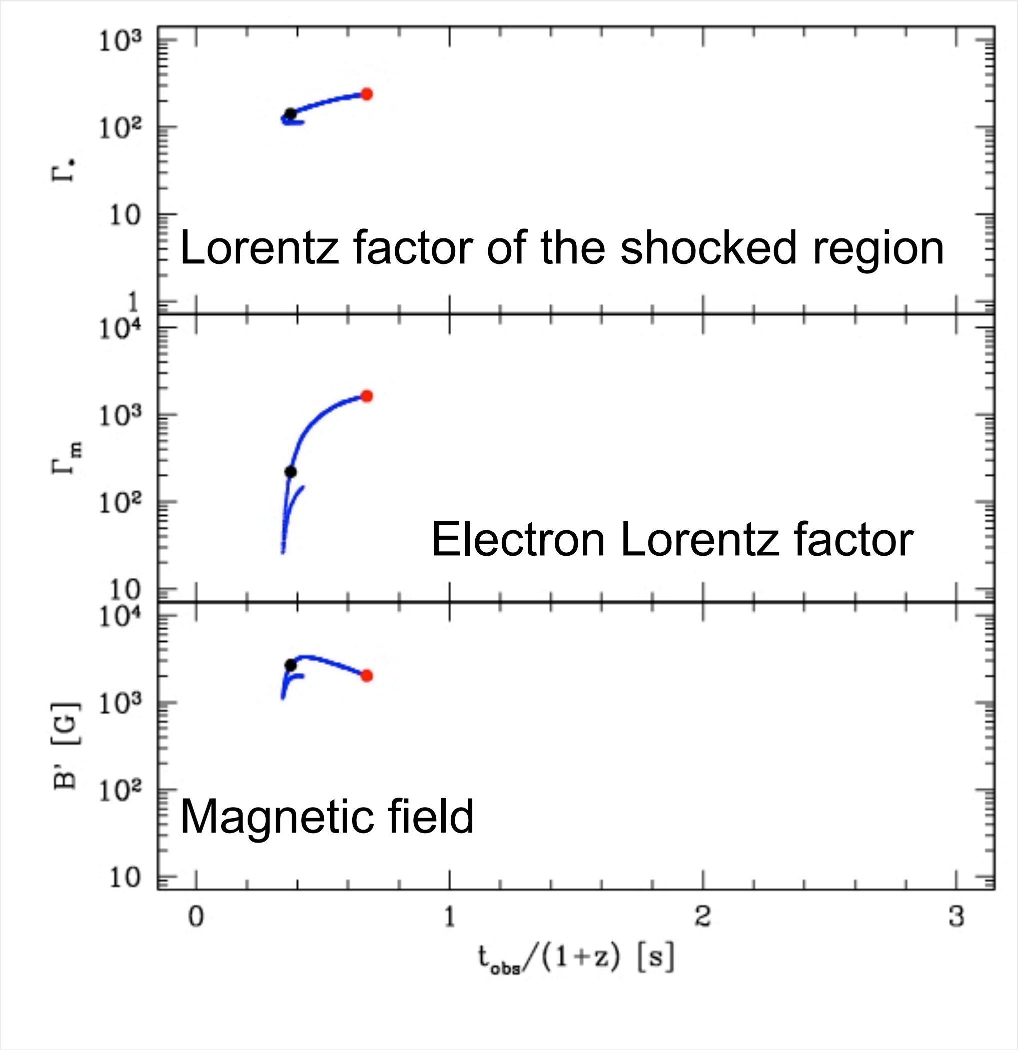

Dissipated energy is distributed between protons, electrons (fraction ε_e) and magnetic field (fraction ε_B)

Internal shock model

Physical conditions in the shocked medium: Lorentz factor Γ^*,
comoving density ρ^*, comoving specific energy density ε^*

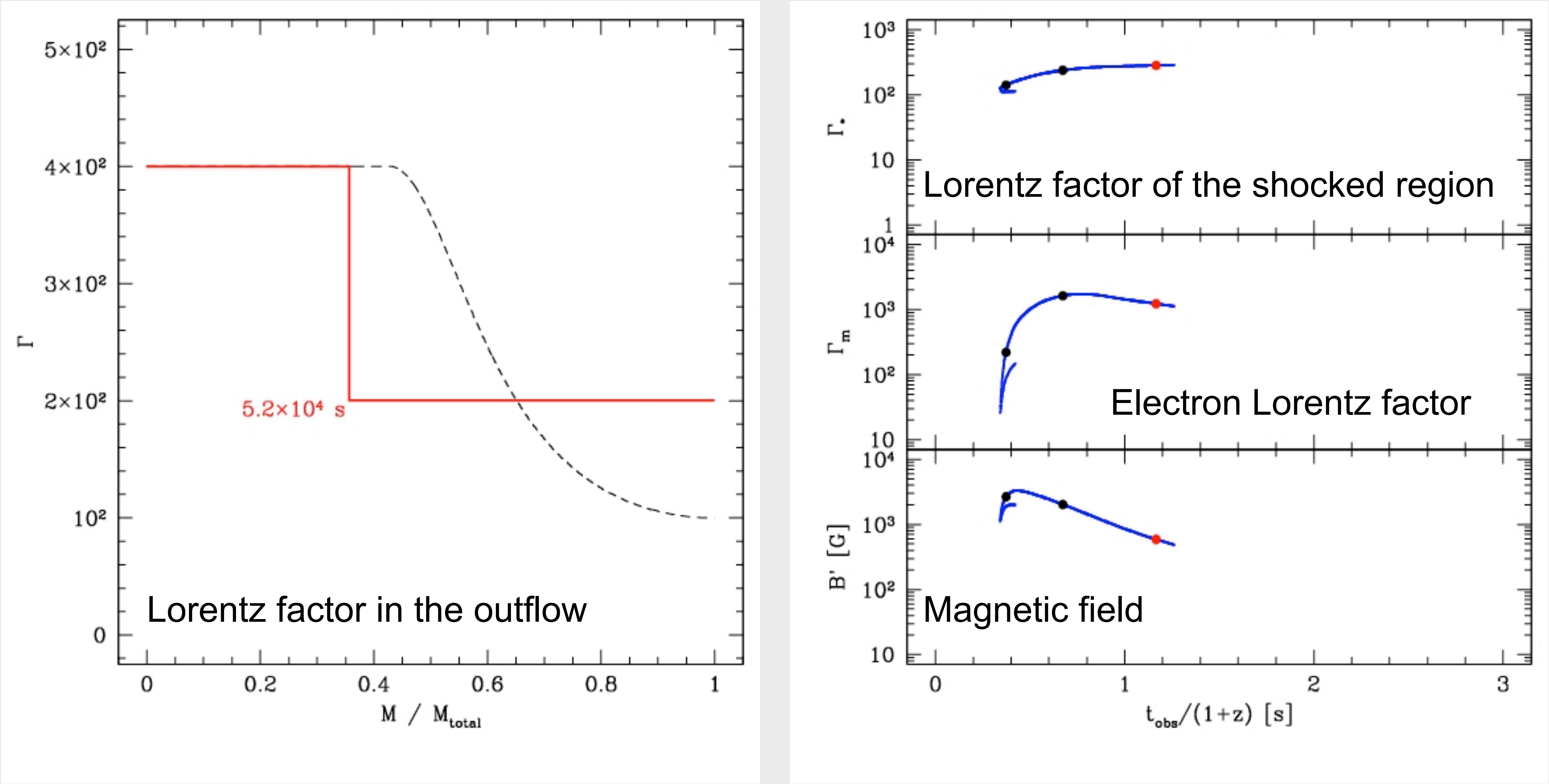

Dissipated energy is distributed between protons, electrons (fraction ε_e) and magnetic field (fraction ε_B)

Internal shock model

Physical conditions in the shocked medium: Lorentz factor $\mathbf{\Gamma^*}$, comoving density ρ^*, comoving specific energy density ε^*

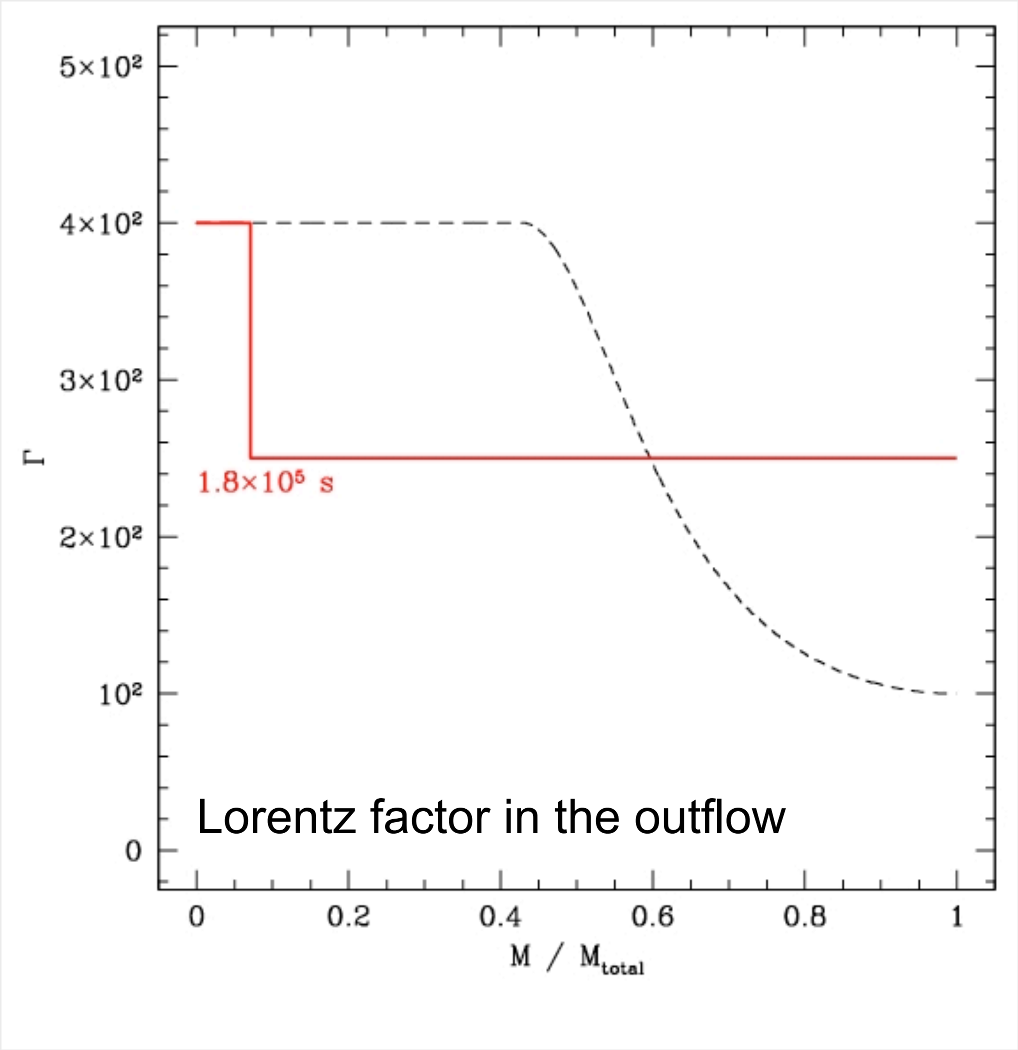

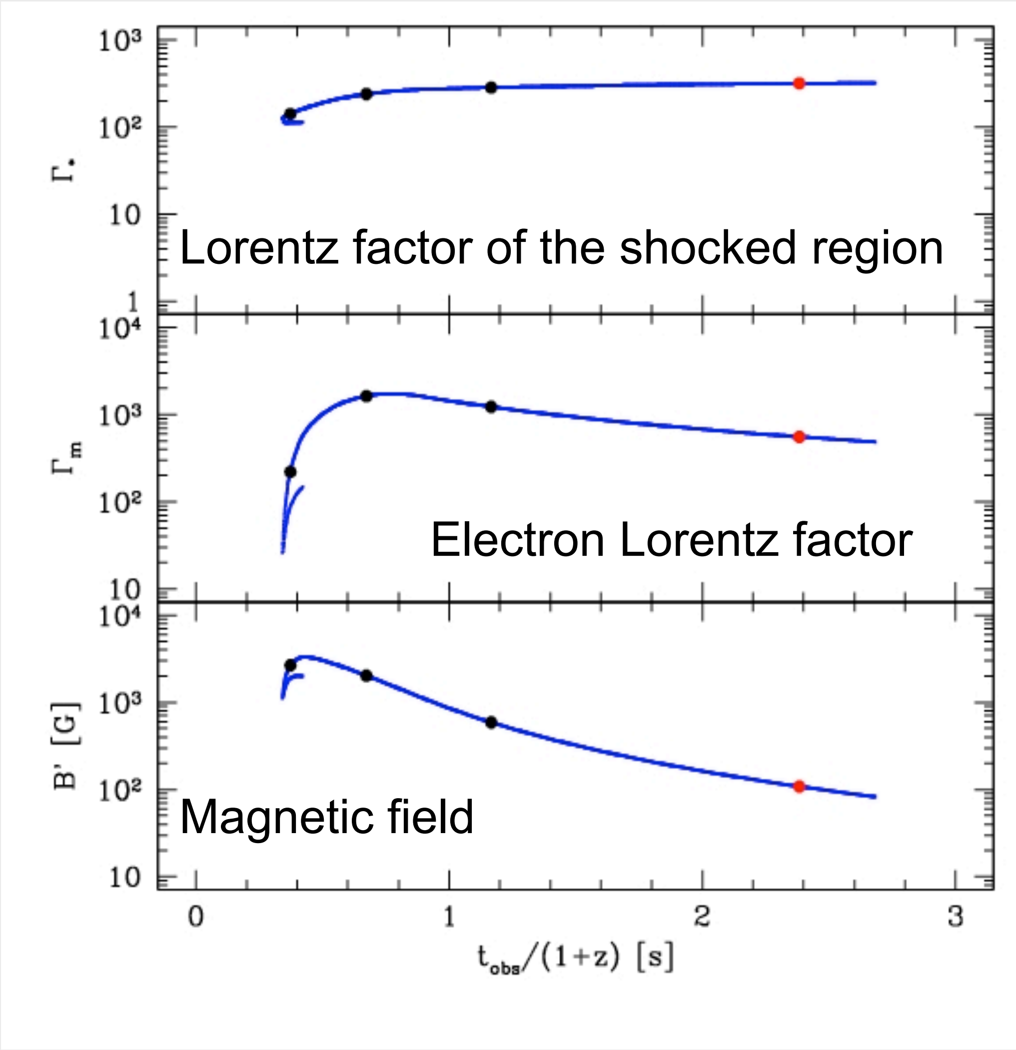

Dissipated energy is distributed between protons, electrons (fraction ε_e) and magnetic field (fraction ε_B)

Internal shock model

Physical conditions in the shocked medium: Lorentz factor Γ^*, comoving density ρ^*, comoving specific energy density ε^*

Relativistic electron density:

$$n'(\Gamma_e, t'=0) \propto \Gamma_e^{-p} \qquad \Gamma_e \geq \Gamma_m$$

$\zeta < 1$ of all electrons is accelerated

Bykov & Meszaros 1996
Spitkovsky 2008

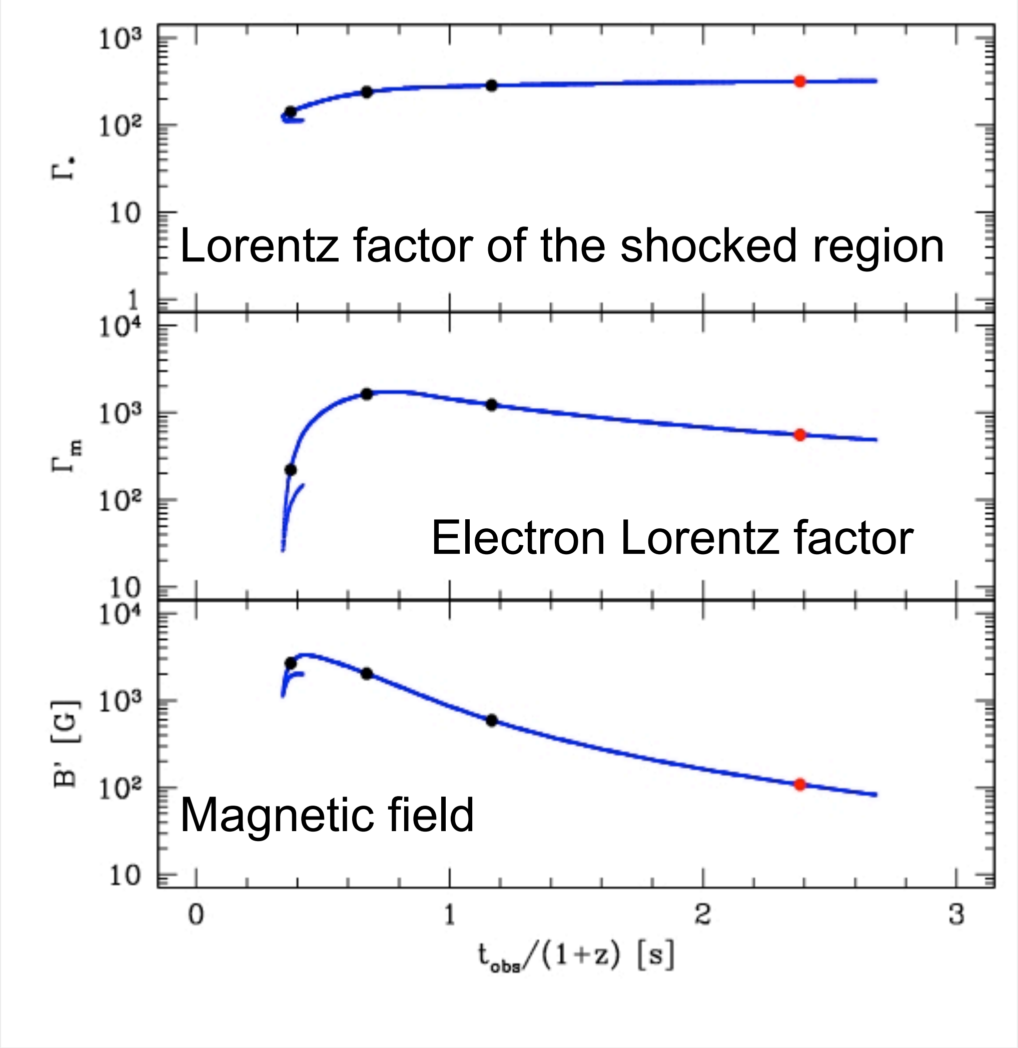

Dissipated energy is distributed between protons, electrons (fraction ε_e) and magnetic field (fraction ε_B)

Internal shock model

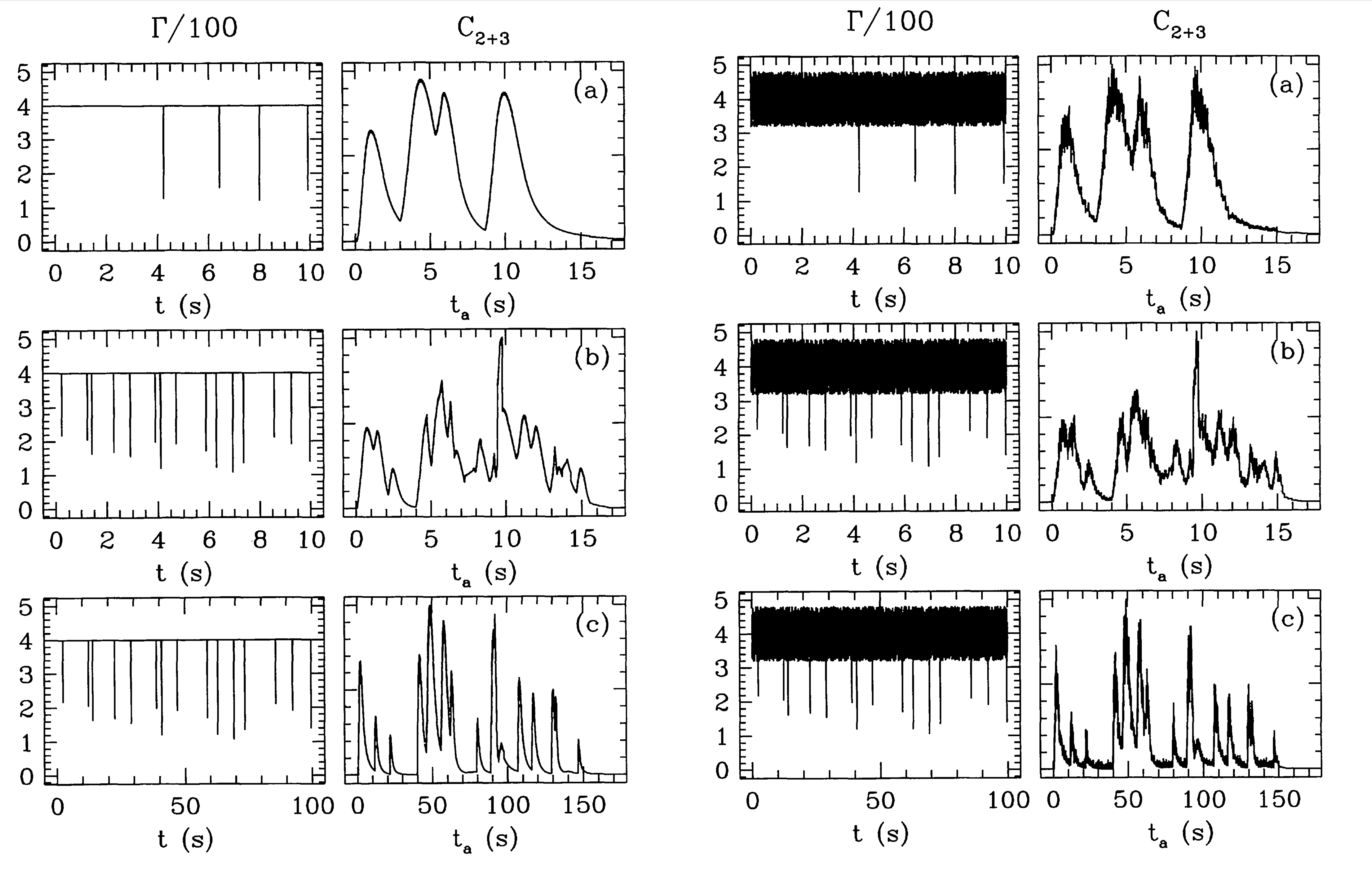

Daigne & Mochkovitch 1998

Internal shock model

SR-0S Strong (engine) ramp-up, no stochasticity | **SR-LS** Strong (engine) ramp-up, low stochasticity | **WR-MS** Weak (engine) ramp-up, medium stochasticity | **WR-HS** Weak (engine) ramp-up, high stochasticity

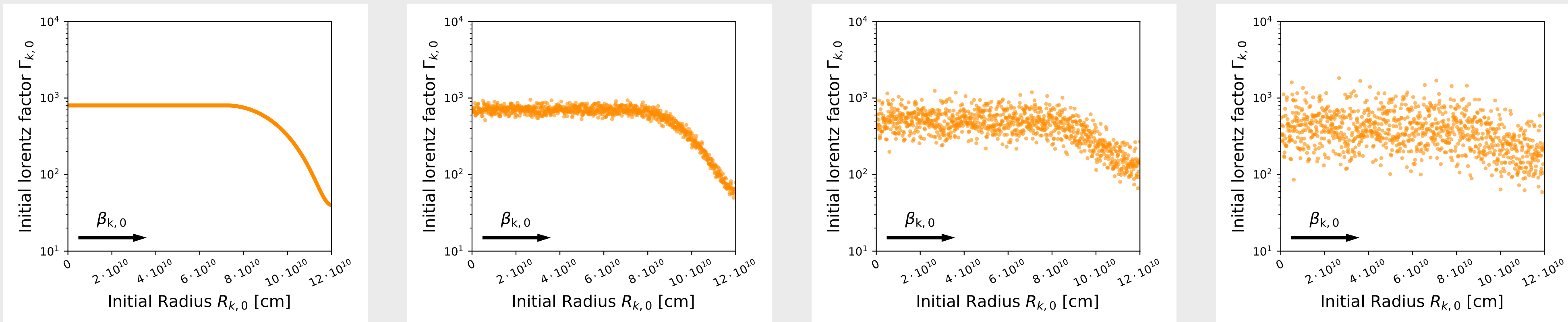

Γ_{min}: 40, Γ_{max}: 800, A_Γ: 0.0 | Γ_{min}: 60, Γ_{max}: 700, A_Γ: 0.1 | Γ_{min}: 120, Γ_{max}: 500, A_Γ: 0.3 | Γ_{min}: 160, Γ_{max}: 400, A_Γ: 0.5

NeuCosmA time-dependent radiation code for calculation of the cosmic ray spectra for each collision (Boncioli et al. 2017; Biehl et al. 2018) + for the extragalactic propagation employed the numerical code *PriNCe* and the distributed fitting network

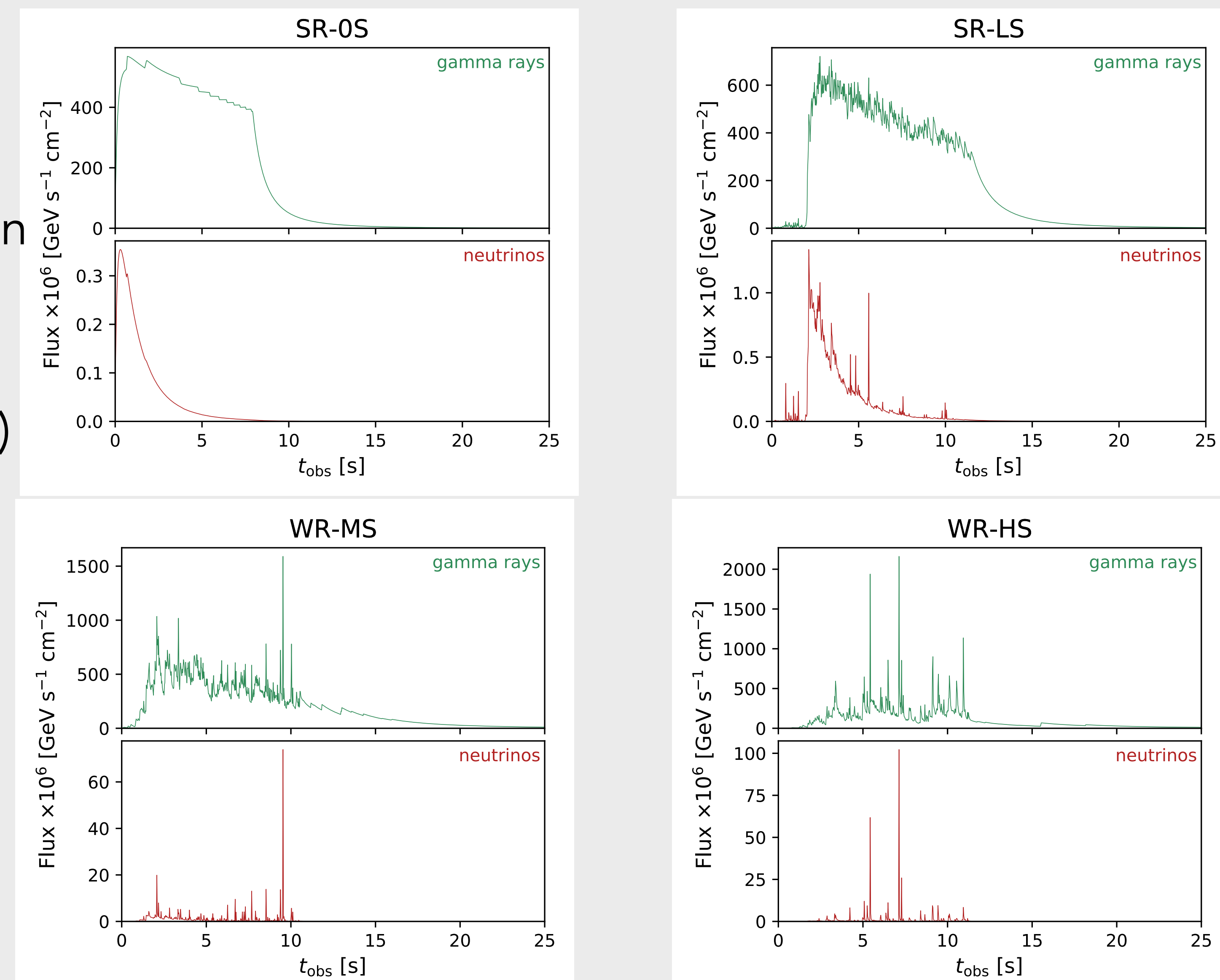

Heinze, Biehl, Fedynitch, Boncioli, Rudolph, Winter 2020

Internal shock model

Assumption: instantaneous shock acceleration

Adiabatic cooling timescale: $t'_{ex} = R / \Gamma^* c$ (comoving frame)
Radiative timescale: t'_{rad}

$t'_{rad} \ll t'_{ex}$ high radiative efficiency

Electron and photon distributions evolve strongly with time!

The present version of the code follows the time evolution of the electron density and the photon density including the following processes:

- adiabatic cooling (spherical expansion)
- synchrotron
- inverse Compton
- synchrotron self-absorption
- $\gamma\gamma$ annihilation

Not included:
* emission from secondary leptons
* IC in optically thick regime (Comptonisation)

ELECTRONS:

$$\frac{\partial n'}{\partial t'}(\Gamma'_e, t') = -\frac{\partial}{\partial \Gamma'_e}\left[\left(\frac{d\Gamma'_e}{dt'}\Big|_{syn+ic} + \frac{d\Gamma'_e}{dt'}\Big|_{ad}\right) n'(\Gamma'_e, t')\right]$$

PHOTONS:

$$\frac{\partial n'_\nu}{\partial t'} = \int n'(\Gamma'_e, t') P_{syn+ic}(\Gamma'_e) d\Gamma'_e - c n'_\nu \int n'(\Gamma'_e, t') \sigma_{abs}(\Gamma'_e, \nu) d\Gamma'_e - c n'_\nu \int_{\nu' > \frac{(m_e c^2)^2}{h^2 \nu}} n'_{\nu'}(t') \sigma_{\gamma\gamma}(\nu, \nu') d\nu'$$

Radiative processes

Radiation: the time evolution of electrons and photons in the comoving frame is solved (time-dependent radiative code)

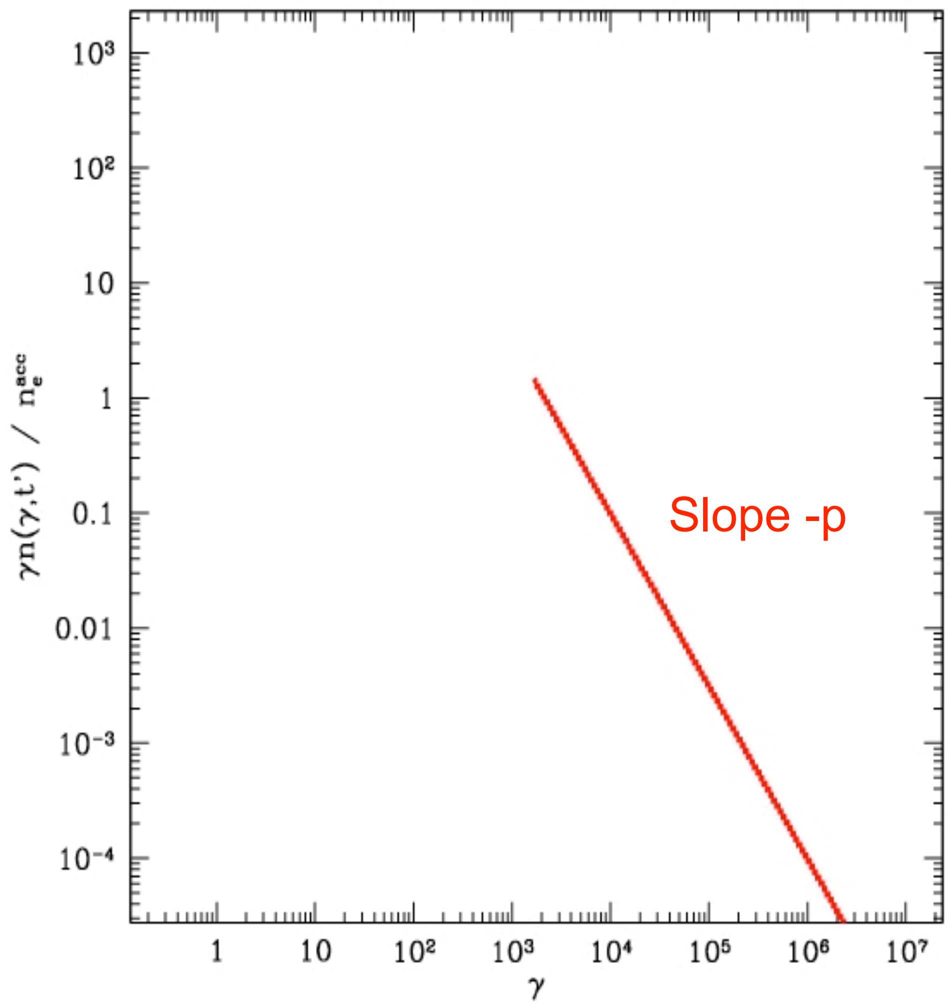

Electron distribution

Radiative processes

Radiation: the time evolution of electrons and photons in the comoving frame is solved (time-dependent radiative code)

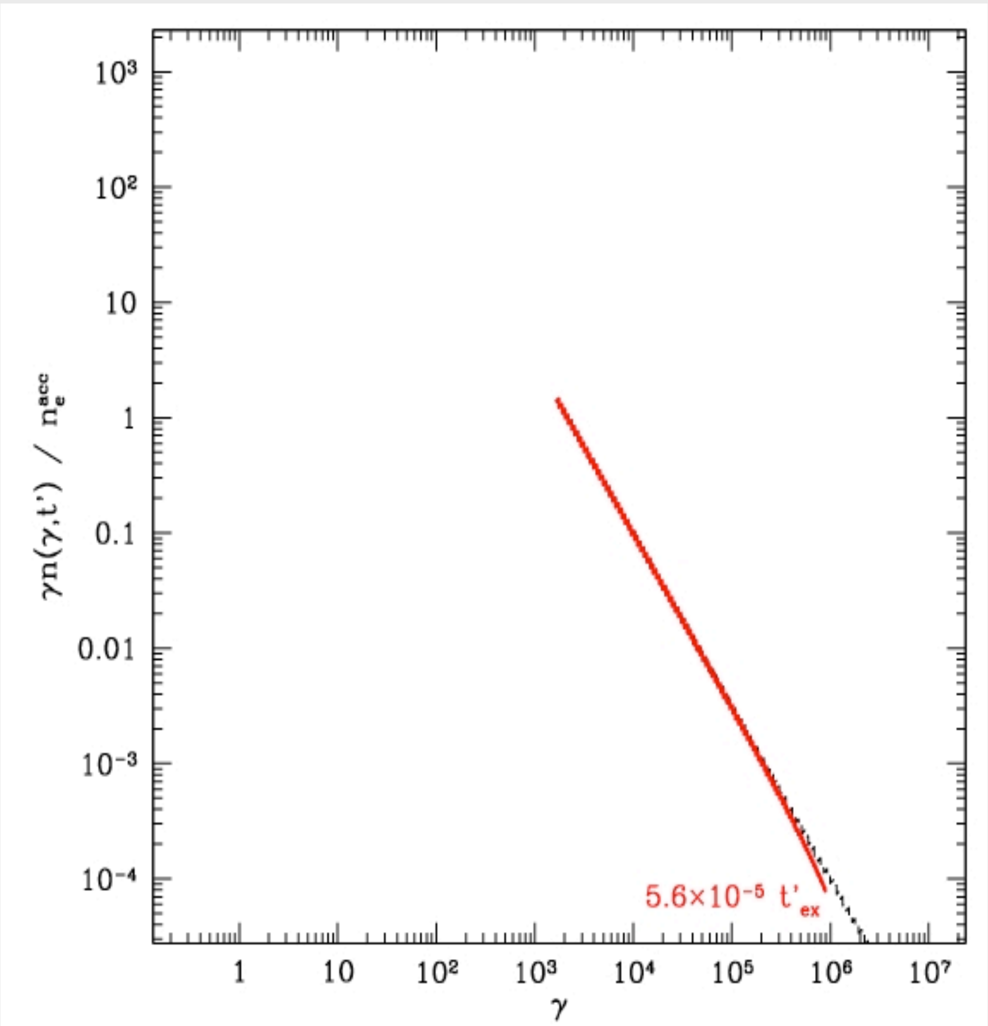

Electron distribution

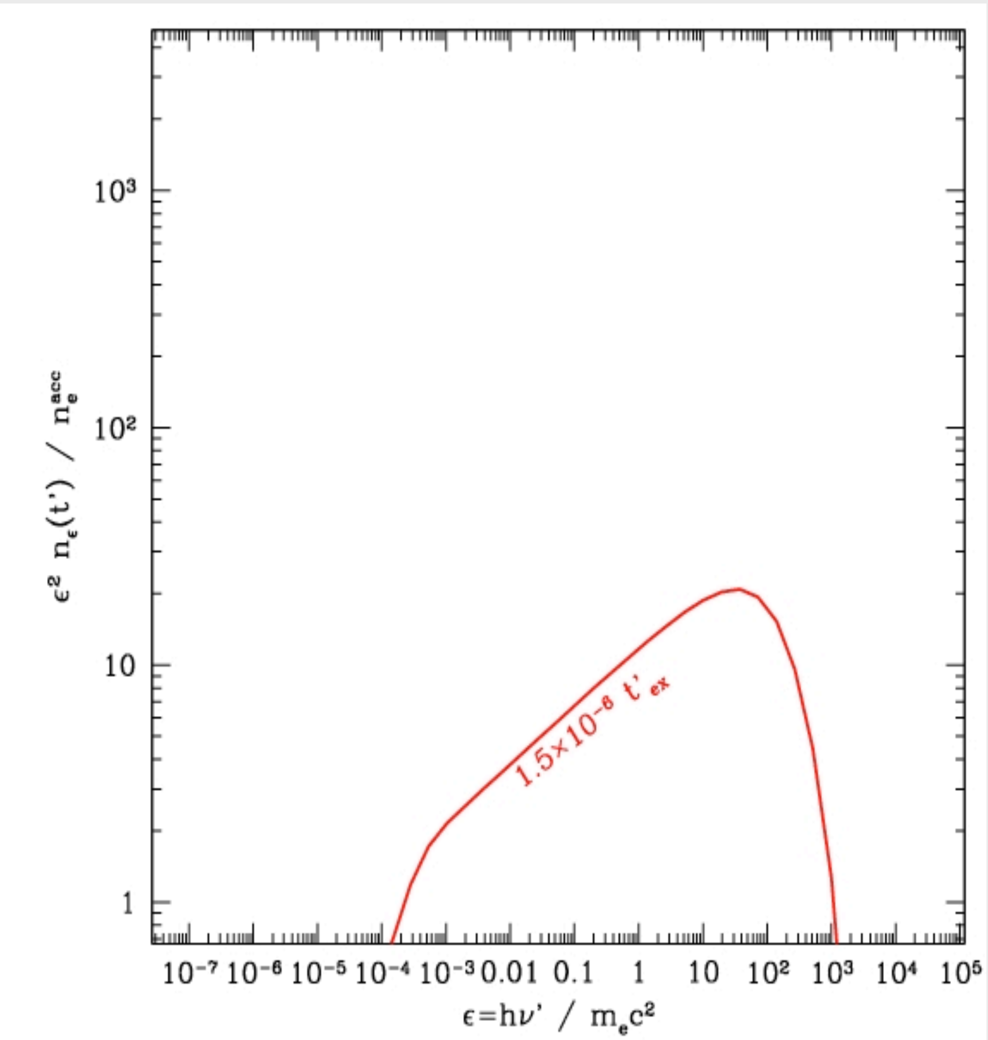

Photon spectrum

Radiative processes

Radiation: the time evolution of electrons and photons in the comoving frame is solved (time-dependent radiative code)

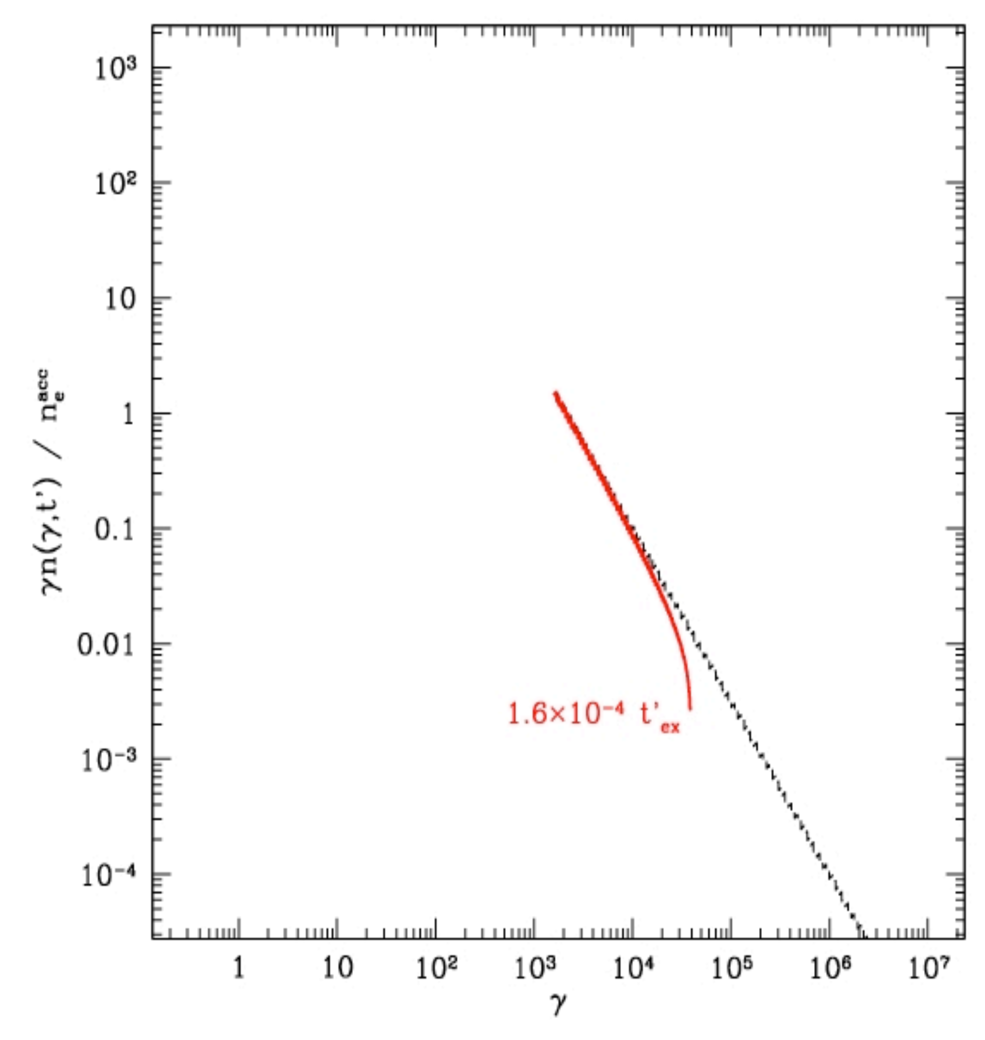

Electron distribution

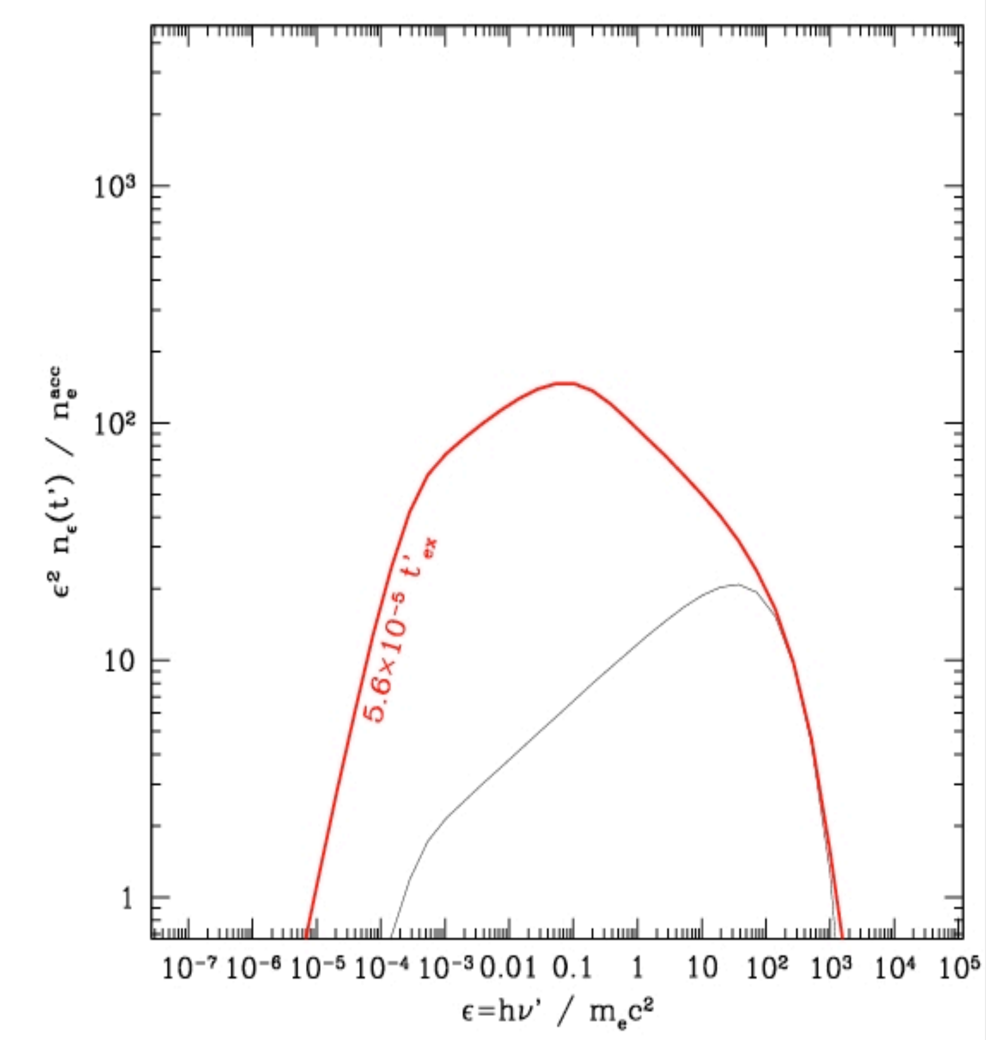

Photon spectrum

Radiative processes

Radiation: the time evolution of electrons and photons in the comoving frame is solved (time-dependent radiative code)

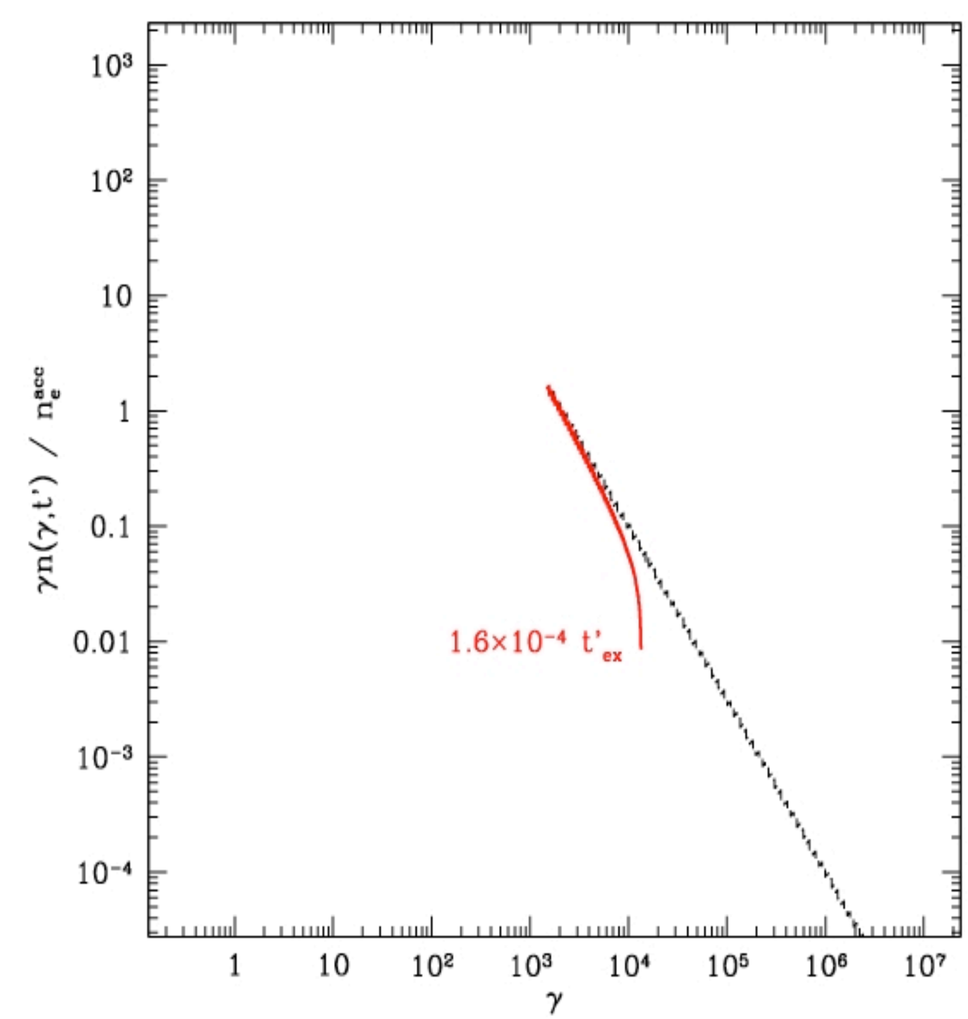

Electron distribution

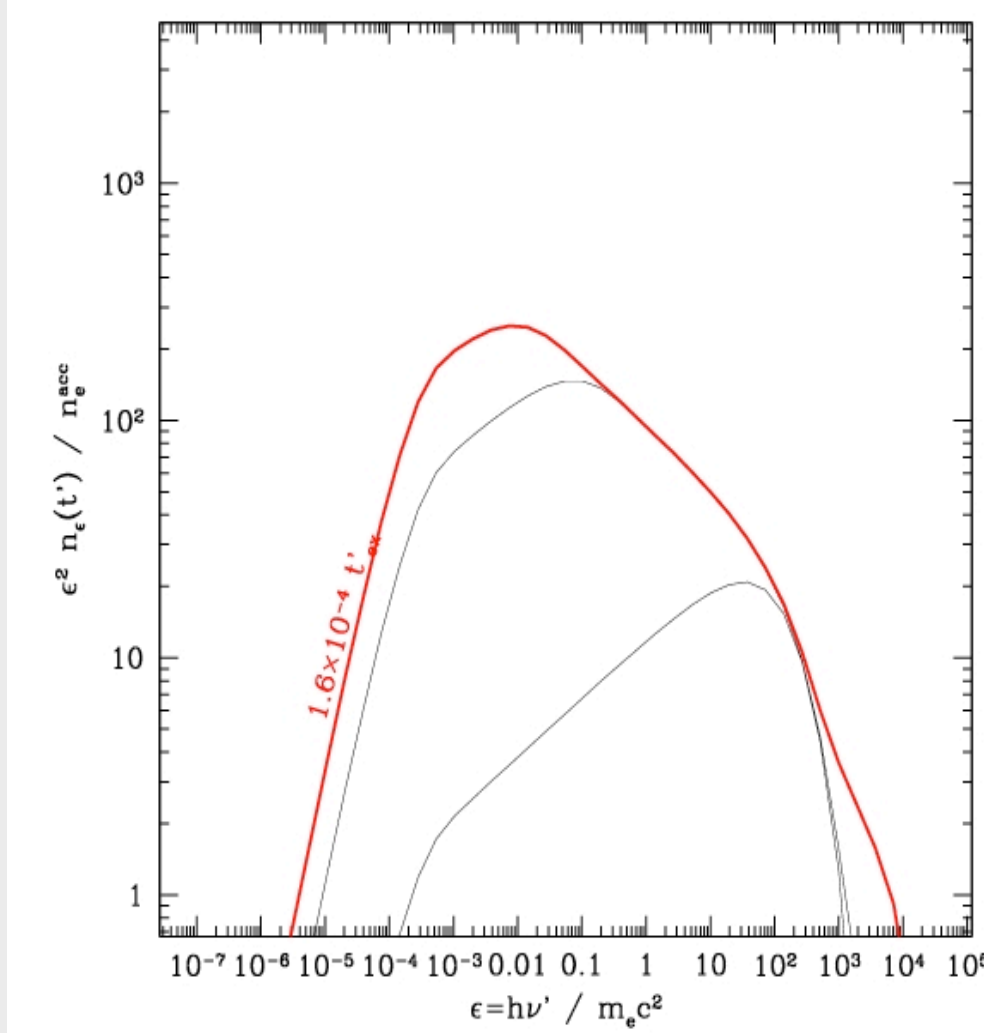

Photon spectrum

Radiative processes

Radiation: the time evolution of electrons and photons in the comoving frame is solved (time-dependent radiative code)

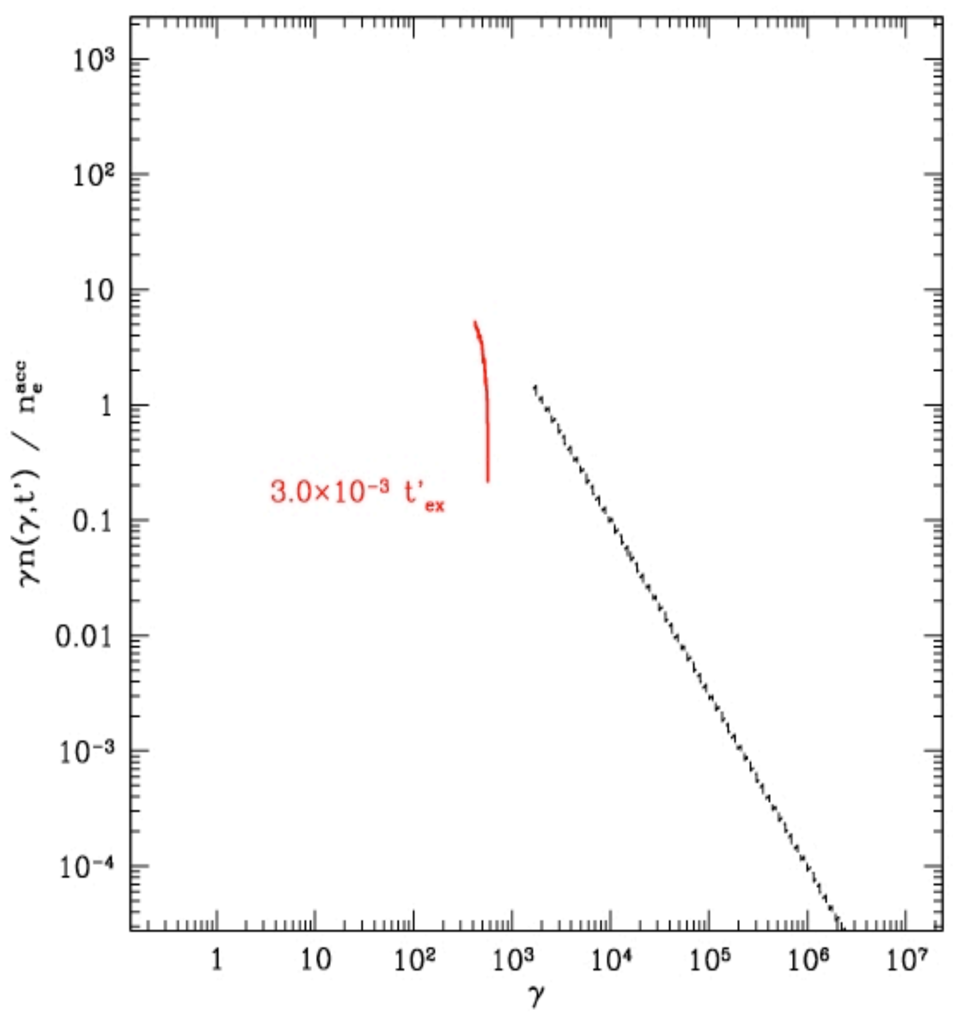

Electron distribution

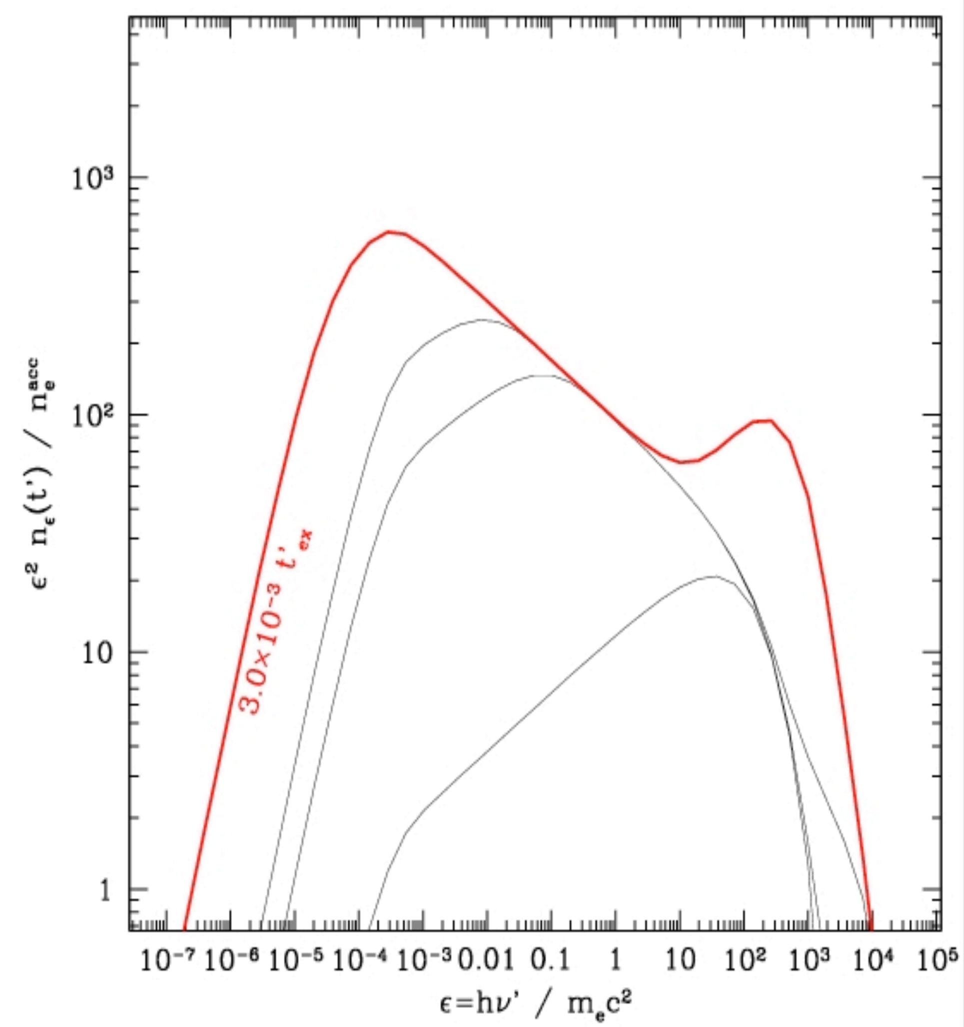

Photon spectrum

Radiative processes

Radiation: the time evolution of electrons and photons in the comoving frame is solved (time-dependent radiative code)

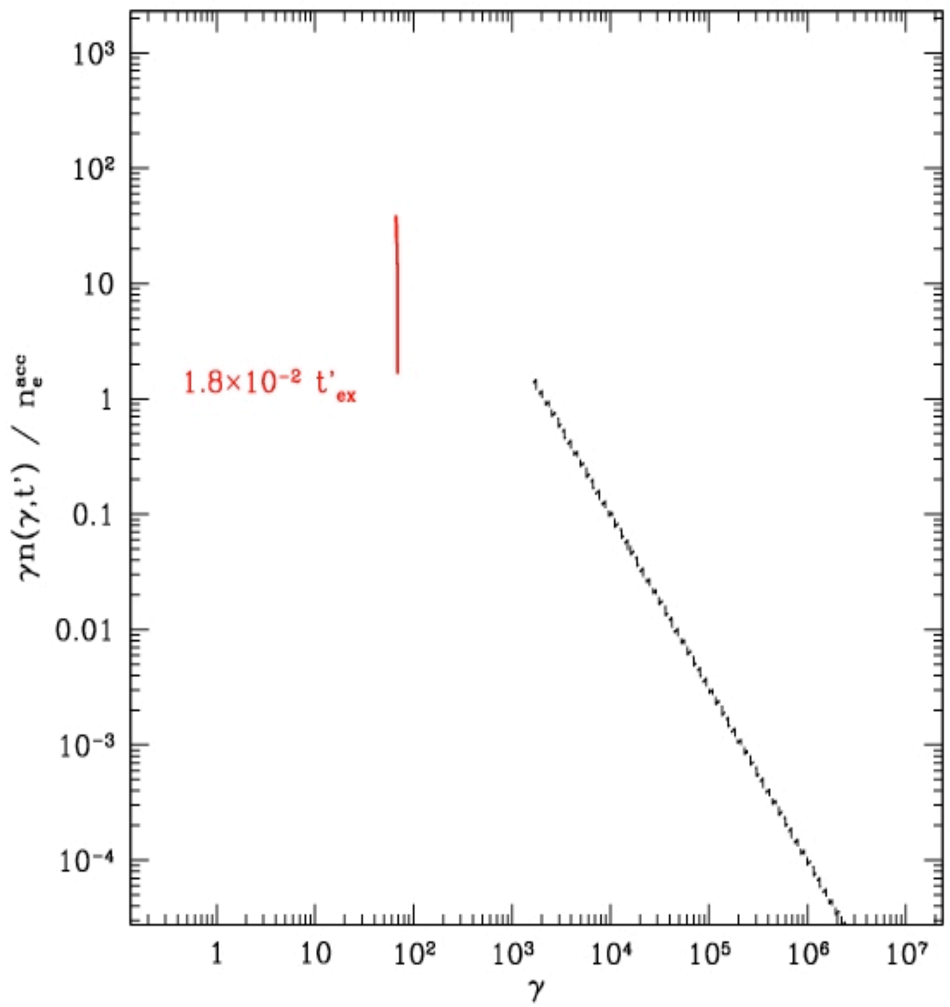

Electron distribution

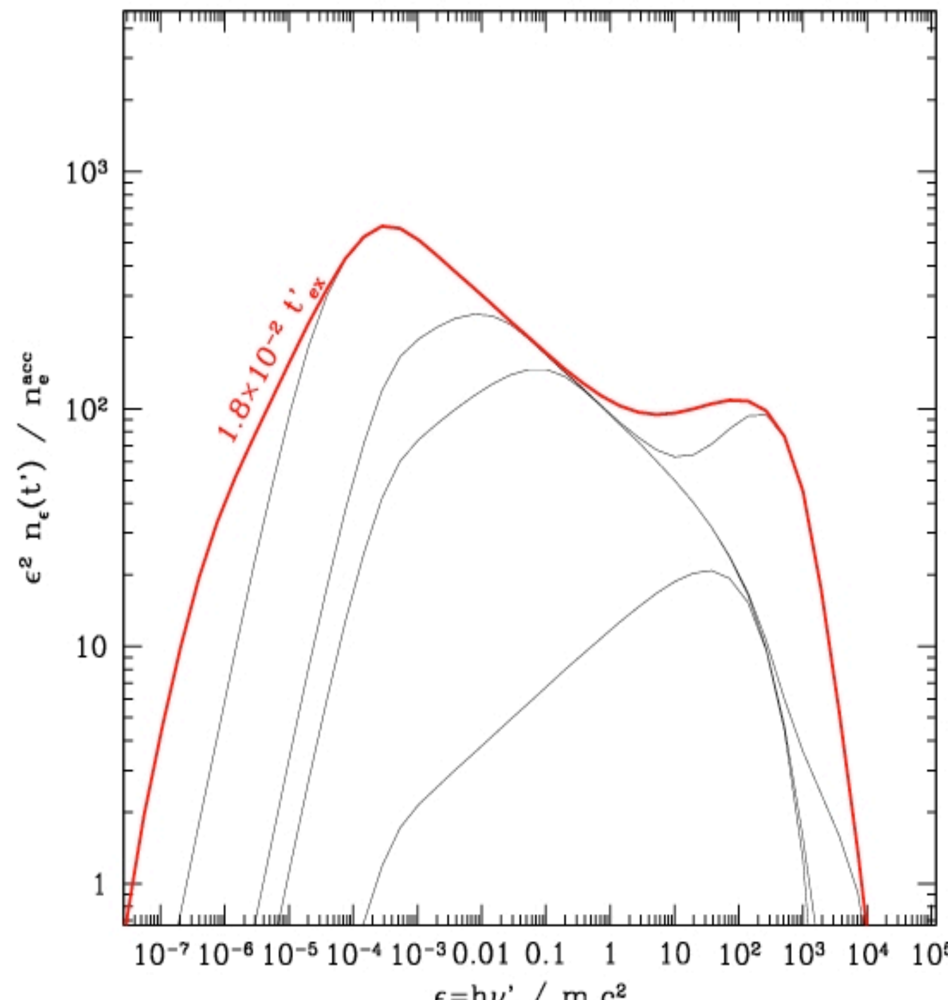

Photon spectrum

Radiative processes

Radiation: the time evolution of electrons and photons in the comoving frame is solved (time-dependent radiative code)

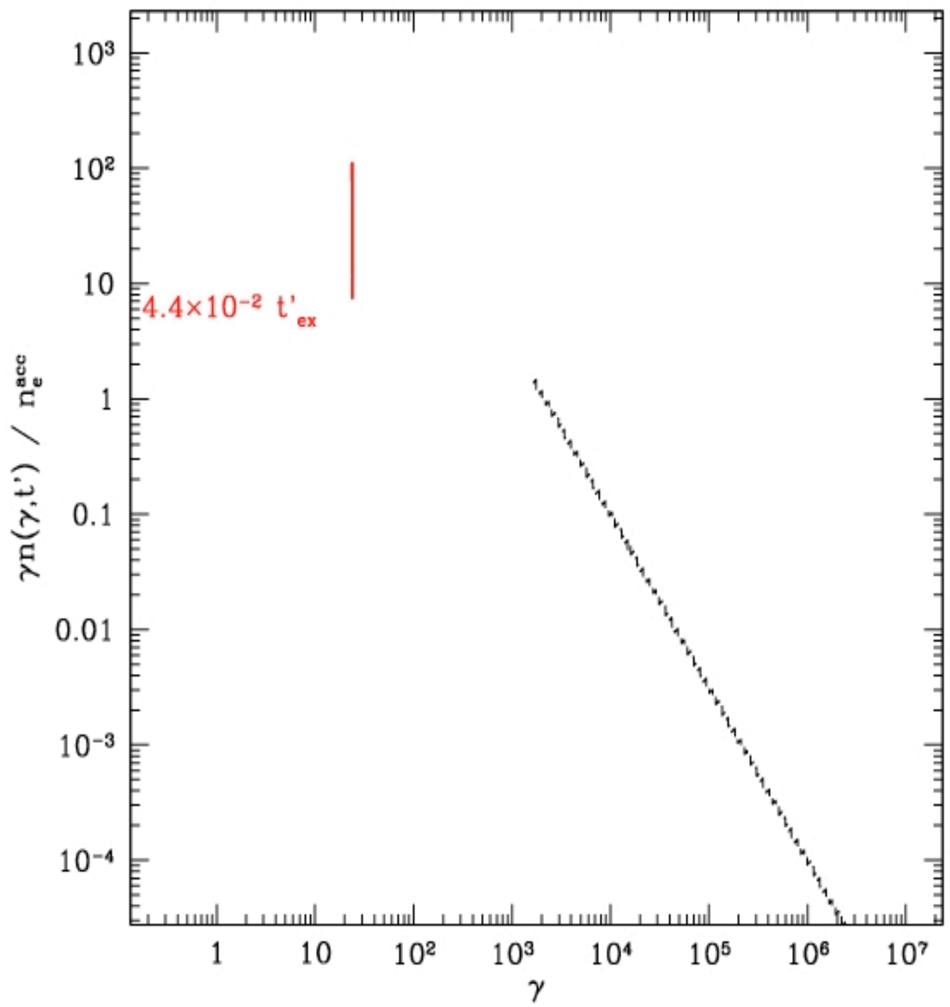

Electron distribution

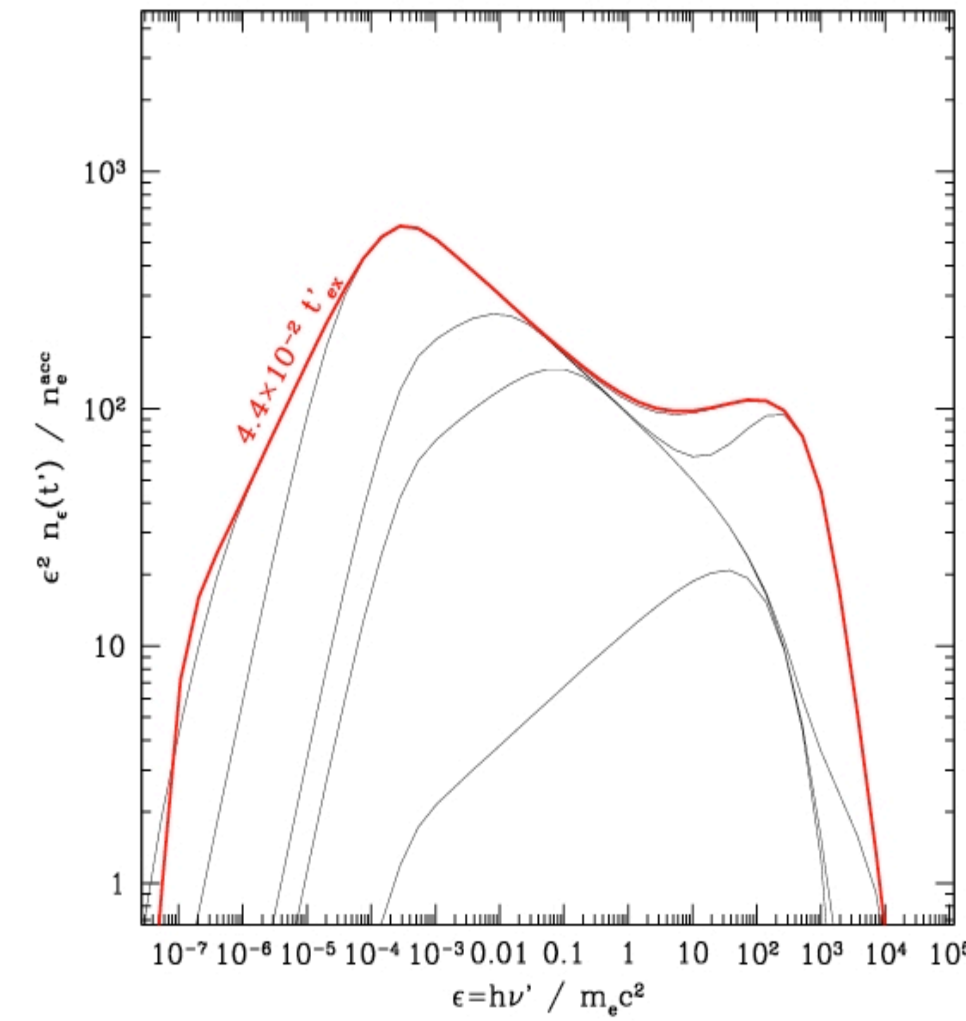

Photon spectrum

Radiative processes

Radiation: the time evolution of electrons and photons in the comoving frame is solved (time-dependent radiative code)

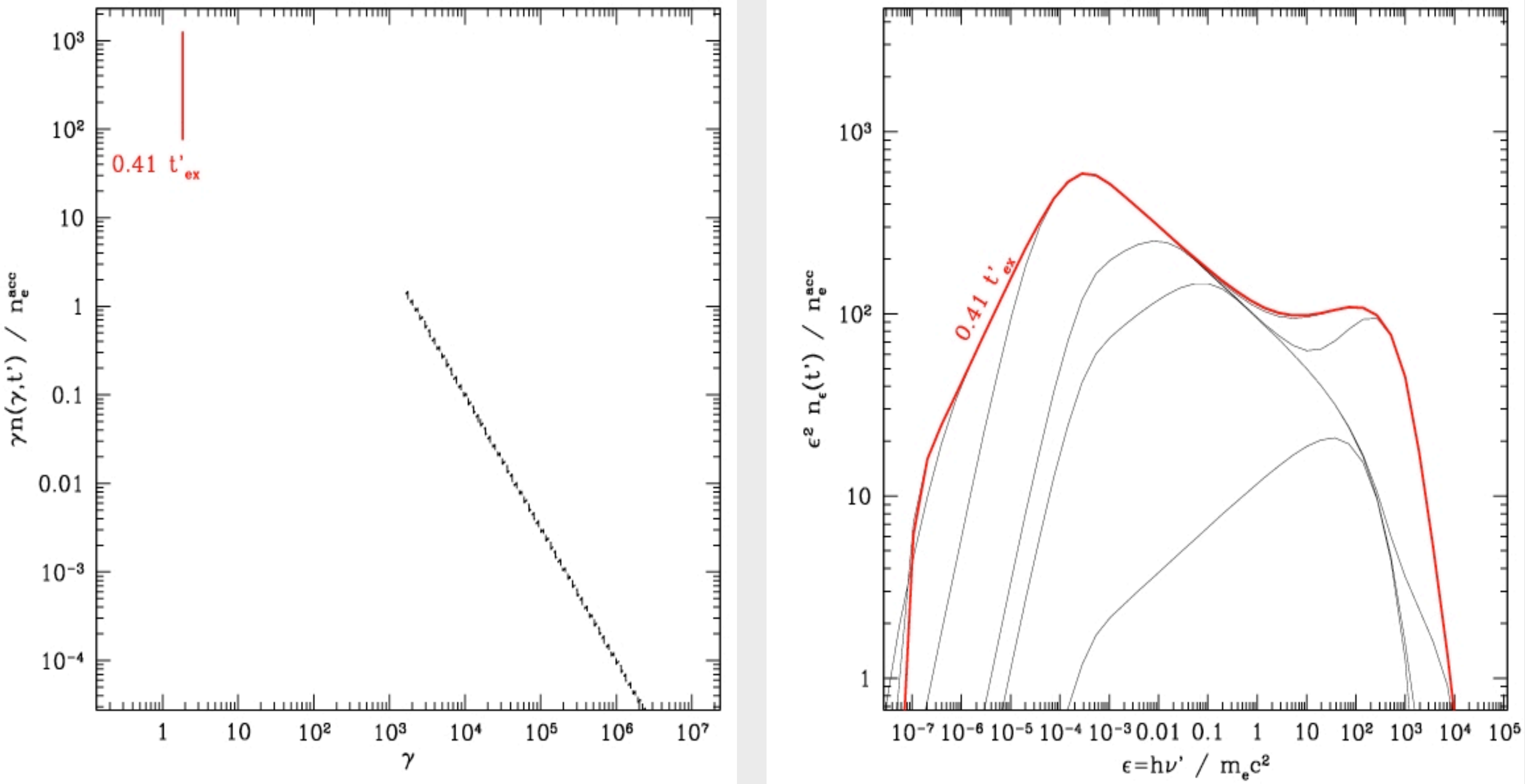

Electron distribution

Photon spectrum

Internal shock model

Radiation: the time evolution of electrons and photons in the comoving frame is solved (time-dependent radiative code)

Comptonization parameter
$Y = L_{ic} / L_{syn}$

IC dominant:
low frequency synchrotron peak
Thomson regime

Synchrotron dominant:
high frequency synchrotron peak
Klein-Nishina regime

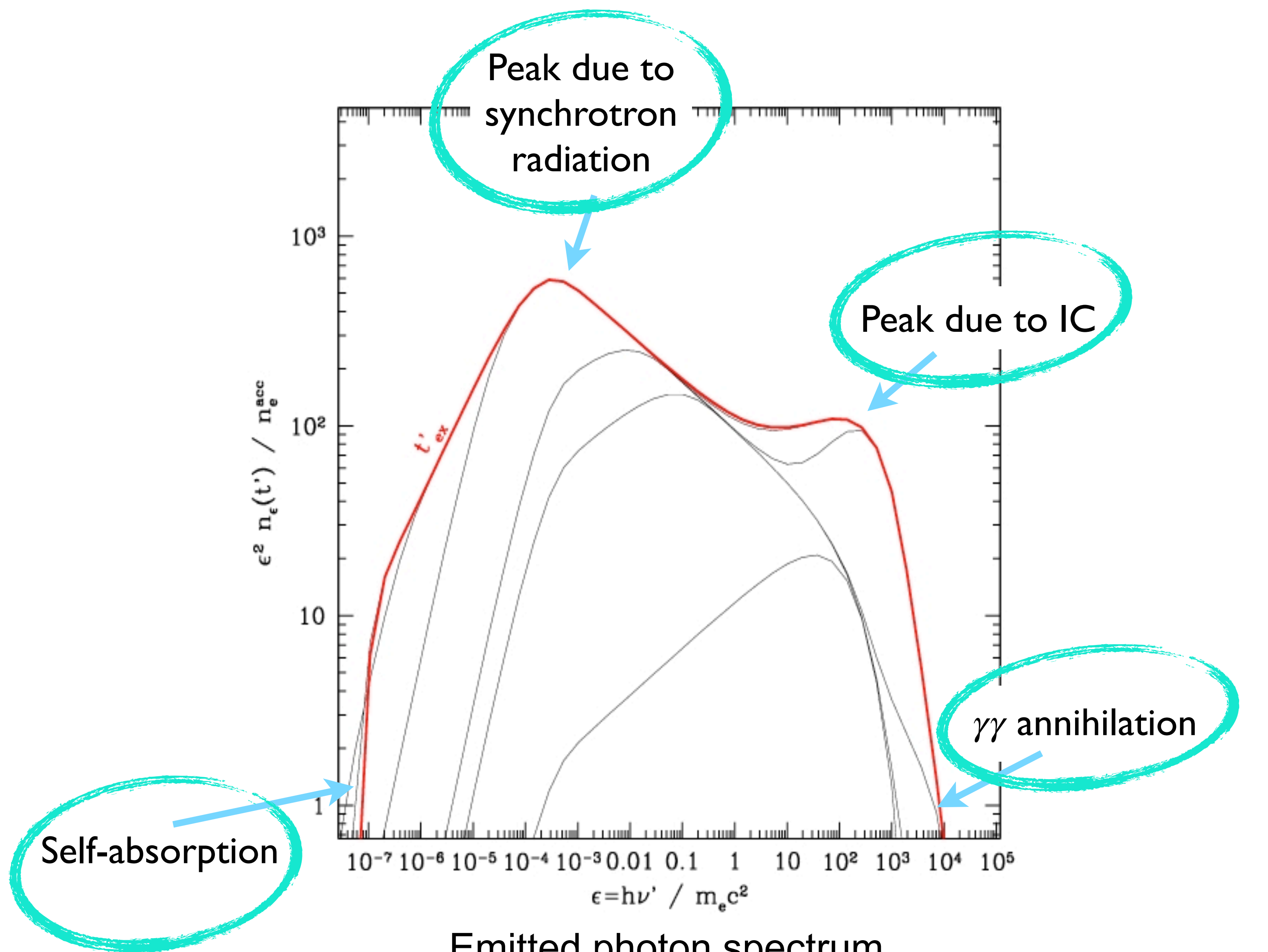

Emitted photon spectrum

Internal shock model

Radiation: the time evolution of electrons and photons in the comoving frame is solved (time-dependent radiative code)

Comptonization parameter

$Y = L_{ic} / L_{syn}$

IC dominant:

low frequency synchrotron peak

Thomson regime

Synchrotron dominant:

high frequency synchrotron peak

Klein-Nishina regime

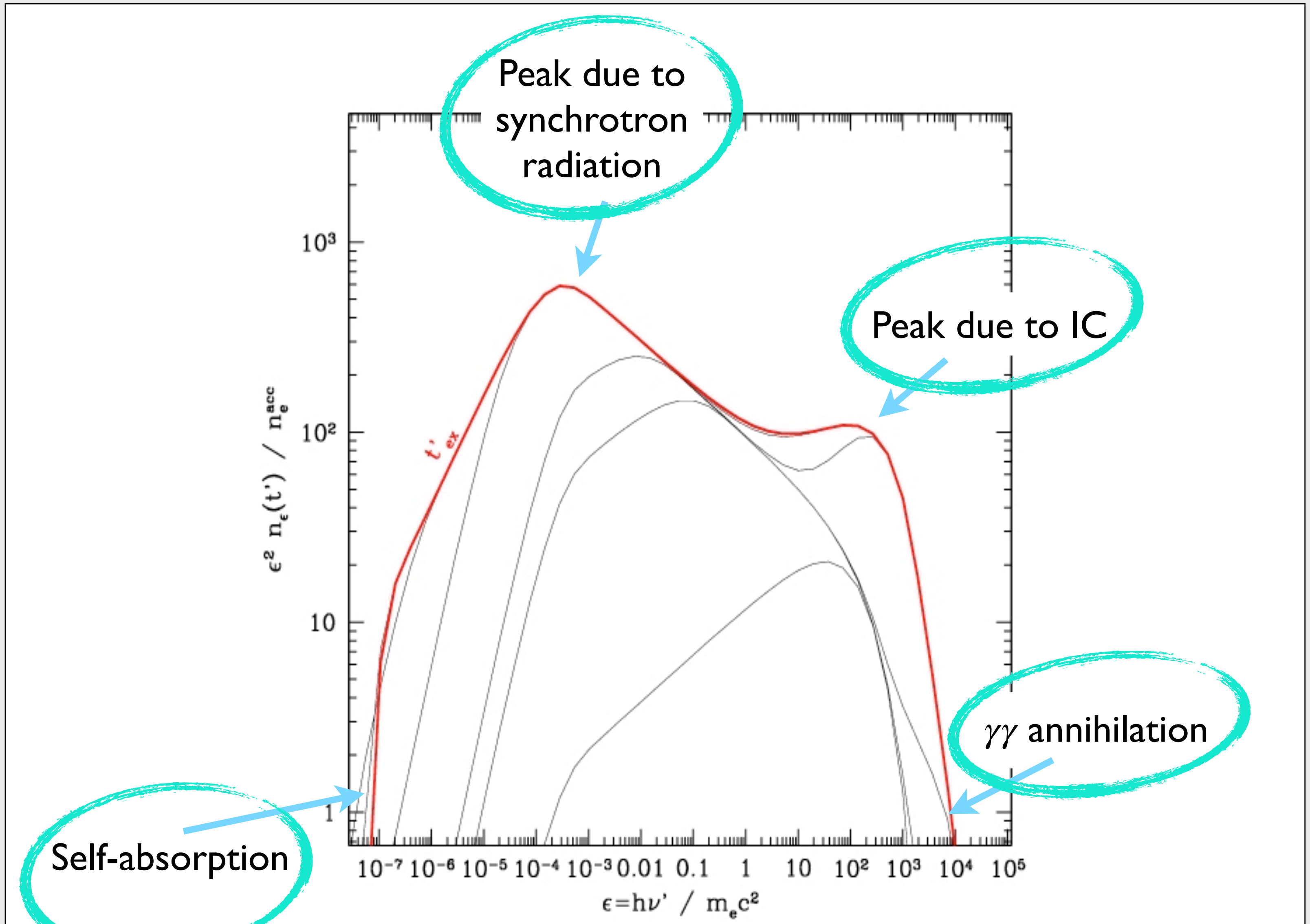

Emitted photon spectrum

This calculation is done at all times along the propagation of each shock wave

All the contributions are added together to produce a synthetic gamma-ray burst (spectrum+lightcurve)

Observed spectra and time profiles

The observed spectra and the light curves are computed from the comoving emission by integration over equal-arrival time surfaces.

relativistic effects (Doppler factor)

geometry (curvature of the emitting surface)

cosmological effect (redshifts)

Instantaneous observed spectrum:

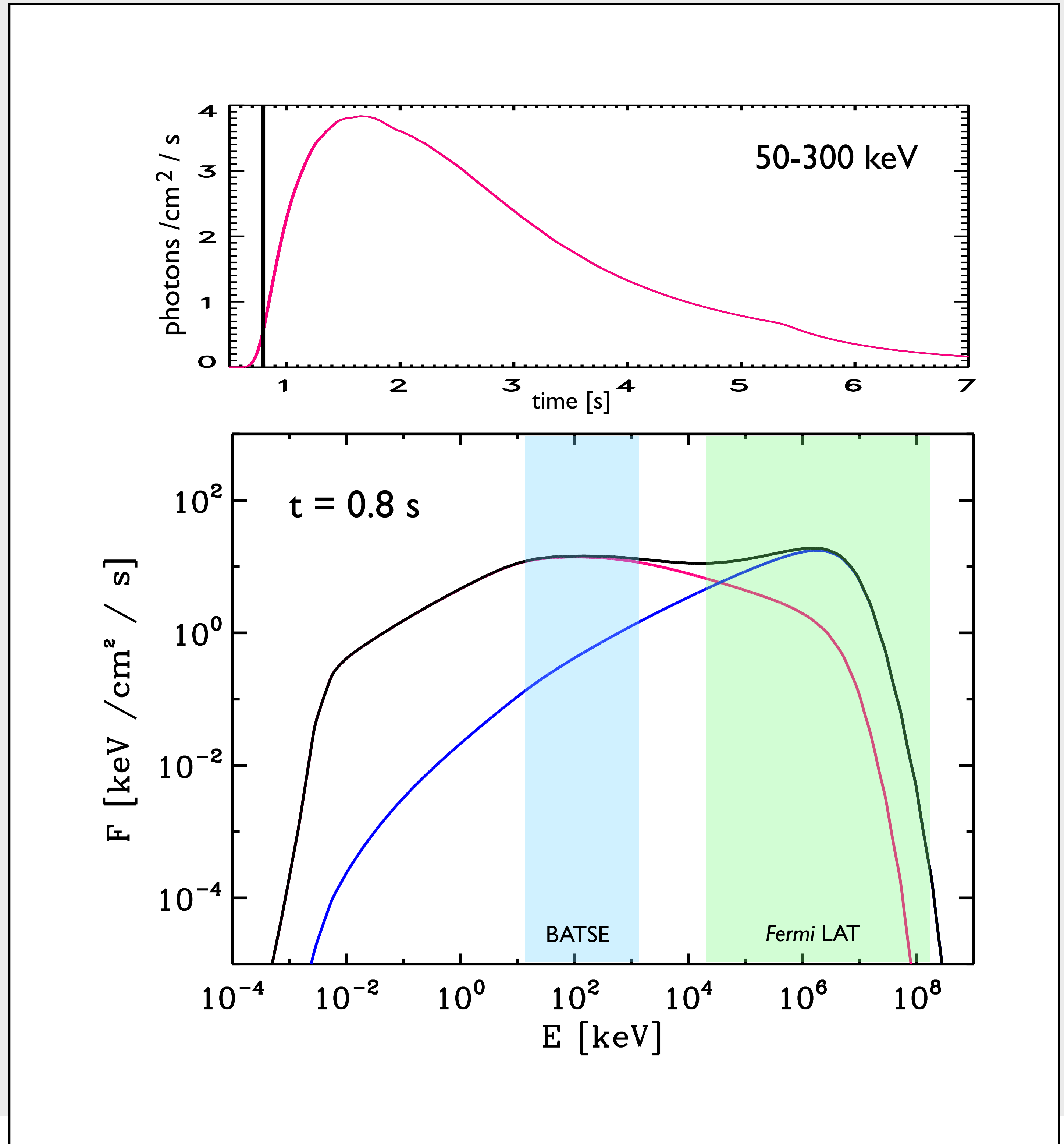

synchrotron
inverse Compton
total

Bosnjak, Daigne & Dubus 2009
Daigne, Bosnjak & Dubus 2011
Bosnjak & Daigne 2014

Observed spectra and time profiles

The observed spectra and the light curves are computed from the comoving emission by integration over equal-arrival time surfaces.

relativistic effects
(Doppler factor)
geometry (curvature of the
emitting surface)
cosmological effect (redshifts)

Instantaneous observed spectrum:

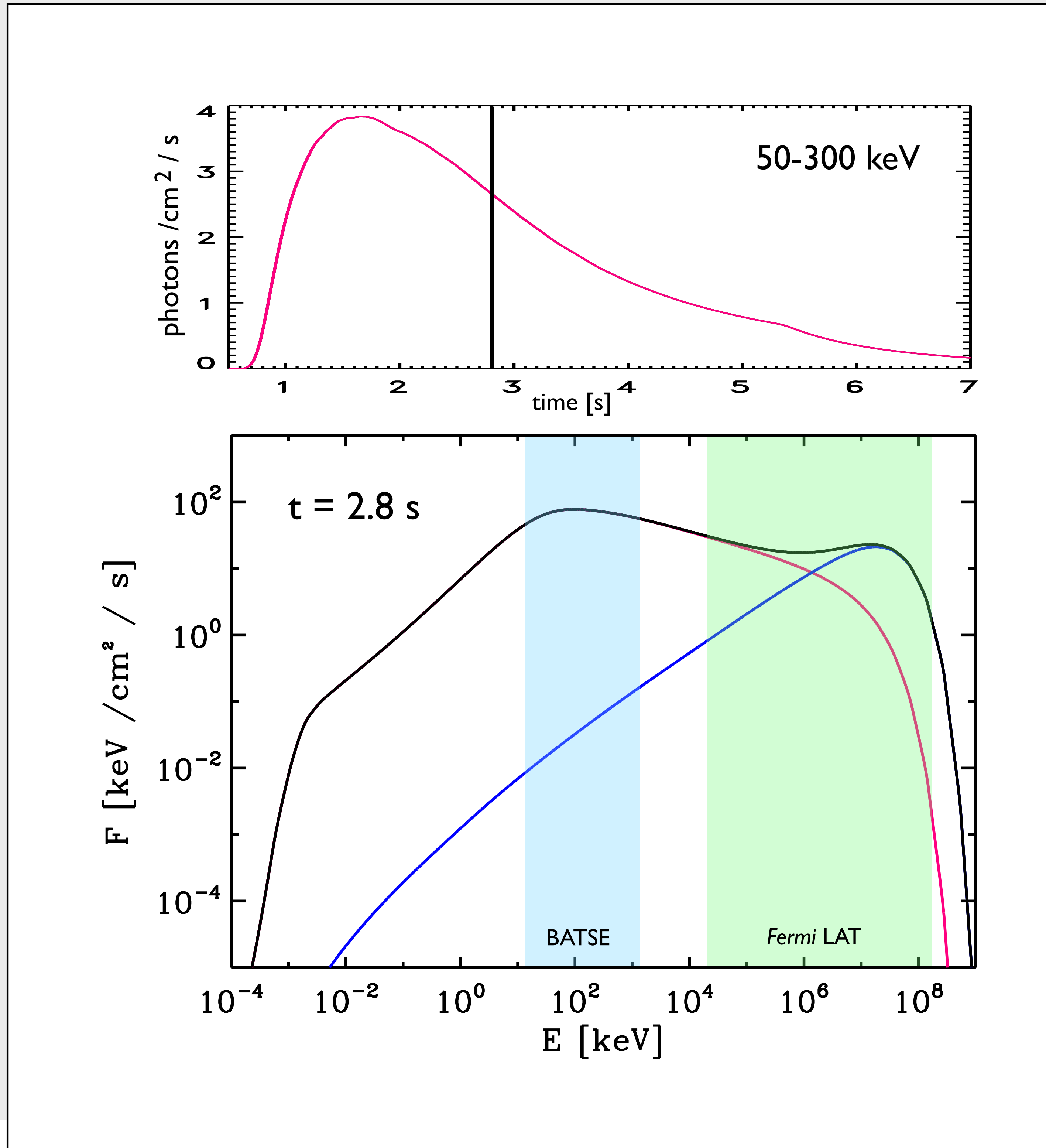

synchrotron
inverse Compton
total

Bosnjak, Daigne & Dubus 2009
Daigne, Bosnjak & Dubus 2011
Bosnjak & Daigne 2014

Steep low-energy slopes

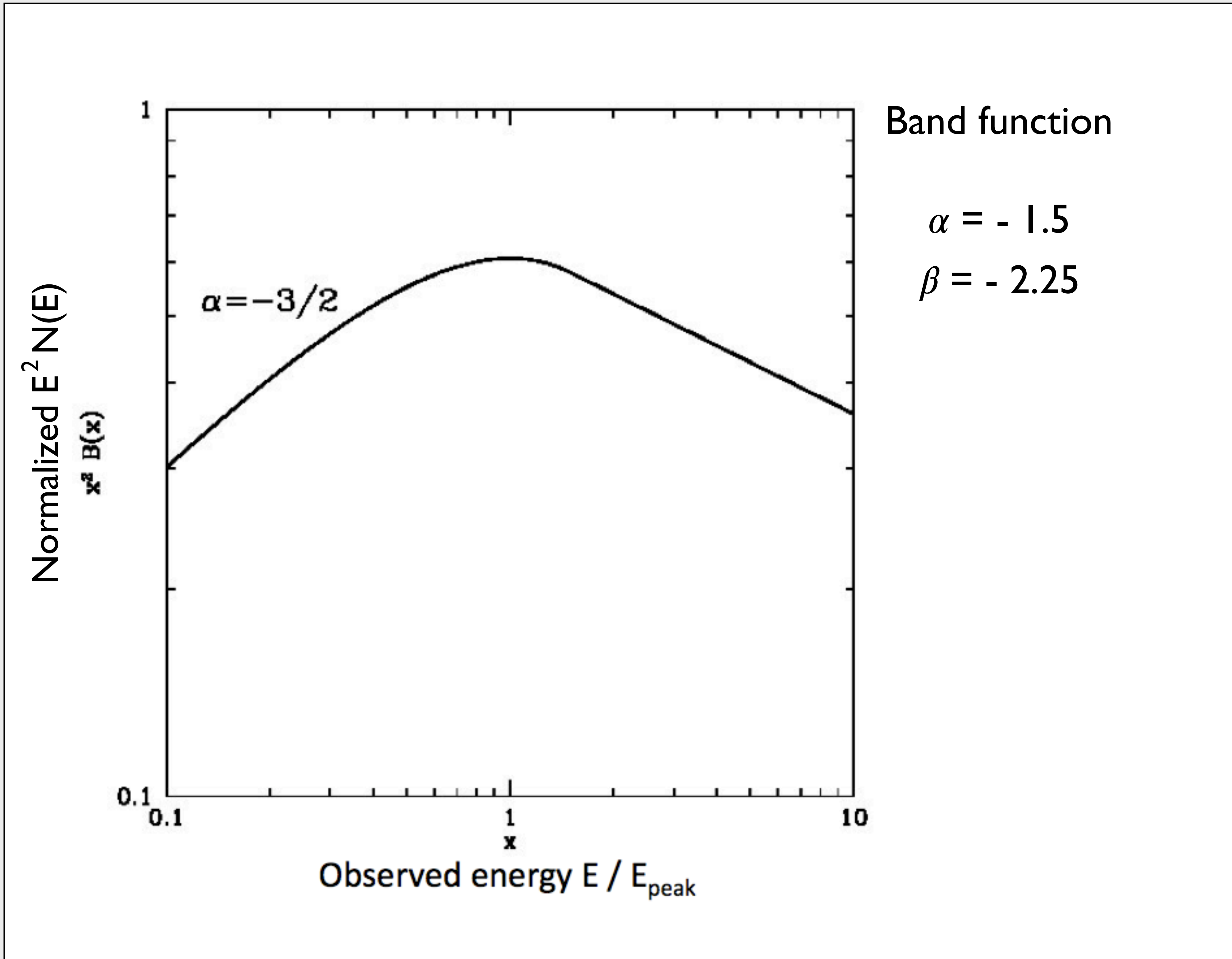

Band function

α = - 1.5

β = - 2.25

Steep low-energy slopes

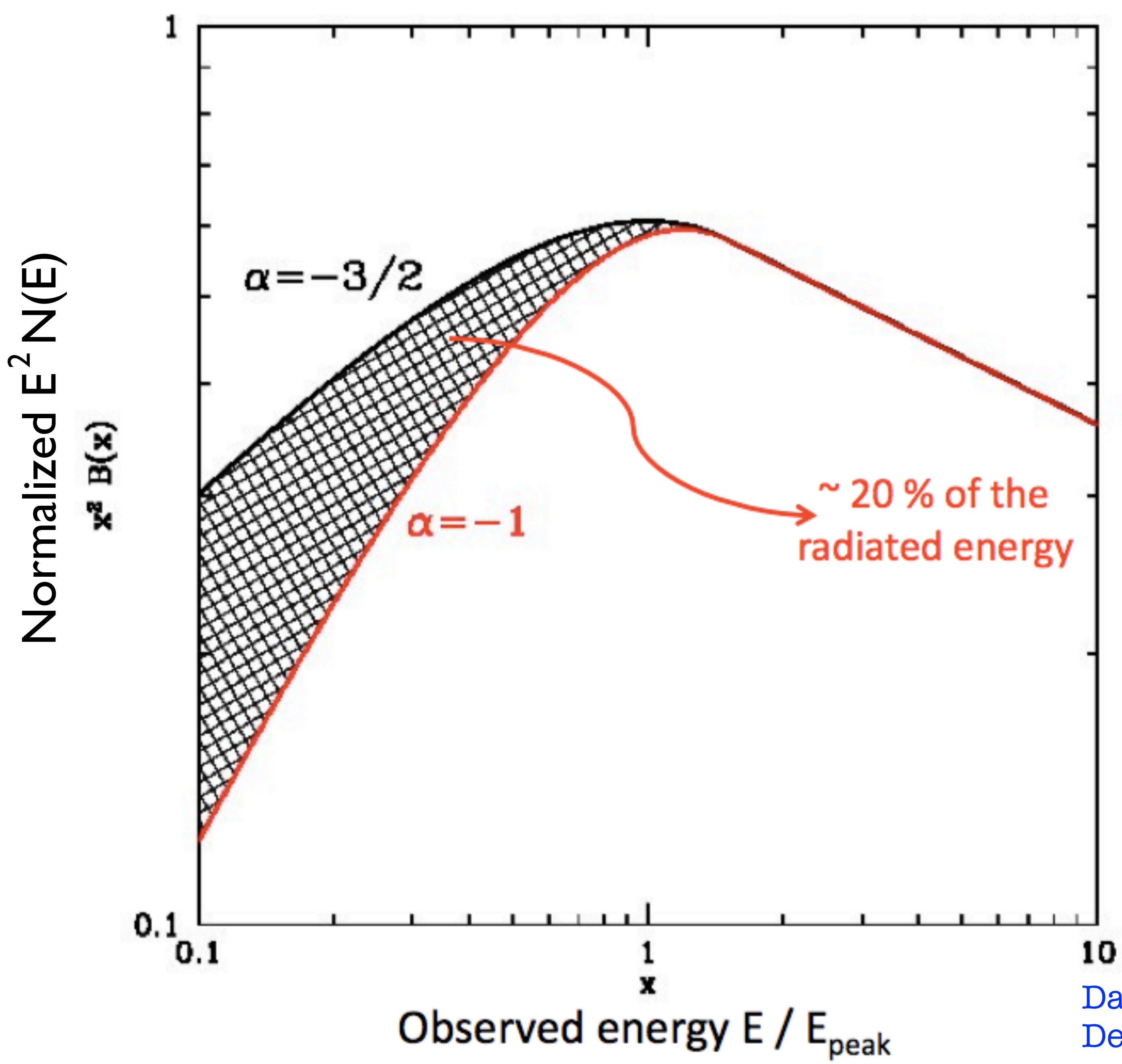

Band function

α = - 1.5 → -1

β = - 2.25

Daigne, Bosnjak & Dubus 2011
Derishev 2001

Inverse Compton scatterings in Klein-Nishina regime have an impact on the synchrotron slope

Radiative models

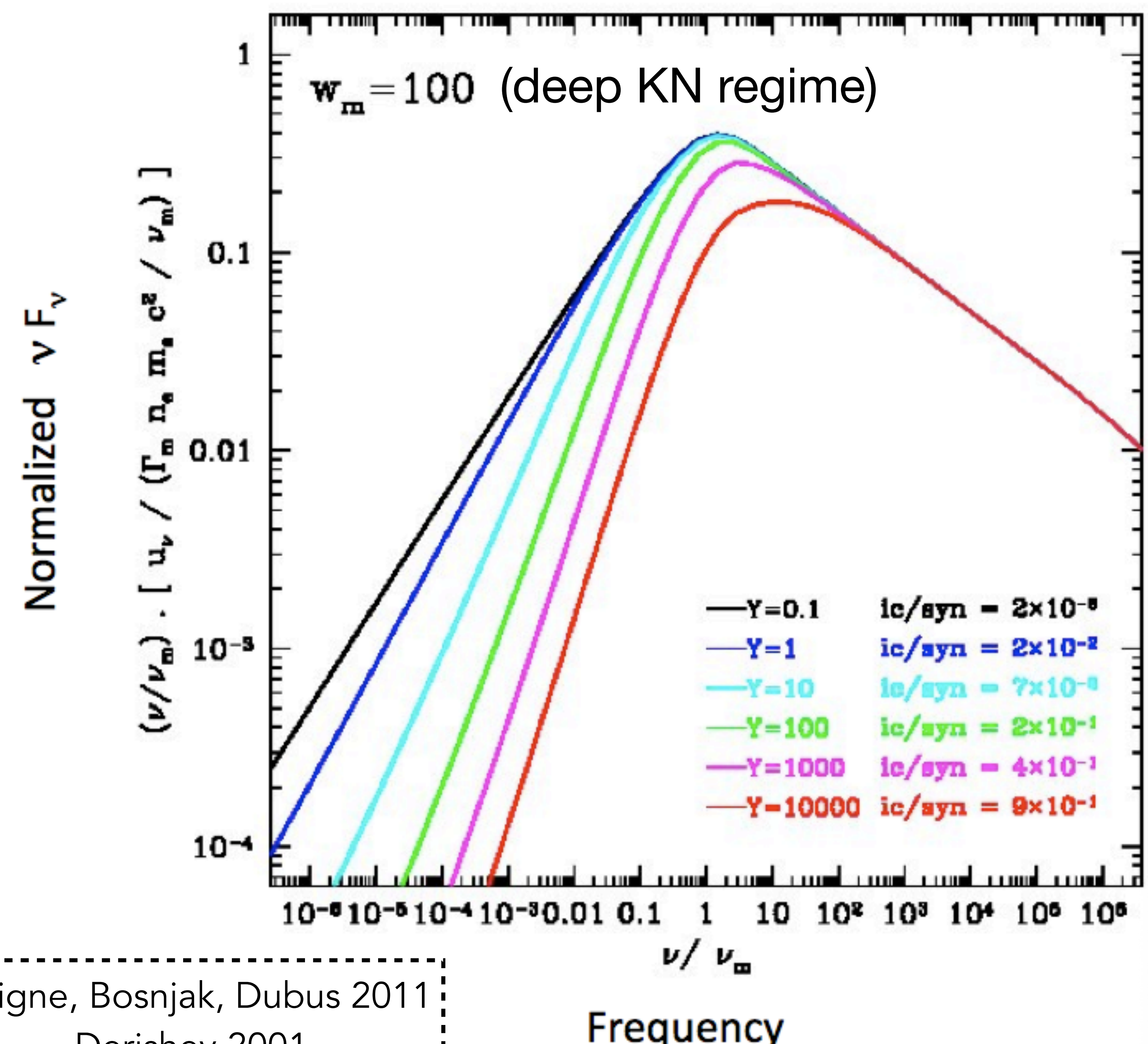

w_m : importance of KN

$$w_{\rm m} = \Gamma_{\rm m} \frac{h\nu'_{\rm m}}{m_{\rm e}c^2}$$

Y : importance of IC vs syn

$$Y = \frac{4}{3}\tau_{\rm T}\Gamma_{\rm m}\Gamma_{\rm c} \simeq \frac{\epsilon_{\rm e}}{\epsilon_{\rm B}}$$

Daigne, Bosnjak, Dubus 2011
Derishev 2001
Nakar et al. 2009

Thomson regime: the electron cooling rate due to IC scatterings remains proportional to γ^2 as for the synchrotron power

KN regime: the electron cooling rate due to IC depends on γ

Results: parameter space study

Bosnjak, Daigne & Dubus 2009
Daigne & Bosnjak 2024

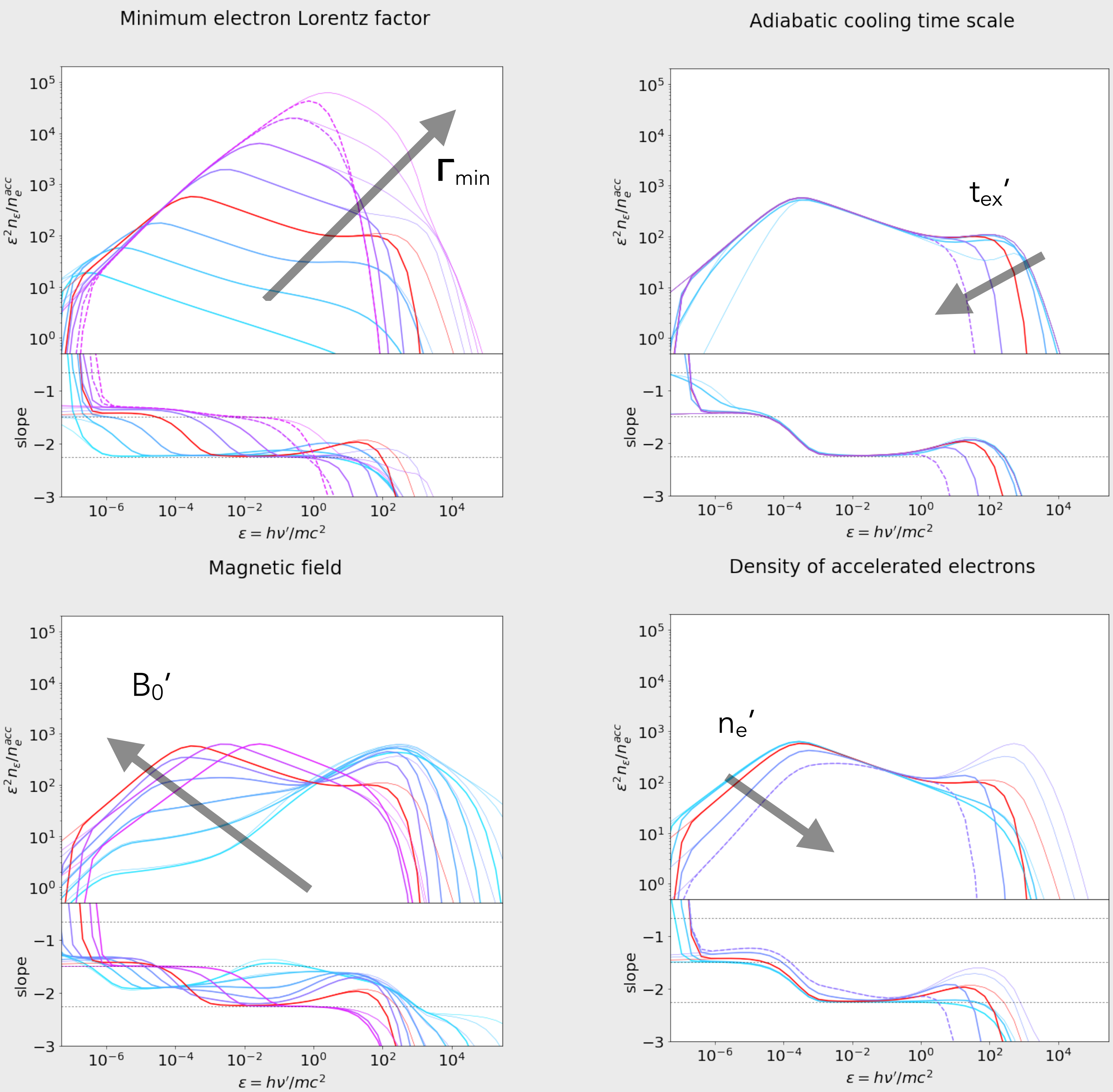

$\tau_{IC} \approx n_e\ (\sigma_T \times \text{KN corr.})\ (c \times t_{rad})$

$Y \approx \tau_{IC} \times (\Gamma_{min}^2 \times \text{KN corr.})$

A strong IC component is obtained when relativistic e- "survive" long enough for scatterings to occur (a low Γ_{min}, a low B' and a low t_{ex}', i.e. $t_{rad}' \rightarrow t_{ex}'$)

Reference spectrum:
$\Gamma_{min} = 1600$
$B_0' = 2000$ G
$n_e = 4.1 \times 10^7\ cm^{-3}$
$t_{dyn} = 80$ s

Results: time-resolved spectra and light curves

Case	Dynamics				Microphysics			Spec. @ max.		Spectro-temporal properties			
	Ejection	$E_{\mathrm{kin,iso}}$ [erg]	$\Gamma(t)$	$\bar{\Gamma}$	ζ	ϵ_B	p	$E_{\mathrm{p,obs}}$ [keV]	α	τ_r/τ_d	$a\,(W(E))$	δ (HIC)	κ (HIC)
A	**$\dot{E}$ = cst**	**1.00×10^{54}**	**smooth**	**340**	**3.00×10^{-3}**	**1/3**	**2.5**	**731**	**−1.5**	**0.38**	**0.29**	**2.28**	**2.16**
					3.40×10^{-3}		2.7	731	−1.5	0.39	0.30	2.15	1.97
					varying			744	−1.4	0.31	0.28	2.23	1.55
					varying		2.7	744	−1.4	0.30	0.29	2.12	1.48
					4.00×10^{-4}		2.1	912	−1.2	0.41	0.14	/	/
					8.80×10^{-4}		2.3	666	−1.1	0.46	0.18	/	/
B	**$\dot{E}$ = cst**	**1.00×10^{54}**	**smooth**	**340**	**1.00×10^{-3}**	**10^{-3}**	**2.5**	**642**	**−1.1**	**0.43**	**0.23**	/	/
					1.10×10^{-3}		2.7	619	−1.1	0.54	0.24	0.97	0.89
					1.15×10^{-3}		2.9	630	−1.1	0.54	0.27	1.23	1.05
					1.20×10^{-3}		3.1	619	−1.1	0.54	0.27	1.31	1.07
					1.23×10^{-3}		3.3	619	−1.1	0.54	0.28	1.32	1.06
					varying			679	−1.1	0.33	0.24	0.96	0.80
					varying		2.7	679	−1.1	0.32	0.27	1.27	0.97
		1.50×10^{54}		360	varying			691	−1.1	0.37	0.24	/	/
		1.50×10^{54}		360	varying		2.7	679	−1.1	0.36	0.26	0.92	0.78
		5.85×10^{53}	sharp		2.00×10^{-3}			744	−1.2	0.68	0.18	/	/
		5.85×10^{53}	sharp		varying			772	−1.1	0.04	0.25	/	/
	$\dot{M}$ = cst	1.85×10^{54}			6.00×10^{-4}			679	−1.1	0.75	0.16	0.13	0.17
	$\dot{M}$ = cst	1.85×10^{54}			varying			630	−1.1	0.60	0.16	/	/
C	**$\dot{E}$ = cst**	**1.00×10^{53}**	**smooth**	**1020**	**1.00×10^{-3}**	**10^{-1}**	**2.5**	**164**	**−0.7**	**0.55**	**0.11**	/	/

Bosnjak & Daigne 2014

Results: time-resolved spectra and light curves

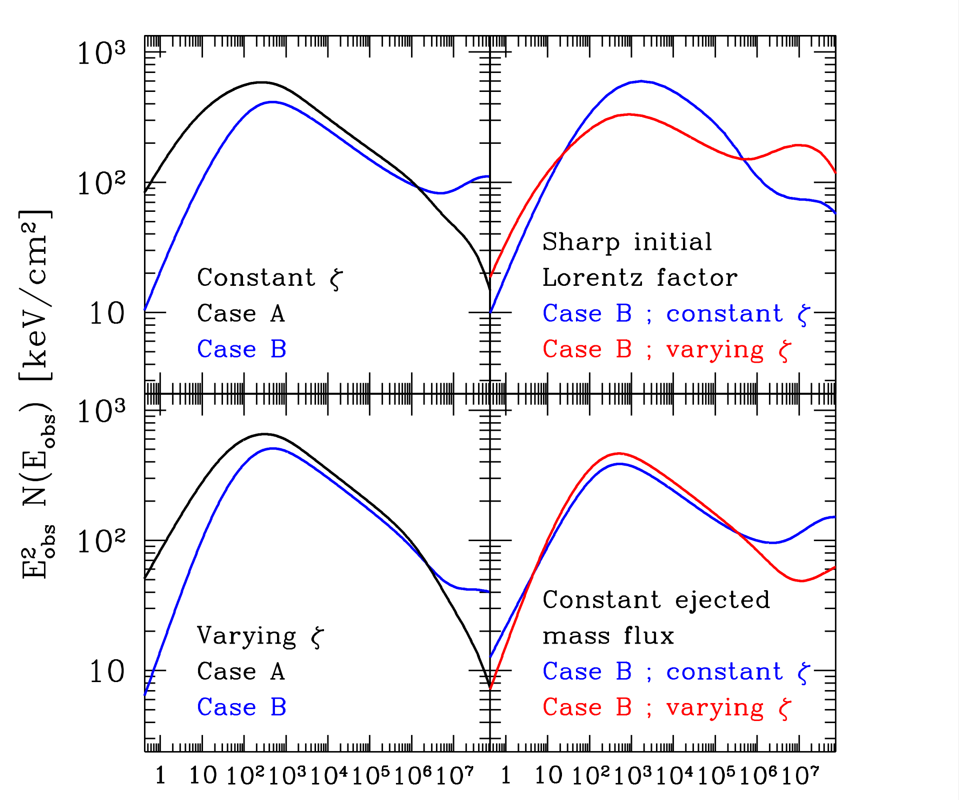

Bosnjak & Daigne 2014

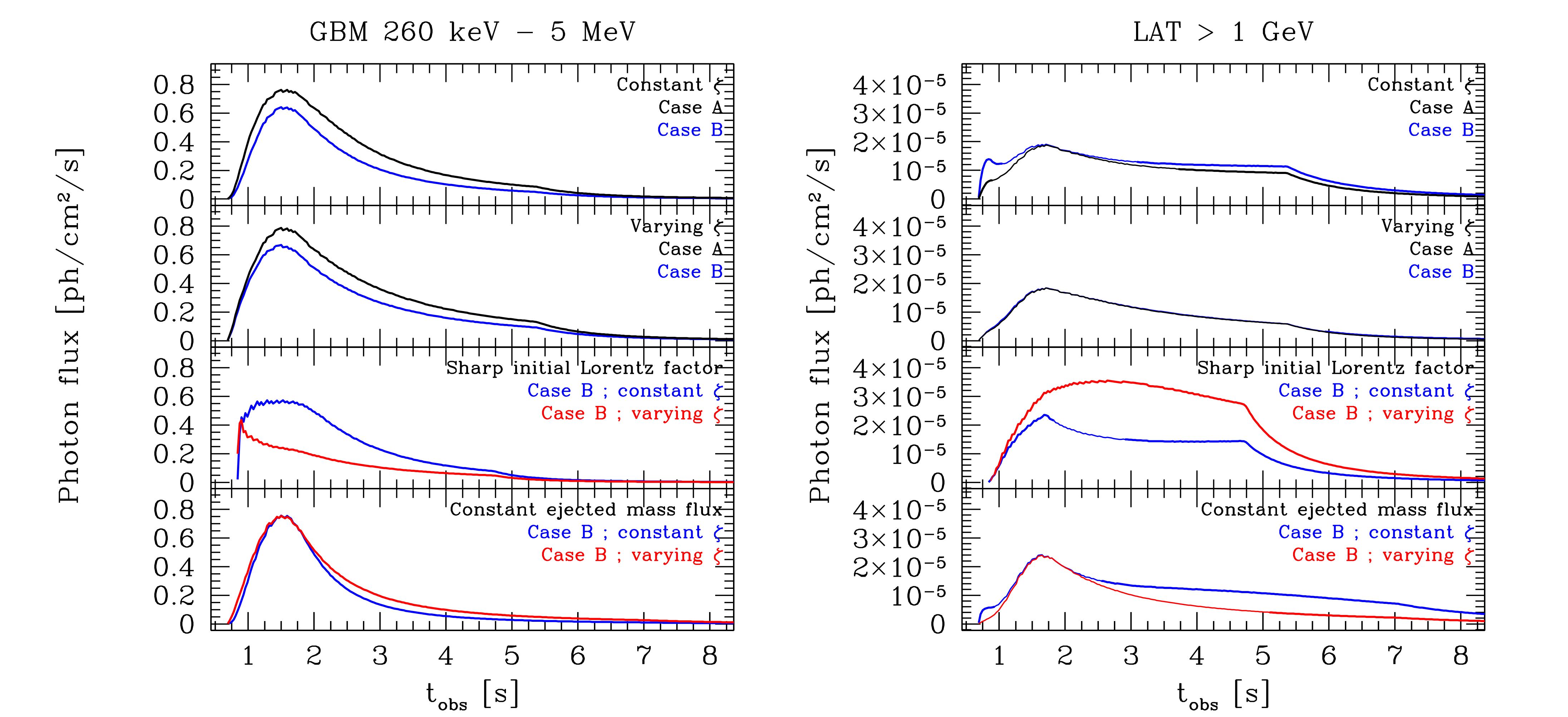

Low-luminosity gamma-ray bursts

- **Motivation**

LL GRBs are fainter about four orders of magnitude ($L \lesssim 10^{49}$ erg/s) from the commonly observed long GRBs

relatively soft ($E_p \lesssim 100$ keV)

not highly beamed (e.g. Soderberg 2006)

low Lorentz factors ($\Gamma \lesssim 50$) (e.g. Cano et al. 2017)

in some cases exhibit substantially longer durations (up to several 10^3 s)

LL GRBs have been proposed as sources of cosmic rays and neutrinos (e.g. Murase et al. 2006; 2008, Zhang et al. 2018; Boncioli et al. 2019; Samuelsson et al. 2020): they are likely to have a much higher event rate in the local universe + heavy nuclei much easily survive inside the sources due to their lower radiation luminosity

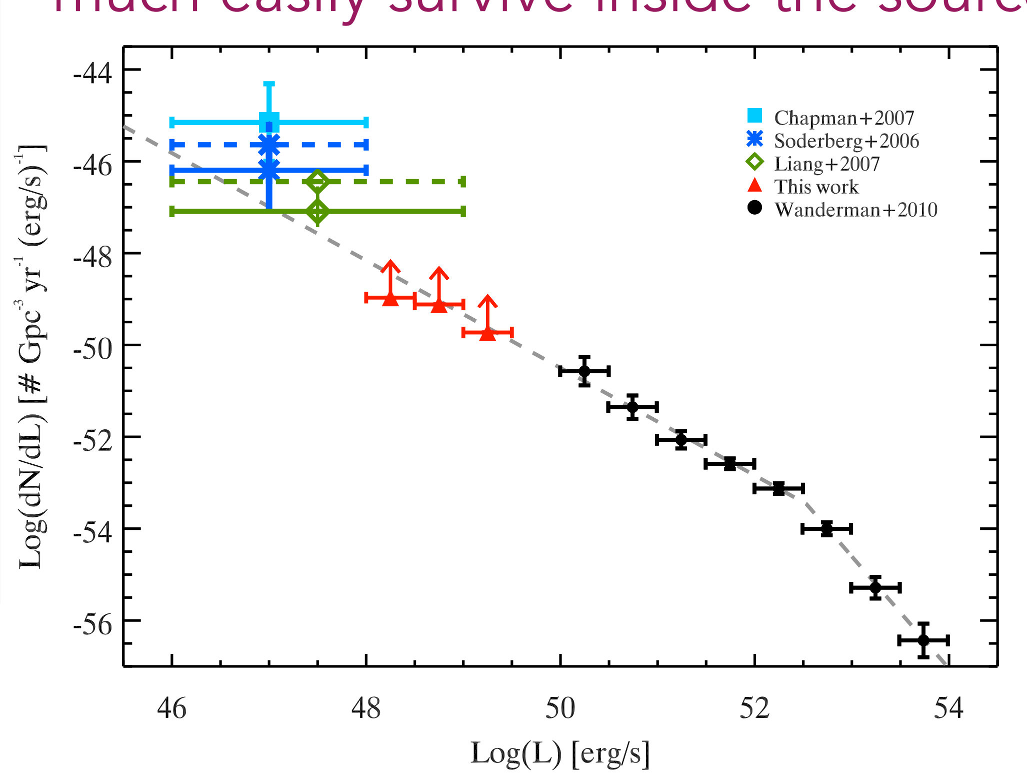

Pescalli et al. 2015

Their low luminosity limits the detection to a distance of ~ 100 Mpc, but LL GRBs are much more common than long GRBs (Liang et al. 2007).

Low-luminosity gamma-ray bursts

GRB 980425

GRB100316D

GRB120714B

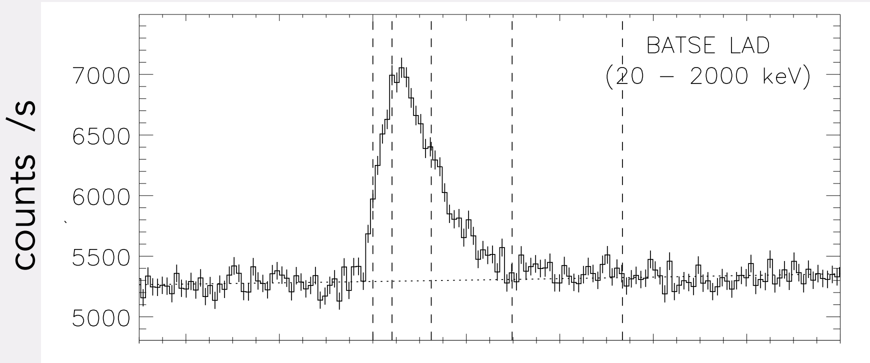

Kaneko et al. 2006

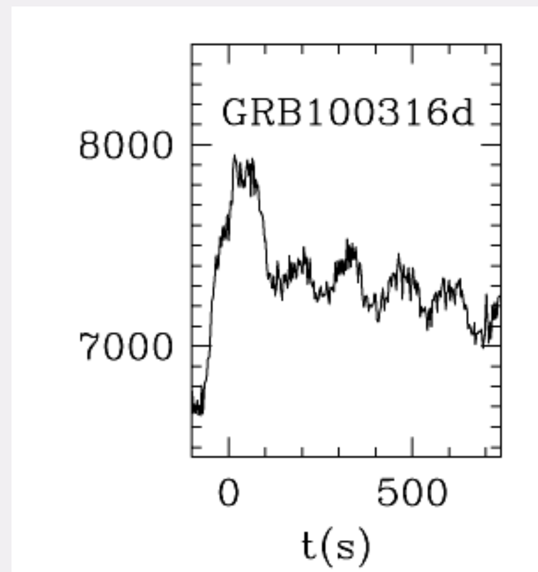

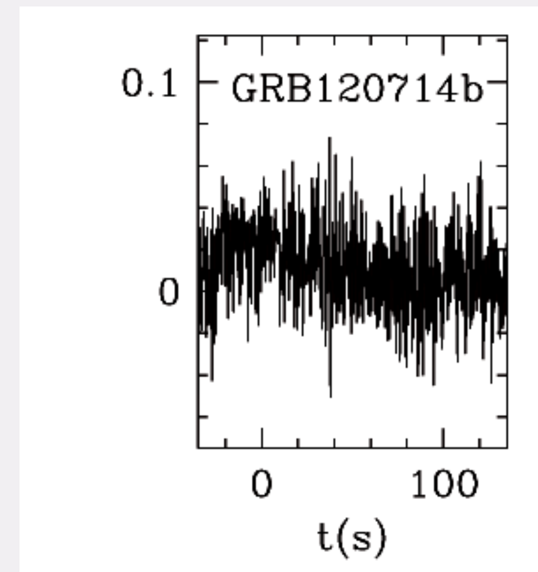

Swift BAT archive; swift.gsfc.nasa.gov

Model inputs:

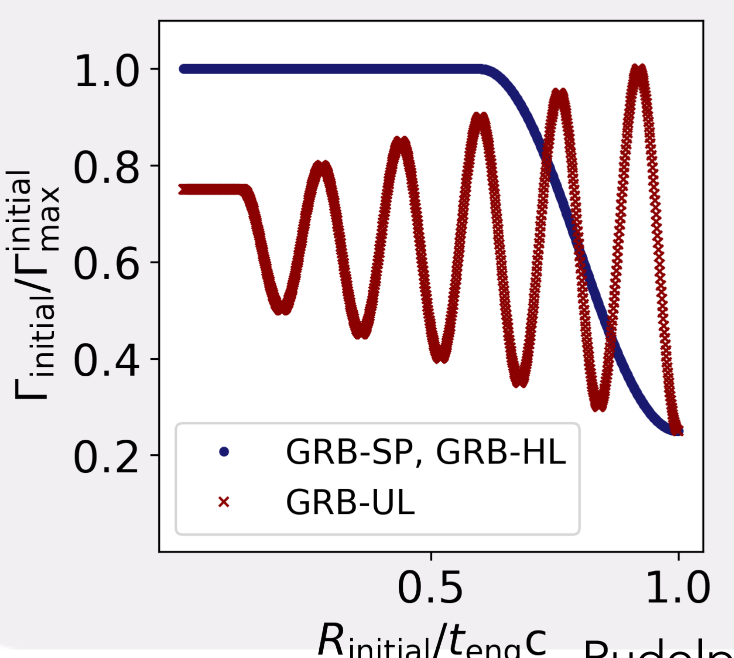

Rudolph 2022

		GRB 980425	GRB 100316D	GRB 120714B
Observed	$E_{\gamma,\,\rm iso}$ (erg)	$1.6 \cdot 10^{48}$	$3.9 \cdot 10^{49}$	$5.9 \cdot 10^{50}$
	T_{90} (s)	35	1300	159
	$E_{\rm peak}$ (keV)	122	30	101
	z	0.0085	0.059	0.3984
		sp-GRB	ul-GRB	hl-GRB
Input	$\Gamma_{\rm initial,\,max}$, $\Gamma_{\rm initial,\,min}$	40, 10	40, 10	80, 20
	$L_{\rm wind}$ (erg s^{-1})	$2.5 \cdot 10^{48}$	$5.8 \cdot 10^{48}$	$3 \cdot 10^{50}$
	$N_{\rm shells}$	1000	1000	1000
	$t_{\rm eng}$ (s)	40	1000	130

Rudolph, Bosnjak, Palladino, Sadeh, Winter 2022

Low-luminosity GRBs: results

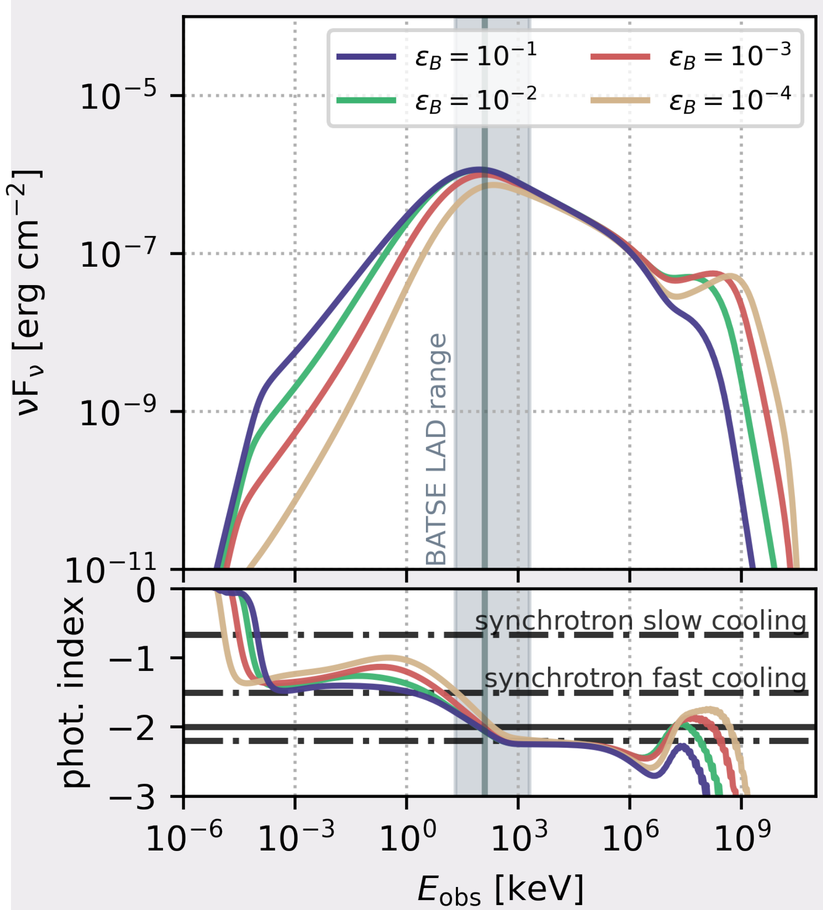

GRB-SP

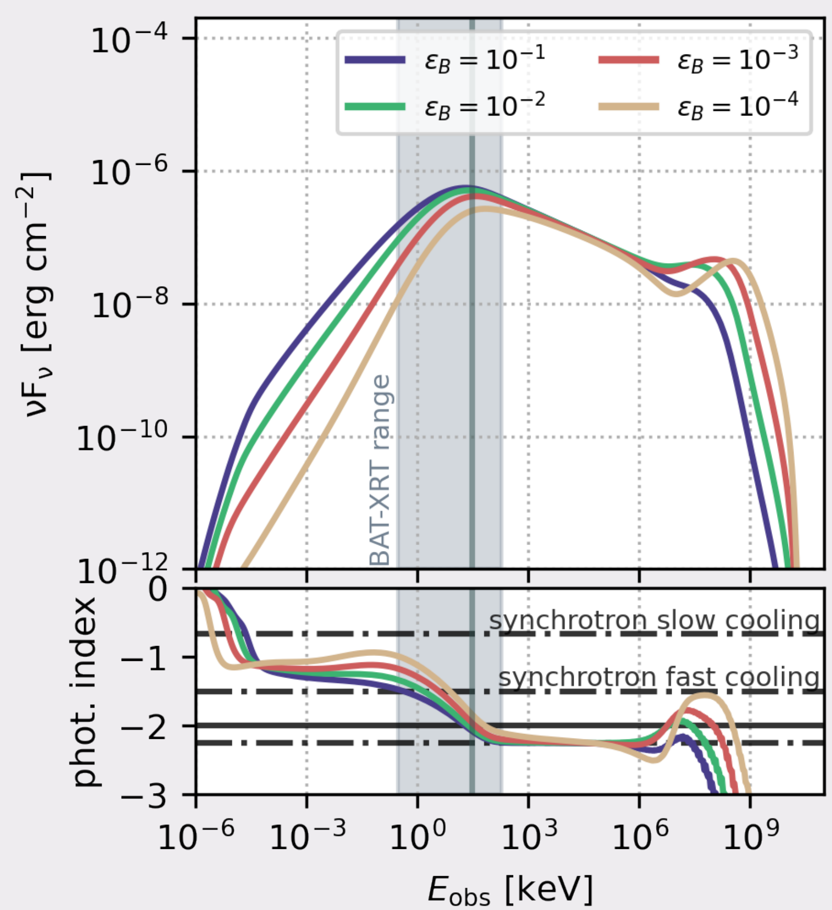

GRB-UL

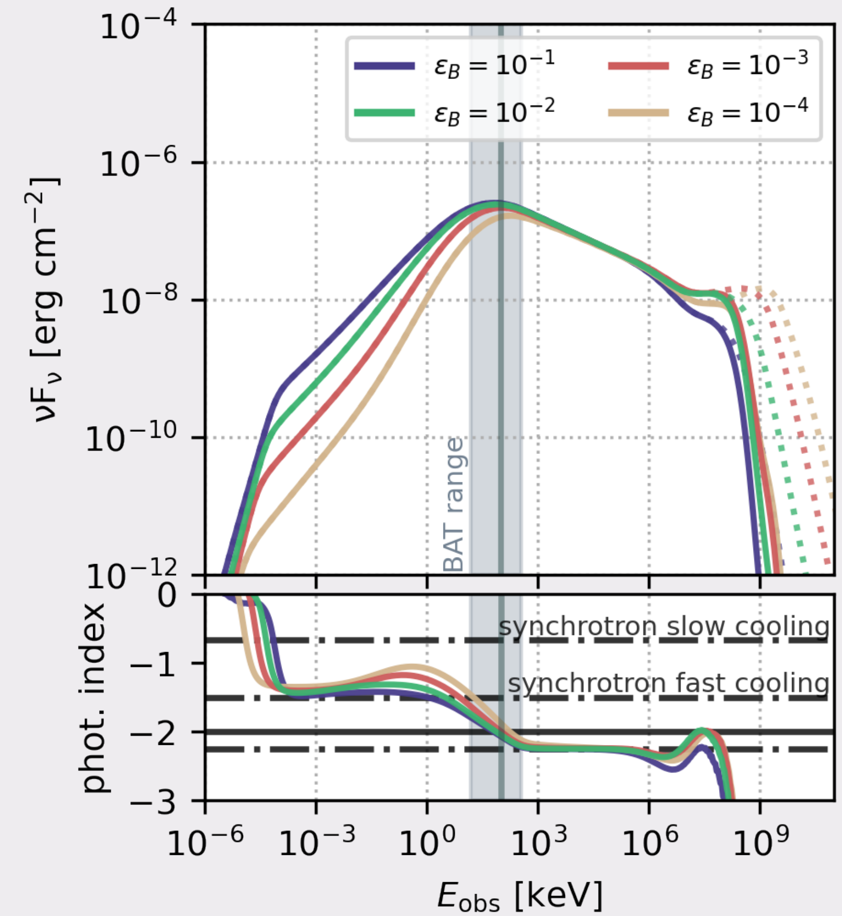

GRB-HL

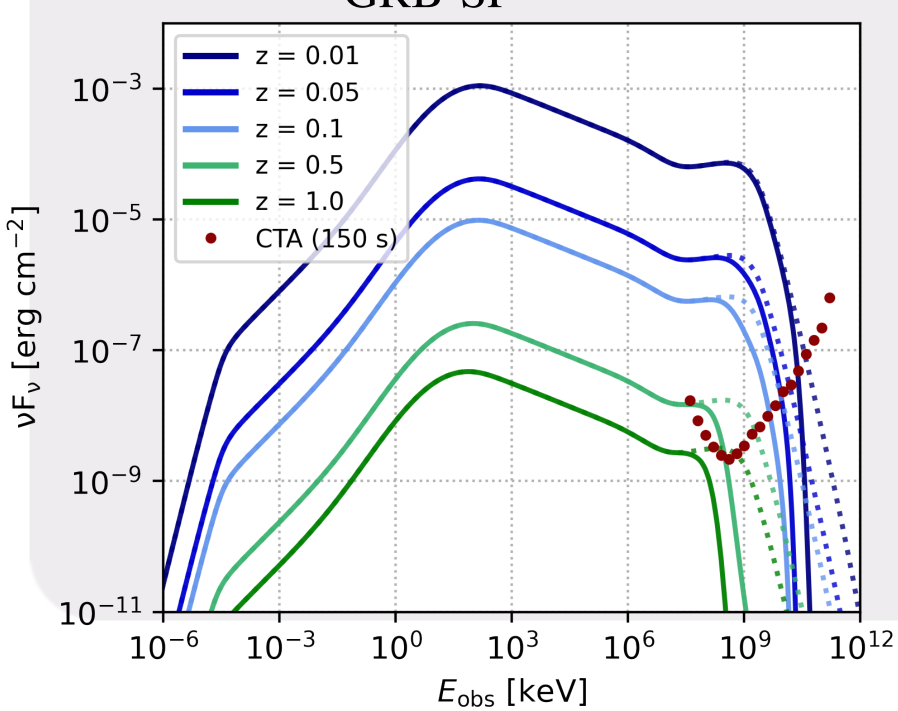

Predicted observed spectra for the prototype hl-GRB with $\epsilon_B = 10^{-3}$ placed at different redshifts.

The minimal fluence nominally detectable by CTA for an observations duration of 150 s.

Rudolph, Bosnjak, Palladino, Sadeh, Winter 2022

Low-luminosity GRBs: results

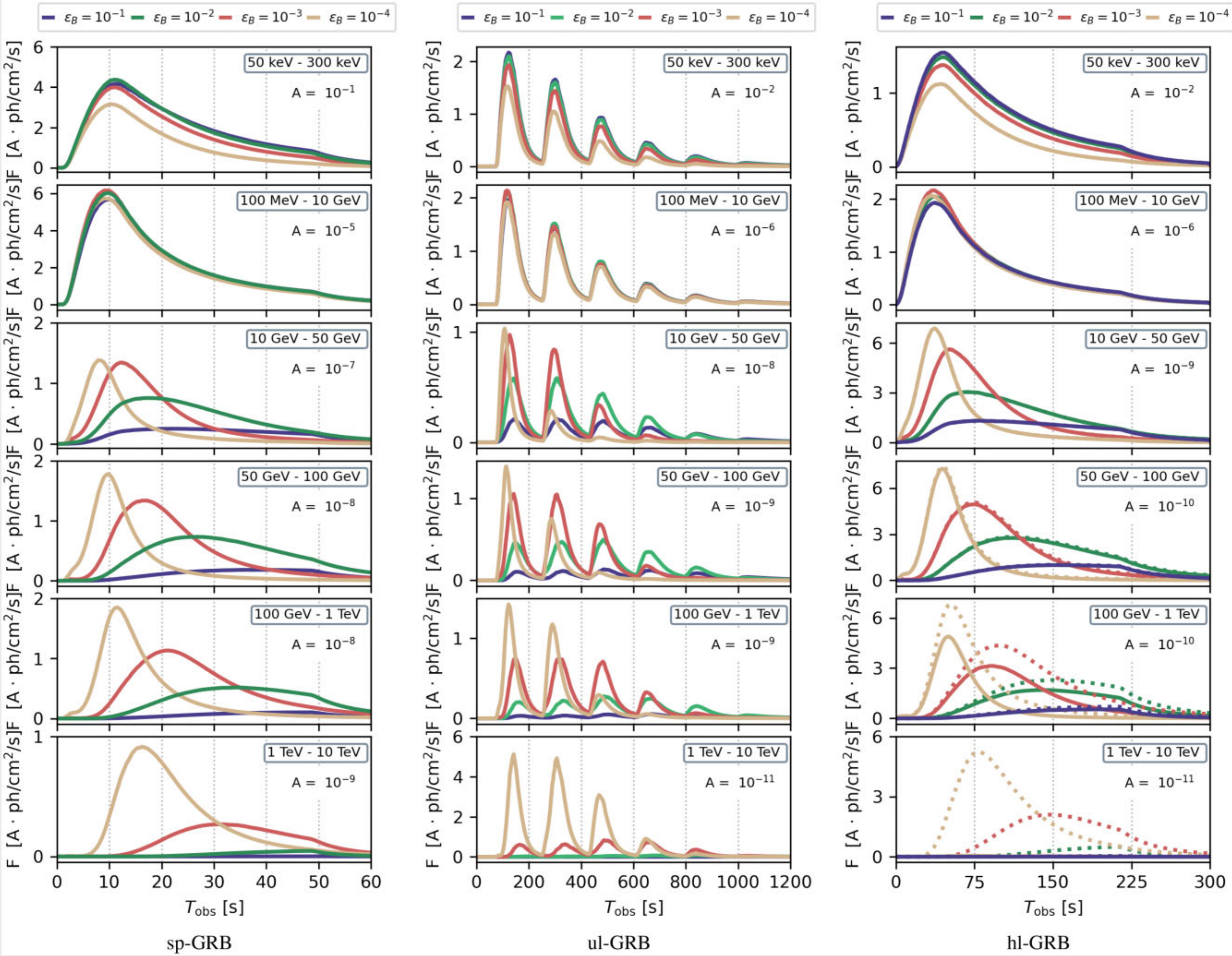

Rudolph, Bosnjak, Palladino, Sadeh, Winter 2022

Maximal energies of cosmic-ray nuclei

The maximal energies are calculated for each collision using the simulated photon spectra and parameters of the jet evolution.

The acceleration rate is balanced with the energy losses (photo-hadronic cooling, photo-disintegration cooling, synchrotron and adiabatic cooling) with NeuCosmA code (Biehl et al 2018).

Iron nuclei (protons) can reach energies up to ≃ 10^{11} GeV (10^{10} GeV).

High ϵ_B yields higher maximal energies.

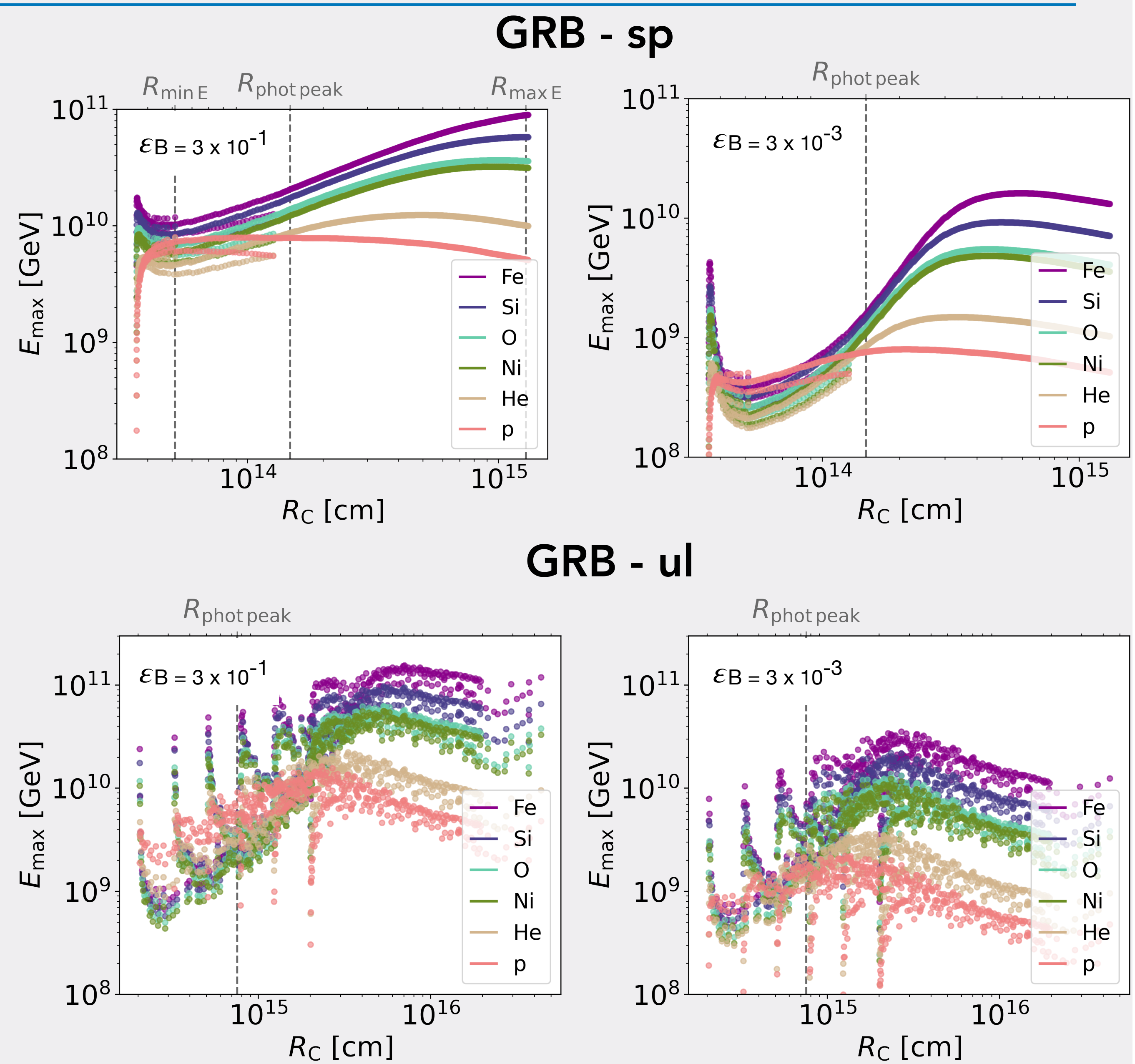

A LL GRB can either have a leptonic inverse Compton VHE component in the photon spectrum (for low ϵ_B) or accelerate cosmic rays to highest energies (for high ϵ_B).

Rudolph, Bosnjak, Palladino, Sadeh, Winter 2022

Lepto-hadronic model

Rudolph, Petropoulou, ŽB, Winter 2023
Rudolph, Petropoulou, Winter, ŽB 2023

AM³ time-rependent code (Gao et al. 2017) following the coupled evolution of photons, electrons, positrons, muons, pions, p, n, and ν

All relevant nonthermal processes included: synchrotron emission, SSA, IC scatterings, photopair and photopion production, $\gamma\gamma$-annihilation, adiabatic cooling & escape

Fireball Parameters and Fiducial Microphysics Parameters Used for the Modeling of Two Energetic GRB Prototypes

Parameter	Symbol	SP_{E54}	$MP_{E54.5}$ ($\delta t_{var} = 1.13$ s)	$MP_{E54.5}$ ($\delta t_{var} = 0.11$ s)
Number of initial shells	N_{shells}^{ini}	1000	1297	1297
Engine active time	t_{eng}	5 s	34 s	3.4 s
Number of collisions	N_{coll}	999	1139	1139
Total energy in nonthermal electrons	$E_{e,\,NT}^{tot}$	1.3×10^{54} erg	3.5×10^{54} erg	3.5×10^{54} erg
Average collision radius	$\langle R_{Coll} \rangle$	1.9×10^{16} cm	2.4×10^{16} cm	2.4×10^{15} cm
Overall dissipation efficiency	ε	7.8%	2.98 %	2.98 %
Power-law index of nonthermal electrons	p_e	2.5	3.0	3.0
Power-law index of nonthermal protons	p_p	2.0	2.0	2.0
Minimum Lorentz factor of nonthermal protons	$\gamma'_{p,min}$	10	10	10
Relative fraction of energy transferred to thermal particles	$f_{TH/e} = \epsilon_{TH}/\epsilon_e$	0	0	0
			SYN-dominated model	
Relative fraction of energy transferred to magnetic field	$f_{B/e} = \epsilon_B/\epsilon_e$	1	1	1
Relative fraction of energy transferred to protons	$f_{p/e} = \epsilon_p/\epsilon_e$	{**0**, 10, **30**, 100}	{**0**, 3, 10, **30**}	{**0**, 0.3, 1, **3**}
Normalization for number fraction of accelerated electrons	$\zeta_{0,e}$ [10^{-4}]	18.7	21.6	119.7
Minimum Lorentz factor of nonthermal electrons	$\gamma_{e,\,min}$ [10^4]	1.2	1.5	0.2
			IC-dominated model	
Relative fraction of energy transferred to magnetic field	$f_{B/e} = \epsilon_B/\epsilon_e$	10^{-3}	10^{-3}	…
Relative fraction of energy transferred to protons	$f_{p/e} = \epsilon_p/\epsilon_e$	{**0**, 10, **30**, 100}	{**0**, 3, 10, **30**}	…
Normalization for number fraction of accelerated electrons	$\zeta_{0,e}$ [10^{-4}]	3.3	3.8	…
Minimum Lorentz factor of nonthermal electrons	$\gamma'_{e,\,min}$	6.5	8.6	…

$$E_{kin,ini} = \varepsilon^{-1} E_{diss} = \varepsilon^{-1}(E_{e,\,NT}^{tot} + E_{p,\,NT}^{tot} + E_B + E_{TH}^{tot})$$
$$= \varepsilon^{-1} E_{e,\,NT}^{tot}(1 + f_{p/e} + f_{B/e} + f_{TH/e});$$

$$f_{p/e} = \epsilon_p/\epsilon_e \qquad f_{B/e} = \epsilon_B/\epsilon_e \qquad f_{TH/e} = \epsilon_{TH}/\epsilon_e$$

Lepto-hadronic model

Rudolph, Petropoulou, ŽB, Winter 2023
Rudolph, Petropoulou, Winter, ŽB 2023

AM³ time-rependent code (Gao et al. 2017) following the coupled evolution of photons, electrons, positrons, muons, pions, p, n, and ν

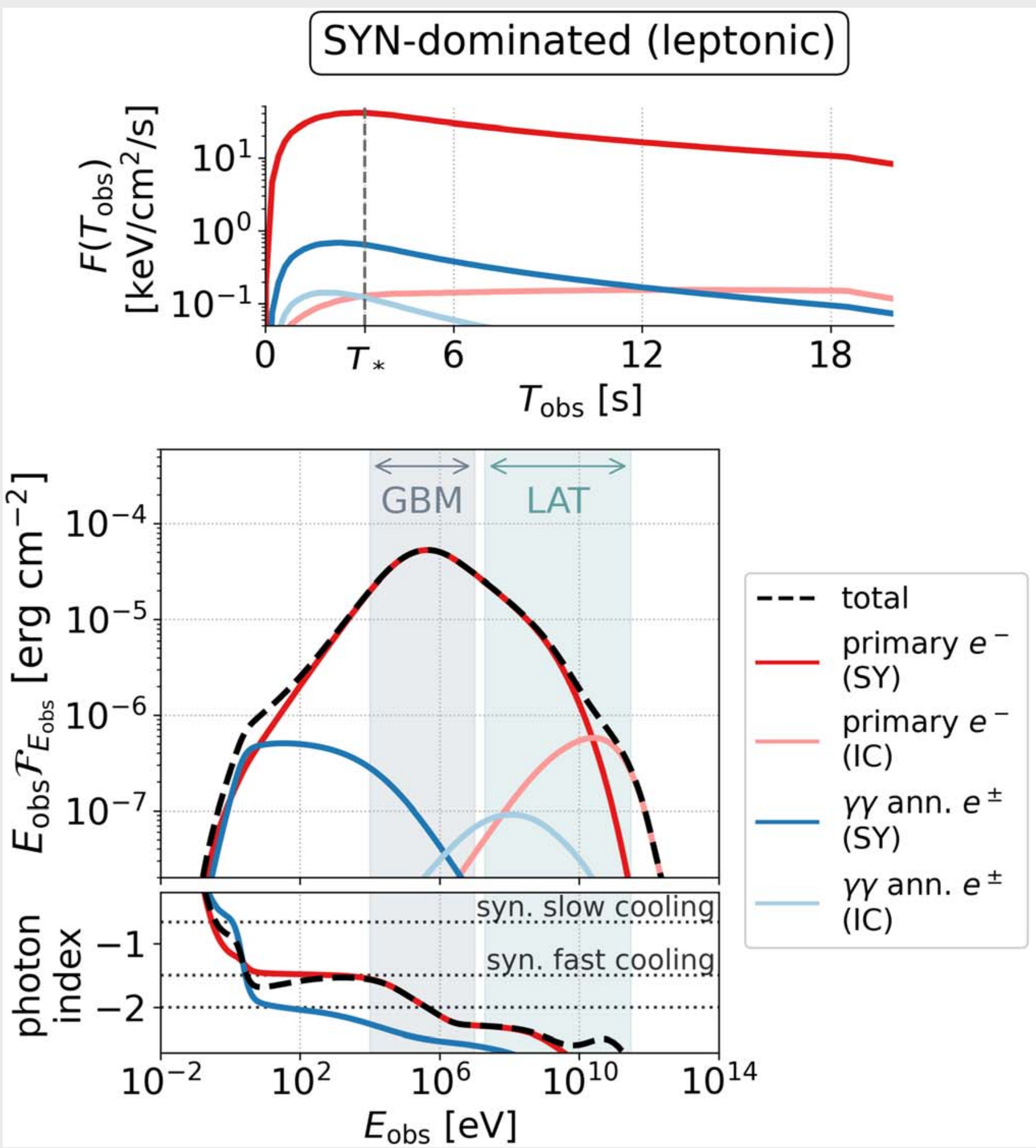

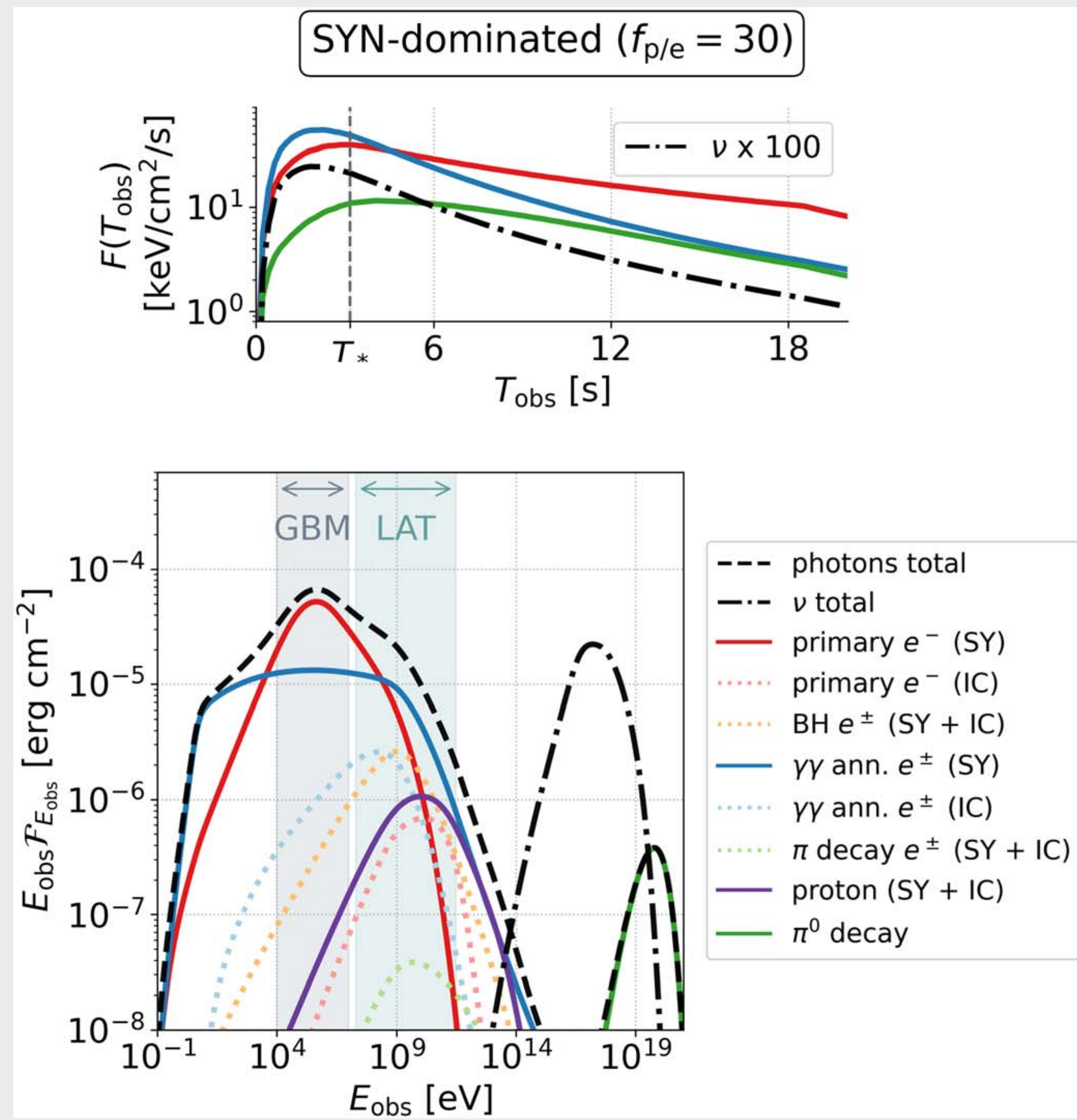

Lepto-hadronic model

Rudolph, Petropoulou, ŽB, Winter 2023
Rudolph, Petropoulou, Winter, ŽB 2023

AM³ time-rependent code (Gao et al. 2017) following the coupled evolution of photons, electrons, positrons, muons, pions, p, n, and ν

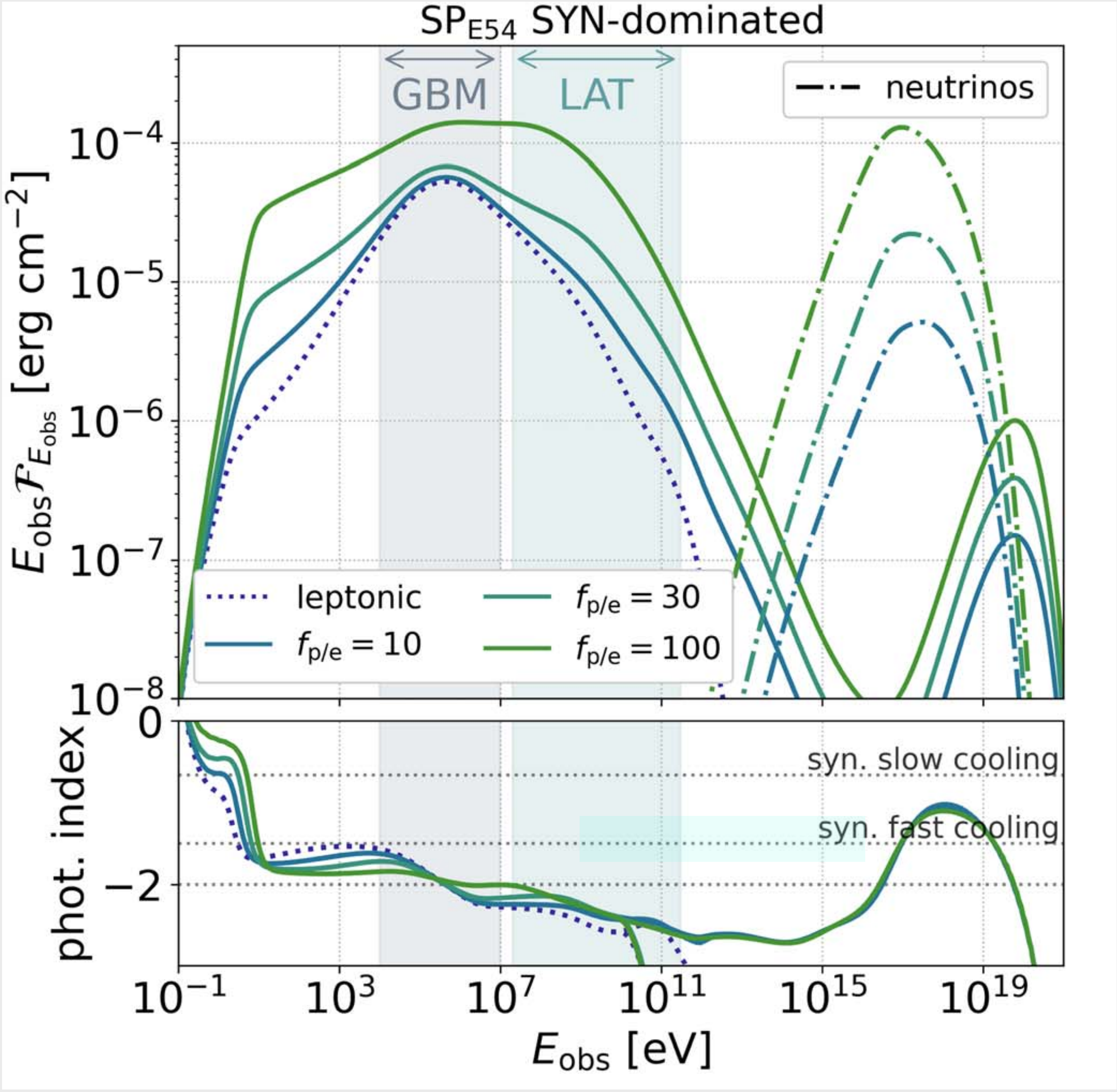

For the chosen baryonic loading, the SYN emission of secondary pairs from $\gamma\gamma$ annihilation follows $n_e' \propto \gamma_e^{-3}$ distribution
→ a broad flat spectrum dominating over all other hadronic-related contributions.

The injection rate of pairs from $\gamma\gamma$ annihilation is high, because of the high luminosity of VHE photons. **These photons are mainly produced from π^0 decays!**

TeV observations: GRB 221009A

First GRB seen by an extensive air shower detector

(LHAASO collaboration, Science 2023)

TeV light curve: a rise to peak after a quiescent phase, then a decay

$E_{iso} \sim 10^{55}$ erg z = 0.151

First time detection of the afterglow onset?

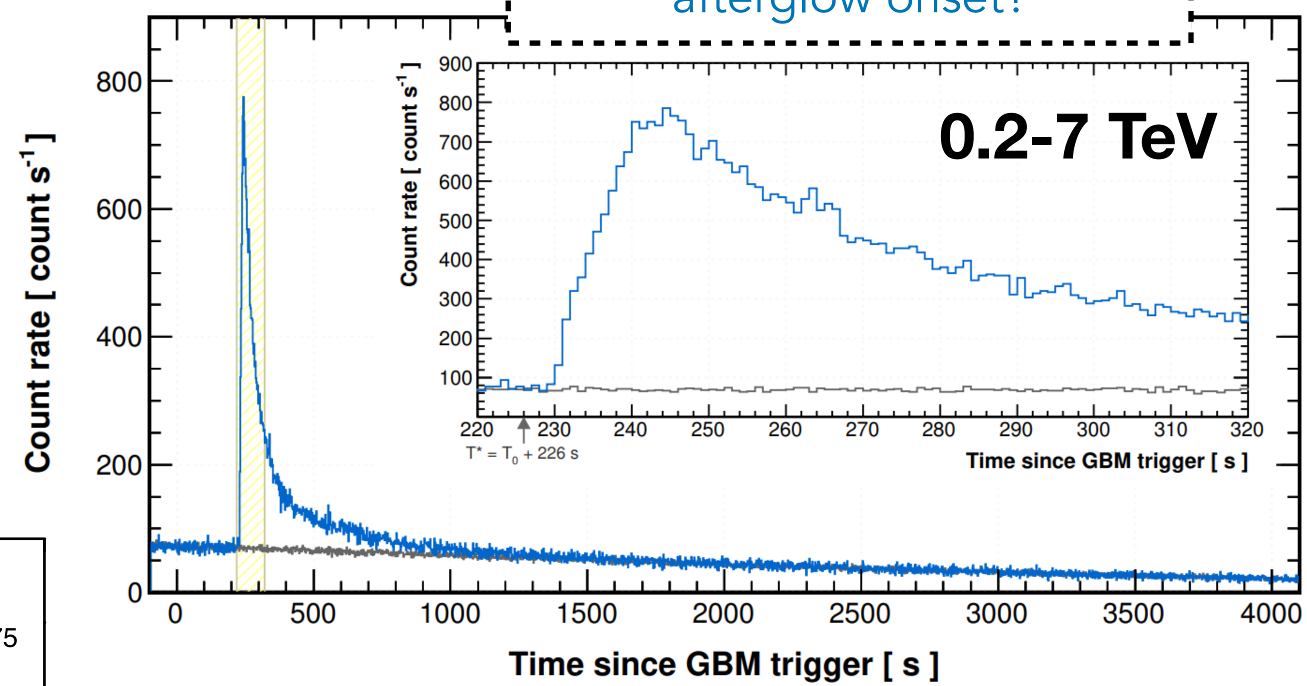

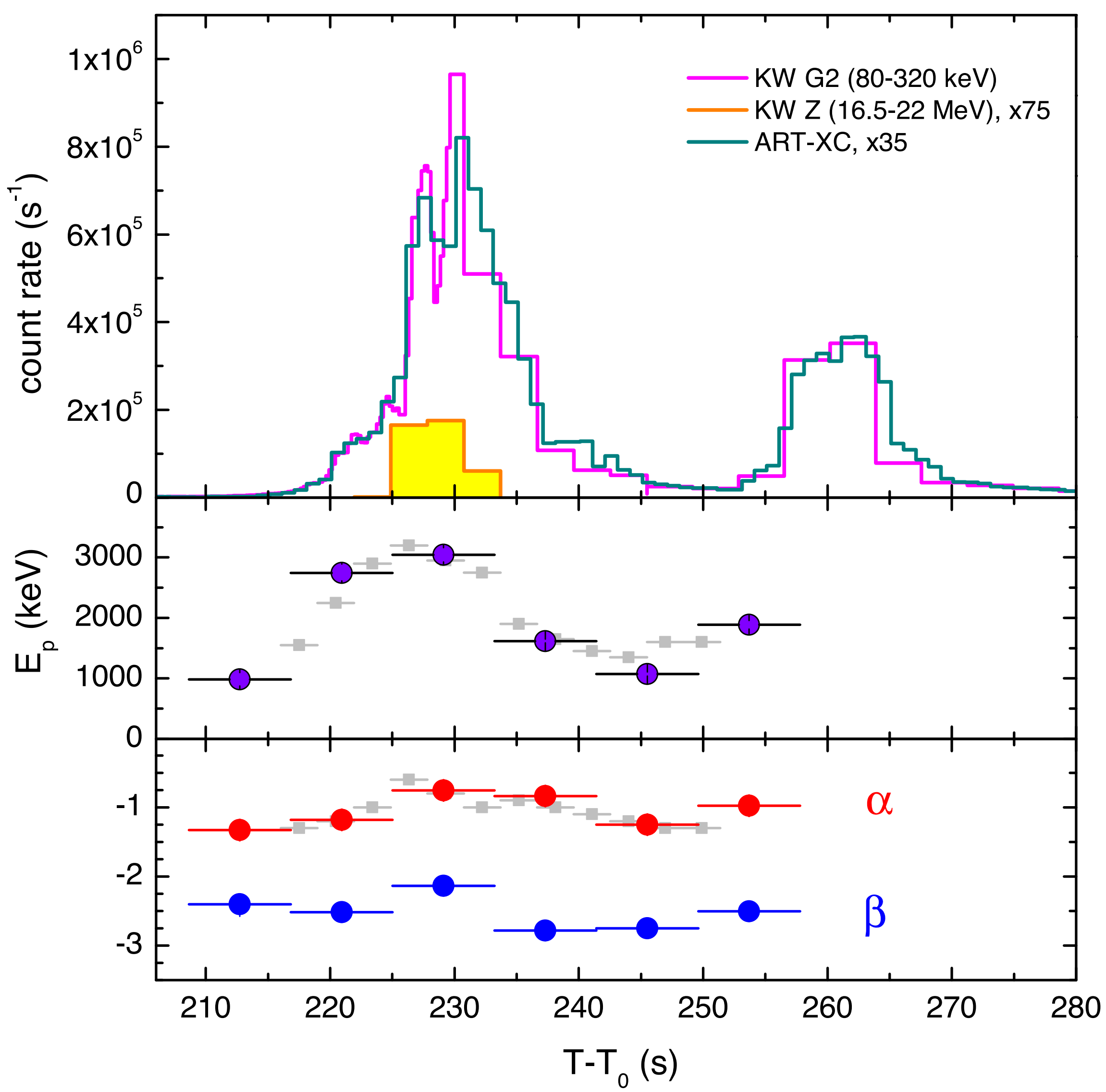

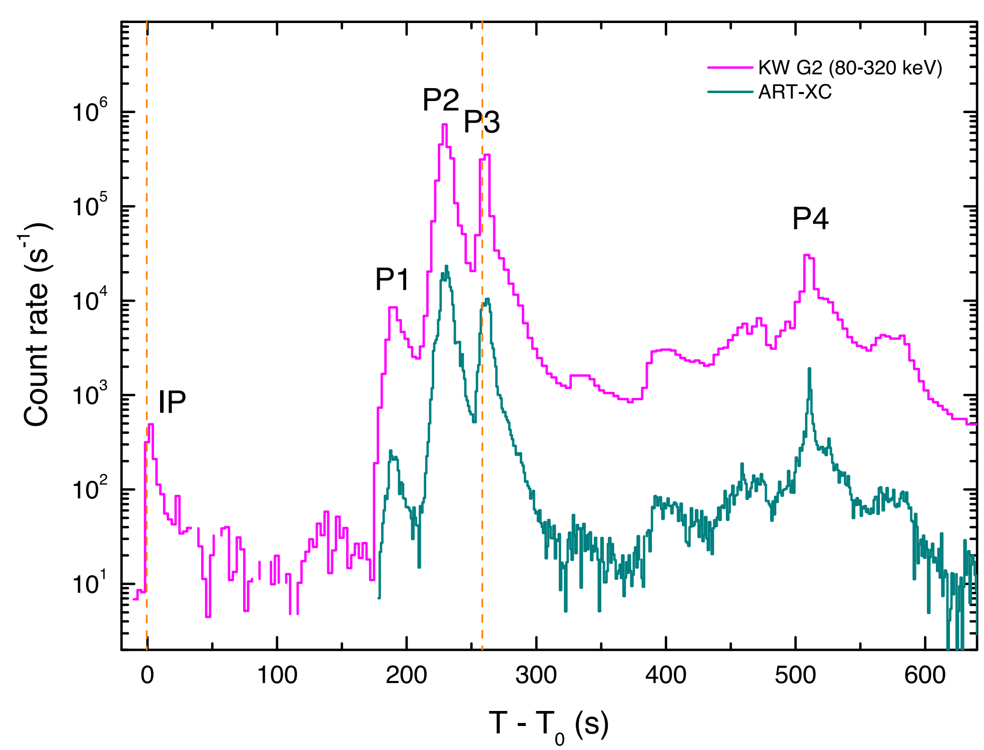

Frederiks et al. 2023: Konus-WIND and ART-XC (4- 30 keV) observations

Lepto-hadronic model: GRB 221009A

Rudolph, Petropoulou, ŽB, Winter 2023
Rudolph, Petropoulou, Winter, ŽB 2023

Multi-messenger model for the prompt emission of GRB 221009A: the varying physical conditions in the outflow and the UHECR feedback on both the photon and neutrino emissions taken into account.

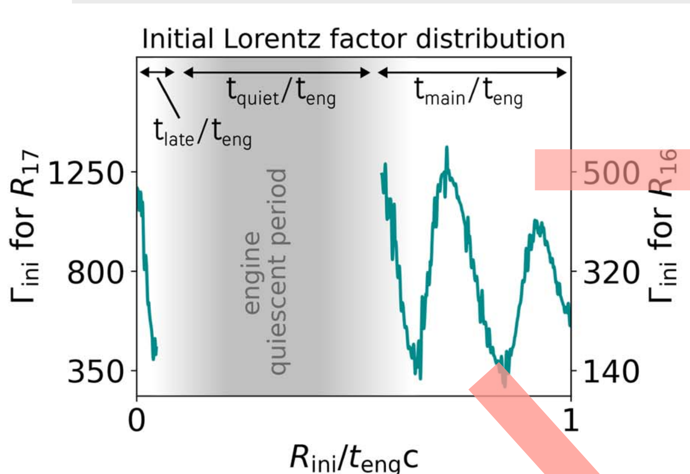

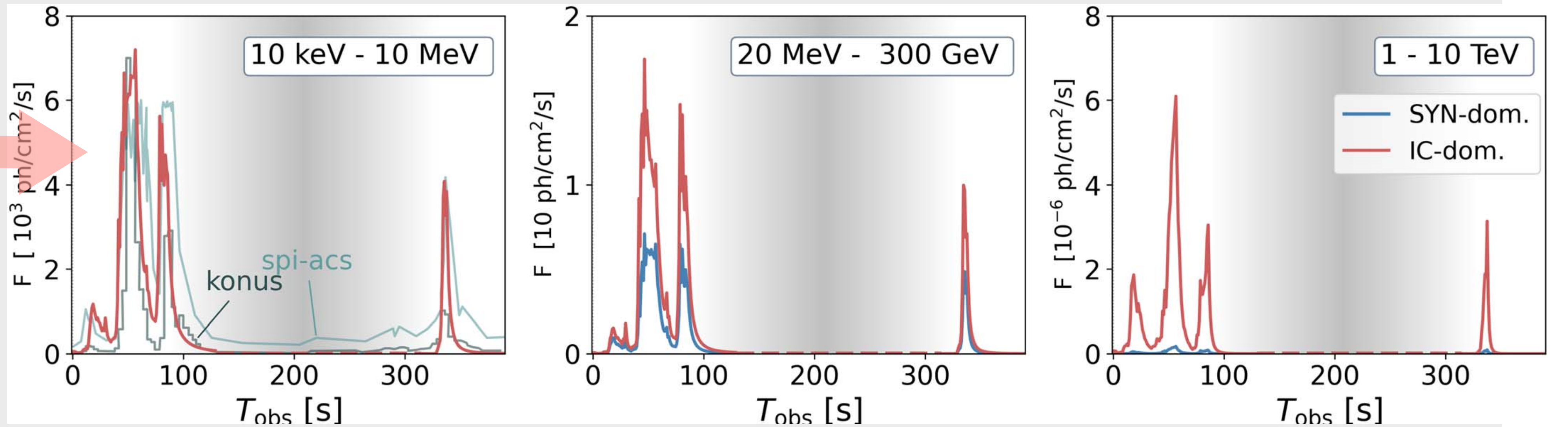

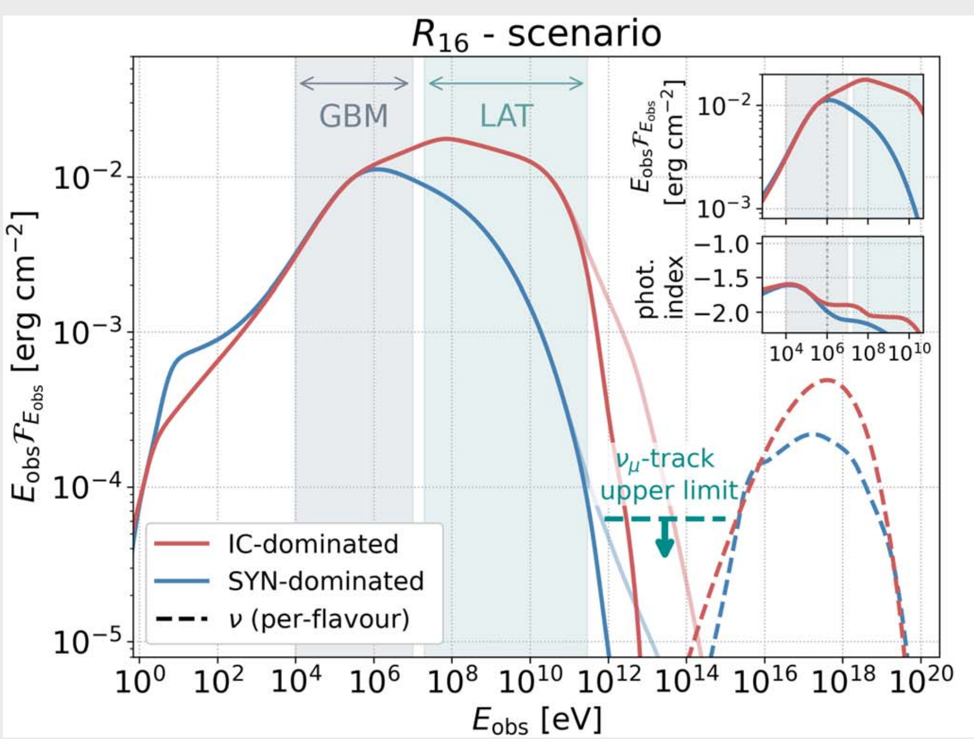

The obtained maximal proton energies are in the range 10^{20} - 2 x 10^{21} eV under the assumption of efficient particle acceleration.

→ compatible with Das & Razzaque 2022 (100 EeV) do describe the LHAASO VHE from EBL interactions.

→ time delay induced by the EGMFs requires extremely low field values paired with large proton energies

→ the EGMF induced delay is very large (LHAASO window of 2000 s)

GRB prompt emission from the synchrotron radiation of relativistic electrons in a decaying magnetic field

‣ Motivation

The theoretically predicted synchrotron spectrum leads to a slope $F_\nu \propto \nu^{-1/2}$ below 100 keV, which is in contradiction to the much harder spectra observed during the prompt GRB emission.

Sari, Piran & Narayan 1998

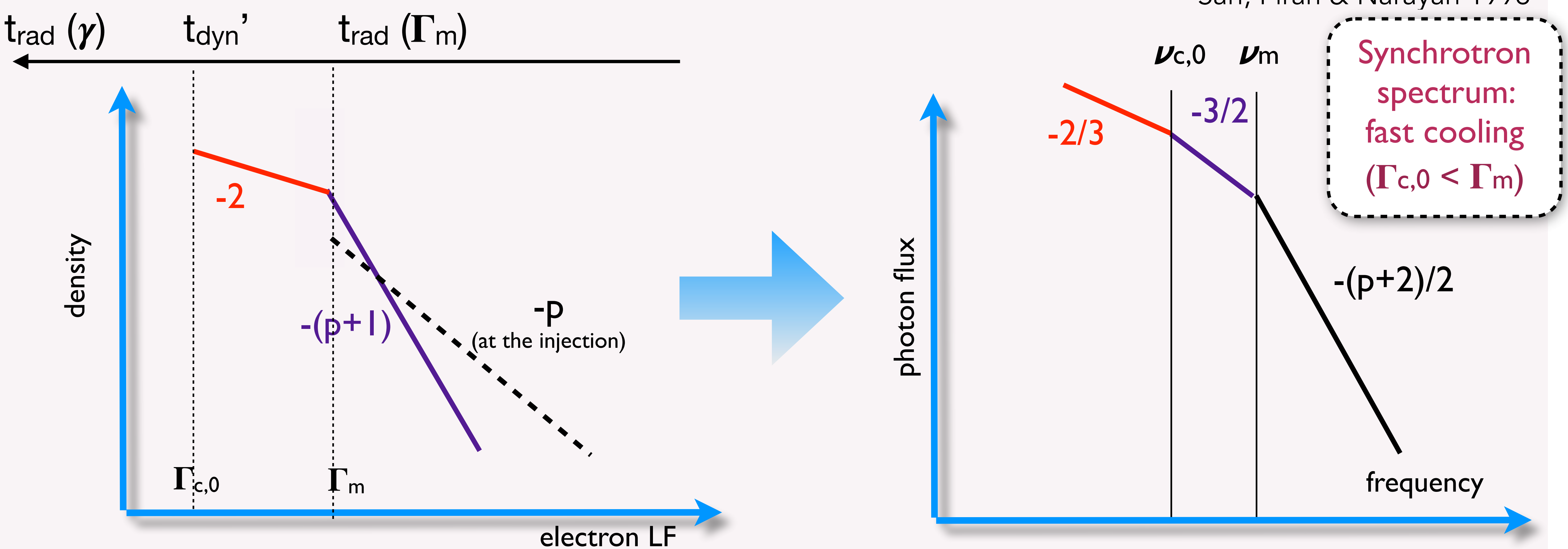

Γ_m: minimum Lorentz factor at injection

$\Gamma_{c,0}$: radiative timescale = dynamical timescale

A possible solution proposed by Daigne et al. 2011; Beniamini & Piran 2013: in **the marginally fast cooling regime** ($\Gamma_{c,0} \simeq (0.1 - 1)\, \Gamma_m$), where the cooling break is very close to the peak frequency, the intermediate portion of the spectrum (slope = -3/2) disappears and the slope -2/3 is recovered (still with a high radiative efficiency)

GRB prompt emission from the synchrotron radiation of relativistic electrons in a decaying magnetic field

- **Motivation**

Marginally fast cooling can naturally emerge if electrons are radiating in a magnetic field decaying on a timescale t_B',

$$B'(t') = B_0' \, e^{-t'/t'_B} \quad \text{where} \quad t'_{syn}(\Gamma_m) < t'_B < t'_{dyn}$$

→ electrons having $\gamma \gtrsim \Gamma_m$ will still experience a magnetic field B'_0 and the peak + high-enegy part of the synchrotron spectrum will not be affected

→ electrons with Lorentz factors $\Gamma_{c,0} < \gamma < \Gamma_m$ will lose their energy more slowly than expected because they will encounter a lower magnetic field when they start to travel outside the initial acceleration site. The cooling break will increase to:

$$\nu_c \simeq \nu_{c,0} \, (t'_{dyn} / t'_B)^2$$

This allows to naturally tend towards the marginally fast cooling regime, even when $\Gamma_{c,0} / \Gamma_m << 1$. The radiative efficiency will remain high as long as $t'_{syn}(\Gamma_m) << t'_B$ so the final condition becomes:

$$\Gamma_{c,0} / \Gamma_m \lesssim t'_B / t'_{dyn} \lesssim 1$$

Radiative models

Radiating electrons probe the magnetic field on >> scale than in the PIC simulations but - when they are in fast cooling - on a much smaller scale than the (magneto-) hydrodynamical scale.

A hierarchy of scales: t'_{acc} (Γ_m) ≪ t'_{rad} (Γ_m) ≪ t_{dyn}'

- the magnetic field may decay on a length scale much shorter than the shocked region scale t'_{dyn} (e.g. Keshet et al. 2009).

Prompt emission models: Pe'er & Zhang 2006; Derishev 2007; Zhao et al. 2014; Uhm & Zhang 2014; Geng et al. 2018 (much larger scales for B' decay)

Afterglow modelling: Gruzinov 2001; Rossi & Rees 2003; Lemoine 2013

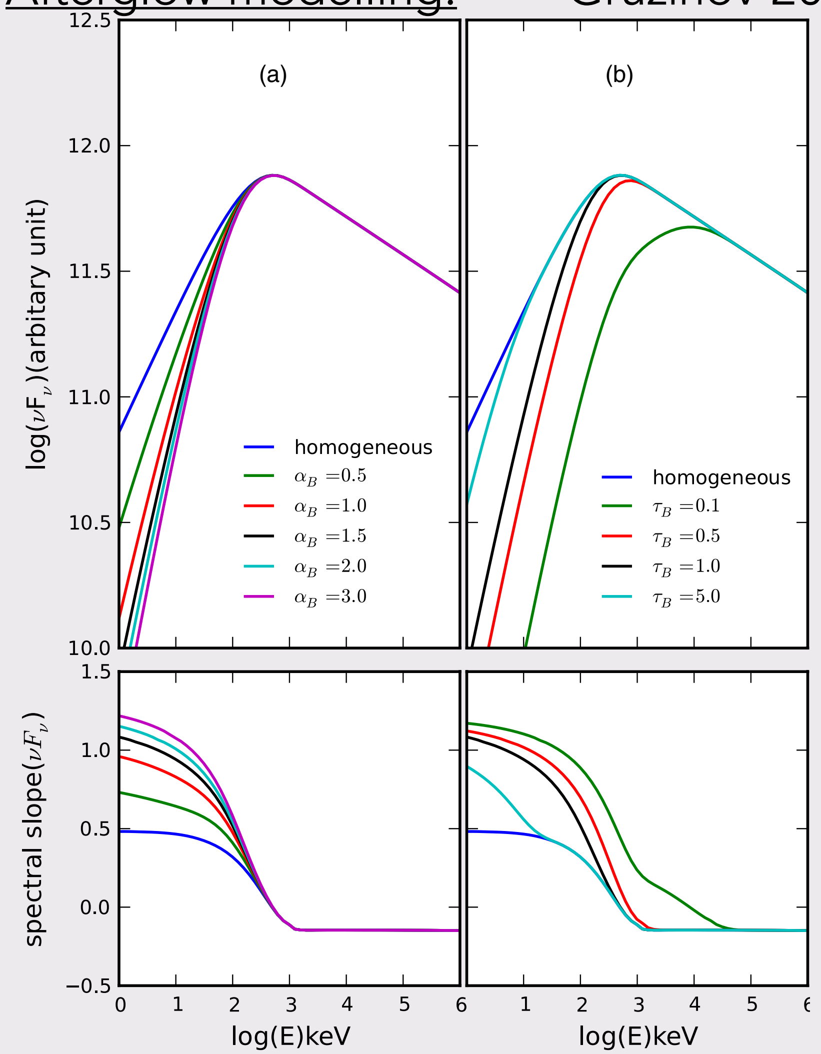

Zhao et al. 2014:

PLD & ED models

Klein-Nishina effects neglected

adiabatic cooling not included

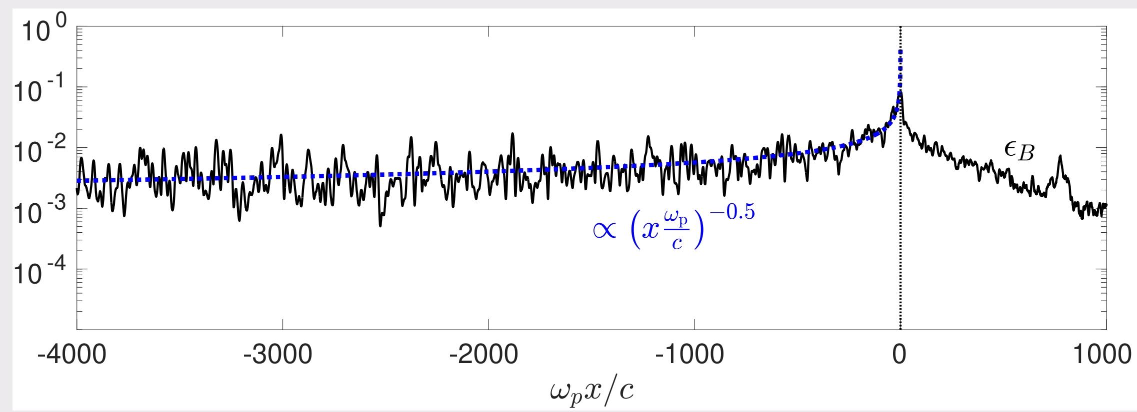

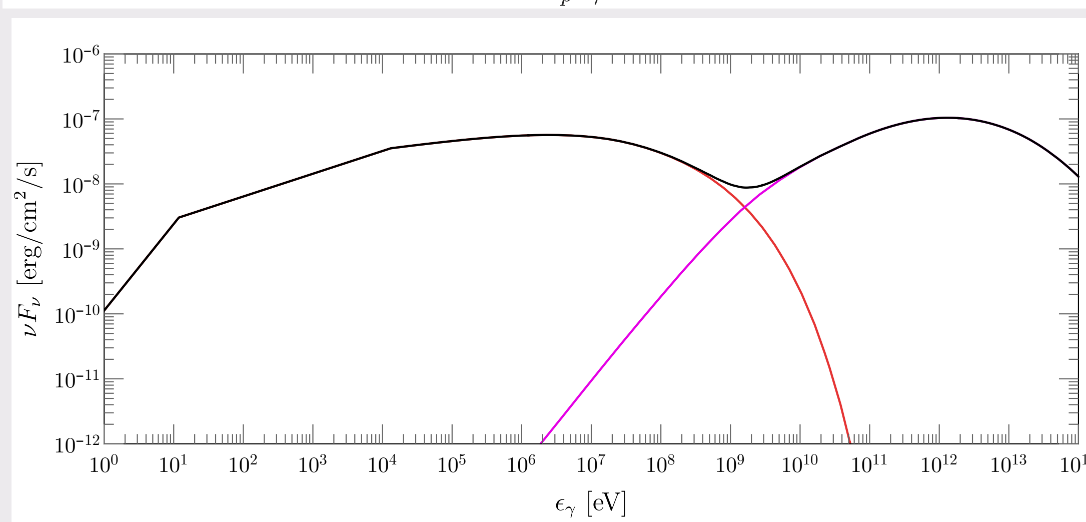

ϵ_B = 0.01 in the shock vicinity

$\epsilon_B \propto (x\ \omega_p / c)^{-0.4}$

E = 8 x 10^{53} erg

z = 0.4

n = 0.03 cm^{-3}

ϵ_e = 0.1

s = 2.3

$\gamma_{e,\,max}$ = 2 x 10^7

Vanthieghem et al. 2020:

- decay of the microturbulence in the shocked region $\epsilon_B \propto (x\ \omega_p/c)^{-0.5}$
- all electrons (but those of the very highest energies) cool in a region in which the turbulence has decayed

Radiative model: exponential decay of the magnetic field

- The magnetic field decay: $B'(t') = B_0' \, e^{-t'/t_B'}$

Electrons radiate efficiently only above an effective Lorentz factor:

$$\Gamma_{c,\mathrm{eff}} \simeq \Gamma_{c,0} \, (t'_{\mathrm{dyn}} / t'_B)$$

which leads to an increase of the cooling break frequency by a factor $\mathbf{(t_{dyn}'/t_B')^2}$

For an extreme decay, we expect a slow cooling spectrum even for $\Gamma_m > \Gamma_{c,0}$

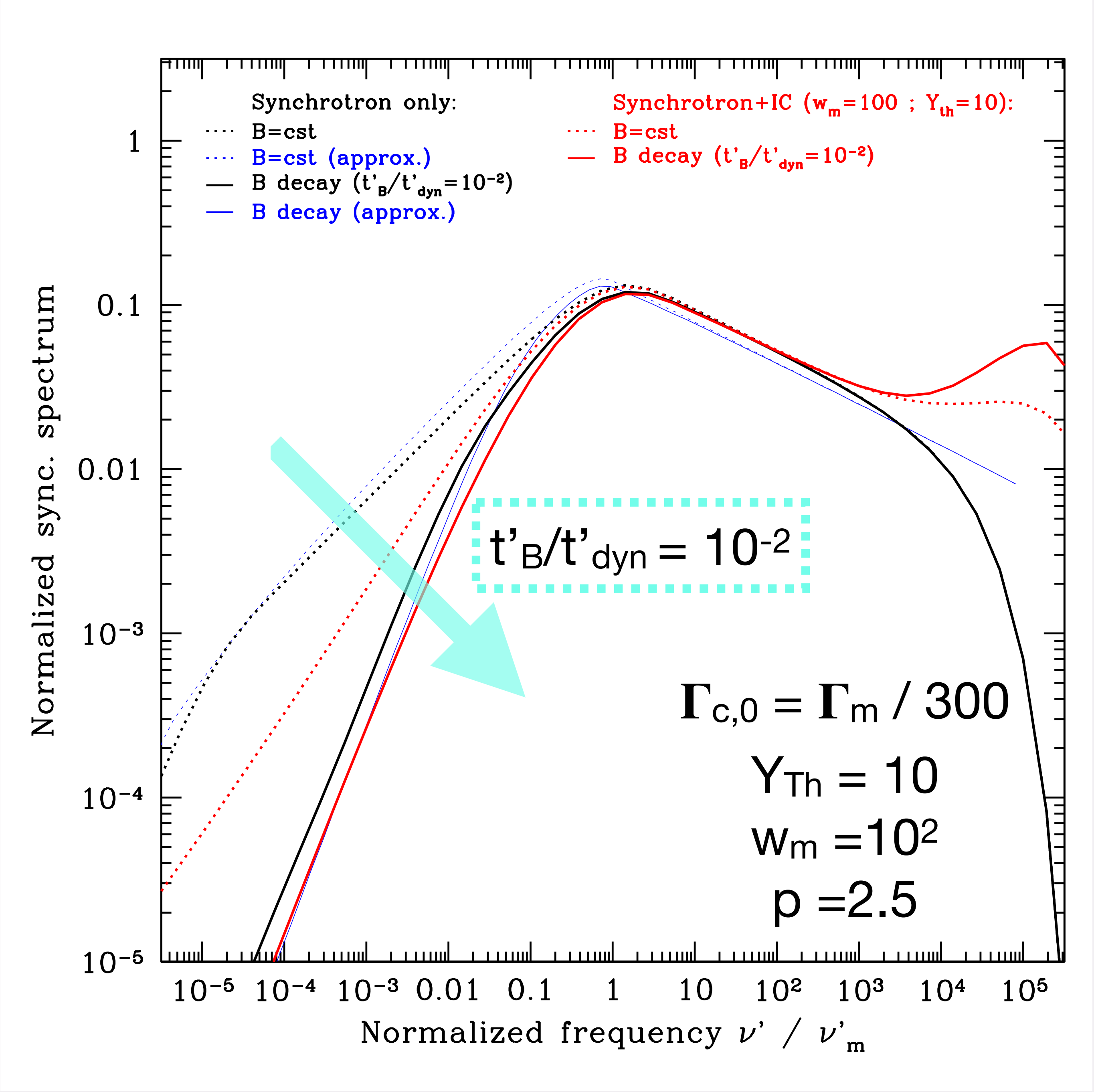

Daigne & Bošnjak 2024

Summary

Internal shock model combining dynamical simualtions that follow the physical conditions (LF, density and energy density) in the shocked regions, and a time-dependent radiative code to compute the emission from shock-accelerated electrons and protons, including the most relevant processes can successfully reproduce many features of the prompt GRB emission.

We modelled low-luminosity GRBs, and investigated the effect of hadronic processes on the energetic GRBs observed by LAT. The low-energy spectral slopes may serve as indicator for the baryonic loading.

When the characteristic decay length of the magnetic field ($B \propto e^{-t'/t_B'}$) is significantly shorter than the dynamical scale ($t_B'/t_{dyn}' \sim 0.01, 0.001$) , the low energy prompt GRB synchrotron spectrum becomes significantly harder. The regime of marginally fast cooling is naturally achieved.

The emitted spectrum in the comoving frame

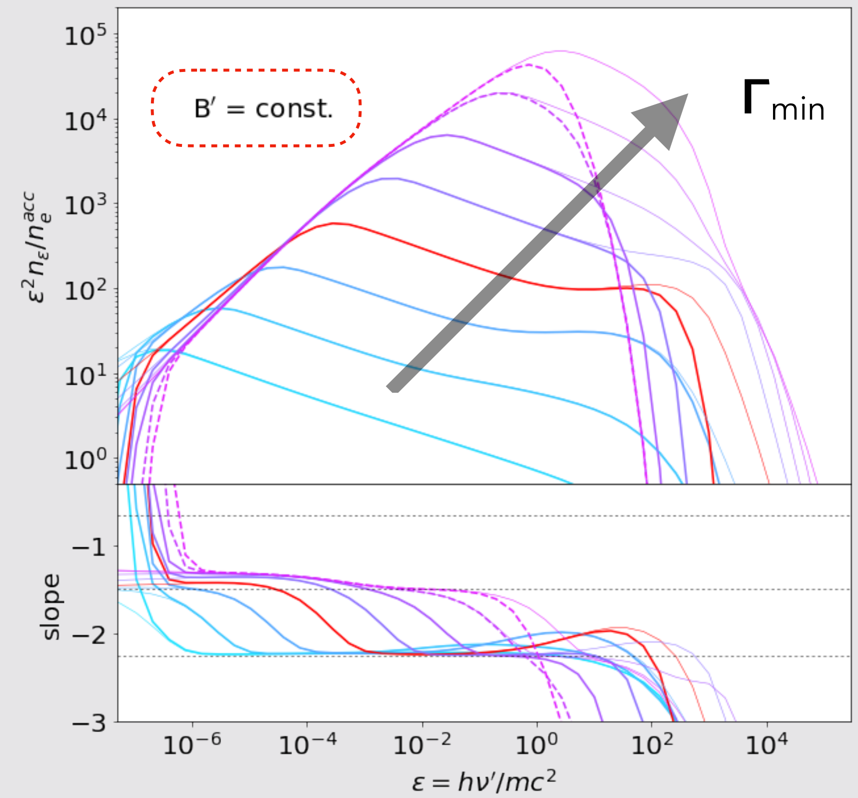

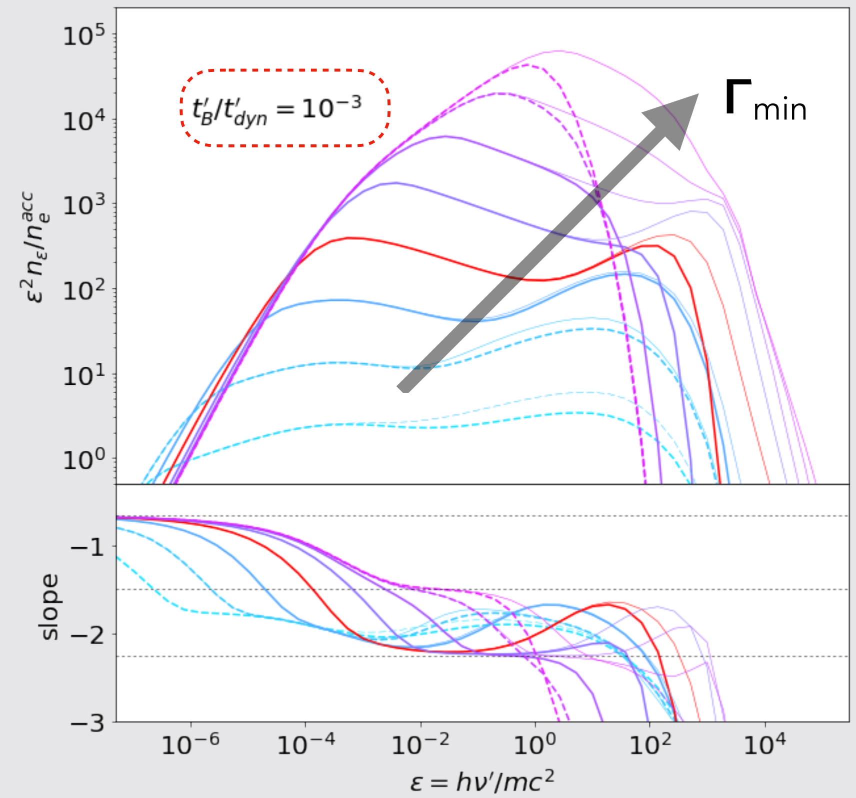

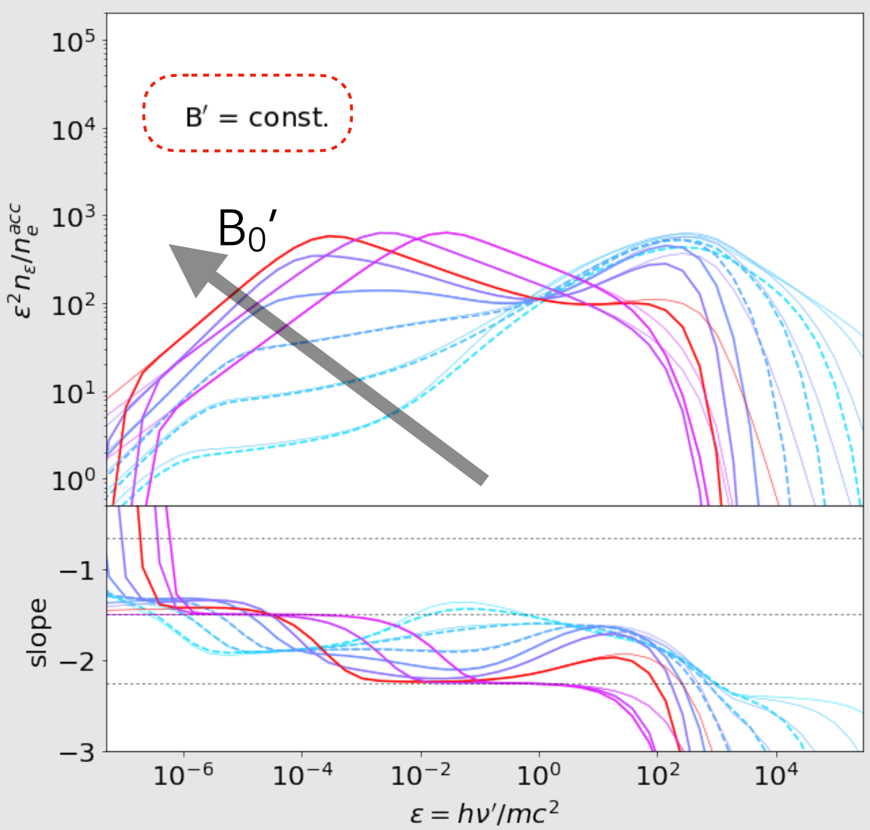

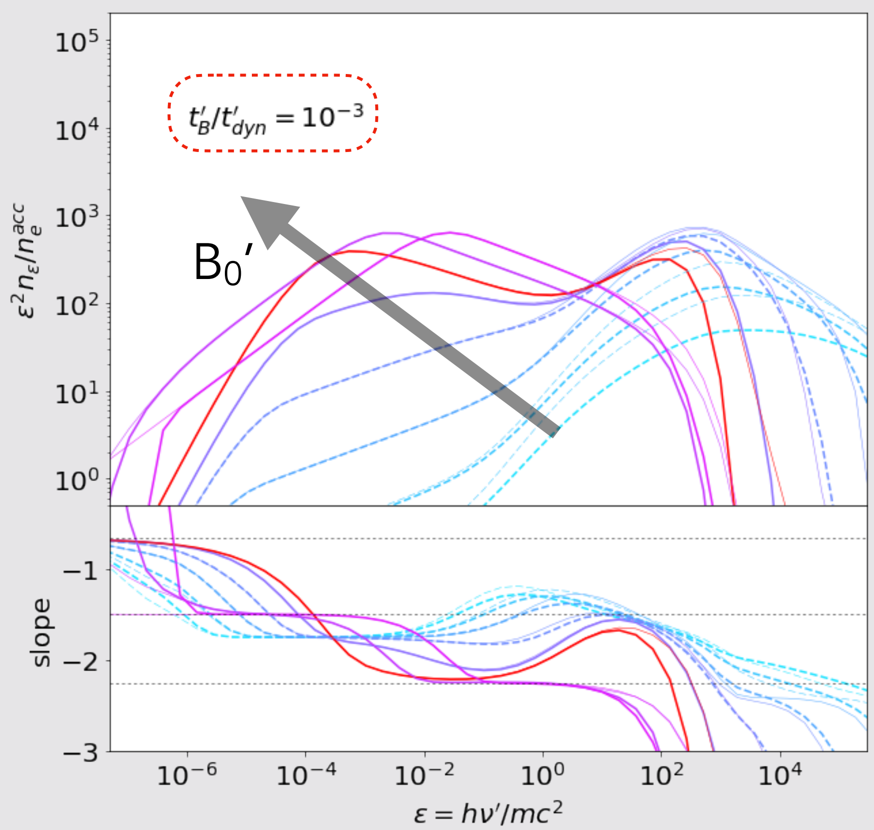

$\tau_{IC} \approx n_e$ (σ_T x KN corr.) (c x t_{rad})

Y ≈ τ_{IC} x (Γ_{min}^2 x KN corr.)

A strong IC component is obtained when relativistic e- "survive" long enough for scatterings to occur (a low Γ_{min}, a low B′ and a low t_{ex}', i.e. t_{rad}' → t_{ex}')

Reference spectrum:
Γ_{min} = 1600
B_0' = 2000 G
n_e = 4.1 x 10^7 cm^{-3}
t_{dyn} = 80 s

Effect of $Y_{Th,0}$ and w_m which govern the importance of inverse Compton scatterings and of Klein-Nishina corrections:

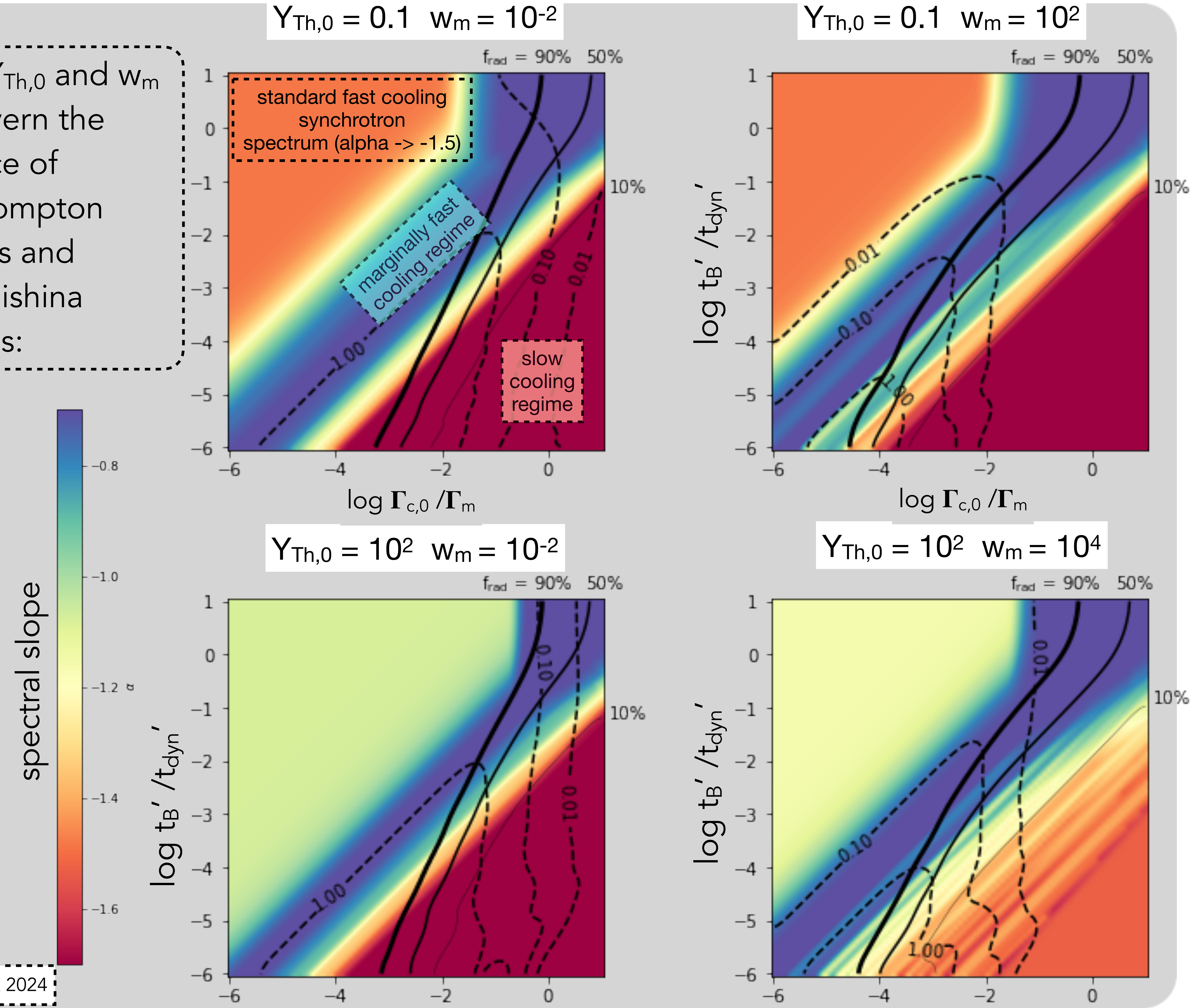

Daigne & Bošnjak 2024

Spectral evolution in the internal shock model: steep low energy slopes

Case A: a single pulse burst with a high magnetic field. The main spectral peak is due to synchrotron emission (Bošnjak, Daigne & Dubus 2009)

$\epsilon_B = 1/3$, $\epsilon_e = 1/3$, $\xi = 3 \times 10^{-3}$, $p = 2.5$, $dE/dt = 5 \times 10^{53}$ erg/s

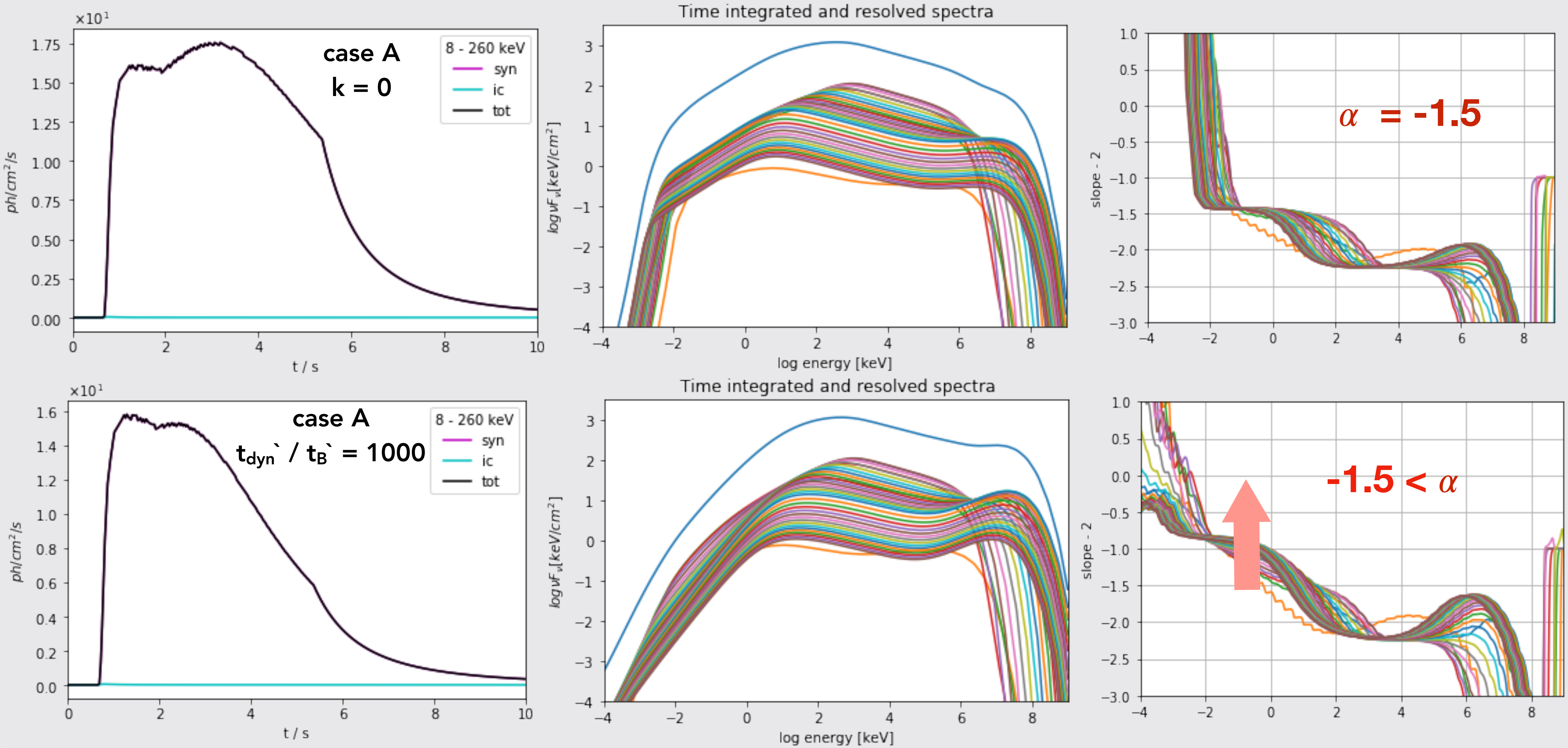

Spectral evolution in the internal shock model: steep low energy slopes

Case B: a single pulse burst with a low magnetic field. The main spectral peak is due to synchrotron emission (Bošnjak, Daigne & Dubus 2009)

$\epsilon_B = 5 \times 10^{-3}$, $\epsilon_e = 1/3$, $\xi = 2 \times 10^{-3}$, $p = 2.5$, $dE/dt = 5 \times 10^{53}$ erg/s

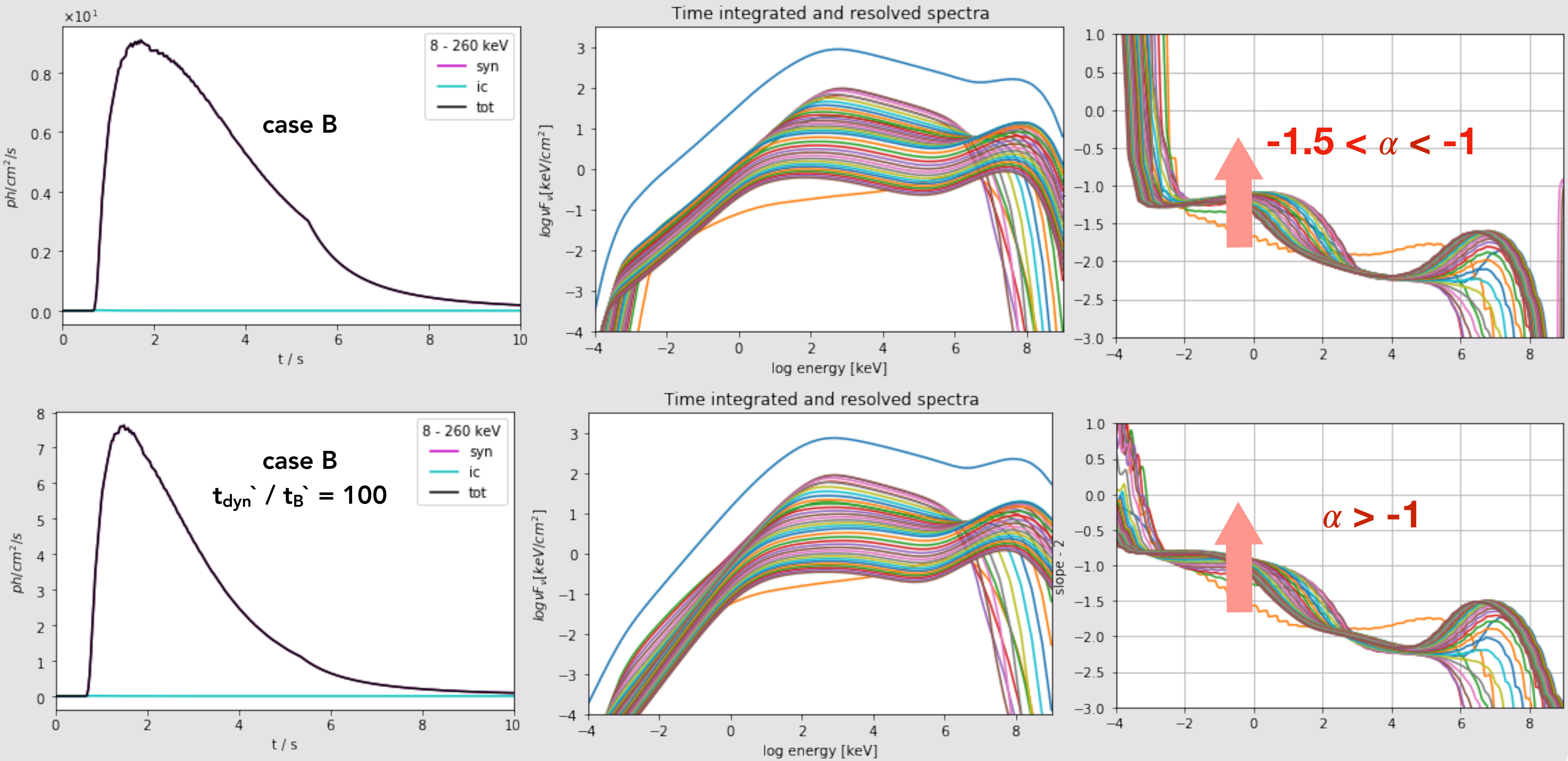

Effect of a decaying magnetic field in the internal shock model: reference case B with $t_B/t_{dyn} = 10^{-3}$:

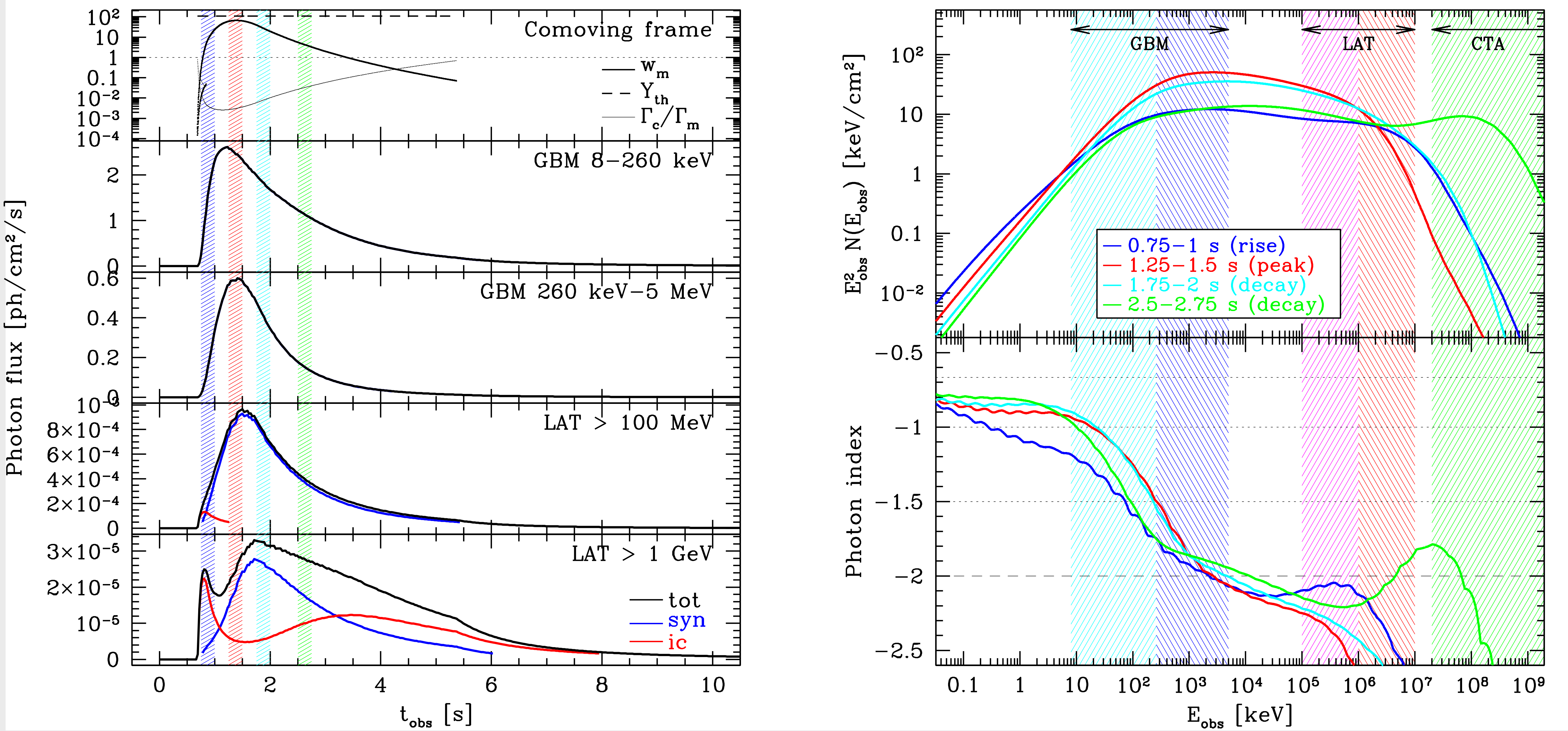

Daigne & Bošnjak 2024